This document is downloaded from DR-NTU (https://dr.ntu.edu.sg)
Nanyang Technological University, Singapore.

Profiling dynamic chromatome reveals HP1BP3 as a key regulator of cell cycle and hypoxia cancer progression

Bamaprasad Dutta

2014

Bamaprasad Dutta. (2014). Profiling dynamic chromatome reveals HP1BP3 as a key regulator of cell cycle and hypoxia cancer progression. Doctoral thesis, Nanyang Technological University, Singapore.

https://hdl.handle.net/10356/59912

https://doi.org/10.32657/10356/59912

Downloaded on 20 Mar 2024 18:29:12 SGT

PROFILING DYNAMIC CHROMATOME REVEALS HP1BP3 AS A KEY REGULATOR OF CELL CYCLE AND HYPOXIA CANCER PROGRESSION

BAMAPRASAD DUTTA

SCHOOL OF BIOLOGICAL SCIENCES

2014

Profiling dynamic chromatome reveals HP1BP3 as a key regulator of cell cycle and hypoxia cancer progression

Bamaprasad Dutta

School of Biological Sciences

A thesis submitted to the Nanyang Technological University in partial fulfillment of the requirement of the degree of Doctor of Philosophy

2014

Acknowledgements

I would like to express my sincere gratitude to my supervisor Dr. Siu Kwan Sze, for his expert guidance and warm encouragement. He shared his wealth of experience on numerous occasions and this has provided me with a great learning experience.

Special thanks go to Dr. Ren Yan for her invaluable discussions and suggestions, which helped me a lot in this project and also for helping me to learn the basic experiments. I am indebted to Dr. Sunil Shankar Adav for sharing his experience and helping.

I would also like to acknowledge the kind support of my current and former laboratory collogues, especially Dr. Park Jung Eun, Tiannan Gao, Li Xin, Arnab Datta, Hao Piliang, Sim Kae Hwan, and Cheow Sok Hwee Esther for extending their helping hand anytime I needed.

I would also like to express my sincere gratitude to my friends Sandip, Barindra, Bhabwana, Manisha and Phat for their kind help and support and also for their encouragement during long period of my PhD study in Singapore.

I would also like to convey deep appreciation for my thesis advisory committee, Dr. Li Hoi Yeung and Dr. Su I Hsin for their excellent advice and constructive criticism during the annual committee meetings and conformation of my PhD candidature. I would also like to express my sincere thanks to our collaborator Dr. Koh Cheng Gee and her lab member for their help in fluorescent microscopy studies

I gratefully acknowledge the financial support rendered by the Nanyang Technological University of Singapore in the form of Research Scholarship. I am also grateful to the academic and technical staffs at the School of Biological Sciences, who have helped me in one way or the other in my research work.

Last but not least, my heartedly gratitude goes to my parents for selfless support, love and understanding during and before my PhD study in Singapore. I thank all my family members who are always proud of my academic achievements and have taken all the troubles to inspire, encourage and support me to reach this stage.

Contents

Contents

Contents

List of figures

Chapter 1

Chapter 2

Chapter 3

List of figures and tables

Chapter 4

List of tables

Chapter 3

Chapter 4

Abbreviations

2-PCPA	(±)-Trans-2-Phenylcyclopropylamine, Hydrochloride
ABC	ATP-Binding Cassette
ACN	Acetonitrile
APEX	Absolute Protein Expression
AQUA	Absolute Quantification
ATM	Ataxia Telangiectasia Mutated
ATR	Ataxia Telangiectasia and RAD3 Related
Bcl2	B-Cell Lymphoma 2
Bub	Budding Uninhibited by Benzimidazoles
CD	Cluster of Differentiation
CDK	Cyclin-Dependent Kinases
ChIP	Chromatin Immunopurification
CID	Collision-Induced Dissociation
CKI	Cyclin-Dependent Kinases Inhibitor
CSC	Cancer Stem Cell
CXCR4	C-X-C Chemokine Receptor Type 4
DAPI	4', 6-Diamidino-2-Phenylindole
DMEM	Dulbecco's Modified Eagle Medium
DMSO	Dimethyl Sulfoxide
DNA	Deoxyribonucleic Acid
DNA-PK	DNA-Dependent Protein Kinase
DNA-PKcs	DNA-Dependent Protein Kinase, Catalytic Subunit
DNase I	Deoxyribonuclease I
DSBs	Double-Strand Breaks
DTT	Dithiothreitol
ECM	Extracellular Matrix
EDTA	Ethylenediaminetetraacetic Acid
EGF	Epidermal Growth Factor
emPAI	Exponentially Modified Protein Abundance Index

Abbreviations

EPO	Glycoprotein Hormone Erythropoietin
ERLIC	Electrostatic Repulsion-Hydrophilic Interaction Chromatography
FBS	Fetal Bovine Serum
FDR	False Discovery Rate
FGF	Fibroblast Growth Factor
GAPDH	Glyceraldehyde-3-Phosphate Dehydrogenase
GFR	Growth Factor Receptors
GO	Gene Ontology
HBSS	Hank's Balanced Salt Solution
HDAC	Histone Deacetylases
HEPES	4-(2-Hydroxyethyl)-1-Piperazineethanesulfonic Acid
HIF	Hypoxia Inducible Factor
HP1BP3	Heterochromatin Binding Protein 1 Binding Protein 3
HPLC	High Performance Liquid Chromatography
HR	Homologous Recombination
ICAT	Isotope-Coded Affinity Tag
IgG	Immunoglobulin G
iTRAQ	Isobaric Tags for Relative and Absolute Quantification
KDM	Histone Lysine Demethylases
LC	Liquid Chromatography
LOX	Lysyl Oxidase
Mad	Mothers against Decapentaplegic
MCAT	Mass-Coded Abundance Tagging
mChIP	Modified Chromatin Immunopurification
mgf	Mascot Generic File
MLL1	Histone-lysine N-methyltransferase HRX
MMP	Matrix Metalloproteinases
MMR	Mismatch repair
MMTS	Methyl Methanethiosulfonate
MNase	Micrococcal Nuclease
MRM	Multiple reaction monitoring

Abbreviations

mRNA	Messenger RNA
MS	Mass Spectrometry
MTA	Metastasis associated
MTT	3-(4,5-Dimethylthiazol-2-Yl)-2,5-Diphenyltetrazolium Bromide
NHEJ	Non-Homologous End Joining
NuRD	Nucleosome Remodelling and Histone Deacetylase
PBS	Phosphate-Buffered Saline
pI	Isoelectric Point
PRMT	Histone Modifier Protein Arginine Methyl Transfereese
PSAQ	Protein Standard Absolute Quantification
PTM	Post-Translational Modification
QconCAT	Concatemer of Standard Peptides for Absolute Quantification
Rb	Retinoblastoma Protein
RNA	Ribonuclic Acid
rRNA	Ribosomal RNA
RT	Room Temperature
SDS-PAGE	Sodium Dodecyl Sulfate Polyacrylamide Gel Electrophoresis
shRNA	Short Hairpin RNA
SILAC	Stable Isotope Labeling by Amino Acids in Cell Culture
SRM	Selected Reaction Monitoring
TBST	Tris-Buffered Saline containing 0.1% Twenn-20
TCEP	Tris 2-Carboxyethyl Phosphine Hydrochloride
TEAB	Triethylammonium Bicarbonate
TMT	Tandem Mass Tags
Tris	2-Amino-2-hydroxymethyl-propane-1, 3-diol
VEGF	Vascular Endothelial Growth Factor
WGA	Wheat Germ Agglutinin

Abstract

Chromatin, a key component of eukaryotic cells composed of DNA and proteins, plays a key regulatory role by controlling accesses to the DNA template that carry genetic instructions for all cellular functions. The chromatin-associated proteome, also called chromatome, is a dynamic system which changes in response to internal and external stimuli. Through the changes, chromatome actively modulates chromatin structure to regulate developmental biology, cell cycle, epigenetics and pathobiology such as cancer development. A handful of chromatin proteomic studies were reported as of now. However, the dynamic chromatin protein binding topology which directly regulates genetic and epigenetic biology in normal development and disease remains unknown. Most characterized genetic mutations in common cancers are linked to tumor initiation and few are related to tumor progression and metastasis. Recent studies showed that epigenetic changes play a key role in tumor malignancy. Emerging clinical and experimental evidences suggest that hypoxic tumor microenvironment might alter the epigenetic marks and induce stemness in normal cancer cells and converting them into the radio- and chemo-resistance malignant cancer cell phenotypes. In addition, recent evidences also revealed the correlation between hypoxia and cell cycle regulation. Thus, characterization of the chromatome dynamics to elucidate chromatin biology by quantitative proteomic approach will provide molecular mechanistic insight of hypoxic microenvironment induced tumor malignancy. Accordingly, our aims are 1) to develop a proteomic method to study the dynamic chromatome by nuclease digestion to release proteins bound to specific chromatin region coupled with quantitative proteomic profiling; and 2) to elucidate the dynamics of chromatin biology during cell cycle and hypoxia induced tumor malignant progression by using our proteomic method developed in aim 1.

In order to establish a suitable proteomic approach to study chromatome dynamics, we used rat liver chromatin as model. We used partial MNase and DNase I digestion together with iTRAQ-based quantitative proteomics to study euchromatin- and heterochromatin-associated proteins in liver cells. A total of 694 chromatin-associated proteins was identified at a high level of confidence that allow us to determine their dynamic interactions with chromatin to infer their euchromatin and heterochromatin associations and their roles in chromatin biology. We reported

several novel chromatin-associated proteins and also validated the localization of Gnl3, Ncl, and Phb proteins by immunofluorescence microscopy analysis. After having established the method, we applied this partial nuclease digestion coupled with iTRAQ-based quantitative proteomic approach to study the dynamic changes of the chromatomes during cell cycle progression and hypoxia microenvironment induced cancer progression. A total of 481 and 1446 proteins were identified at high confidence level during the cell cycle and hypoxia stress based experiments respectively. Data mining suggested that identified proteins were involved in chromatin-dependent events including transcriptional regulation, chromatin re-organization, and DNA replication and repair, while the quantitative data of differential released chromatin-associated proteins by partial nuclease digestion revealed the temporal interactions of these proteins with euchromatin and heterochromatin during interphase progression and different hypoxia stress conditions. When combined with biochemical and functional assays, these data revealed a strikingly dynamic association of protein HP1BP3 with the chromatin during different stages of interphase and also during different oxygen tensions, and uncovered a novel regulatory role for this molecule in the maintenance of chromatin structural integrity and transcriptional regulation. We report that HP1BP3 protein maintains heterochromatin integrity during G_1-S progression and determine the G_1 phase duration by regulating G_1/S transition, which critically influence cell proliferative capacity. Cell cycle chromatomic data together with other functional studies revealed the role of chromatin regulatory protein KDM1 in the regulation of S/G_2 transition. Functional characterization of HP1BP3 during cancer progression showed that HP1BP3 mediated heterochromatinization was activated during hypoxia, which transformed the normal cancer cells into aggressive and malignant cancer cell phenotype through increasing cell survivability, cell motility, radio- and chemo-resistance, and stemness. Based on our experimental evidences and observations we suggested that HP1BP3 mediated heterochromatinization will be the potential target for new cancer therapy.

Chapter 1

1 General introduction

1.1 Introduction

1.1.1 Chromatin

1.1.1.1 Chromatin structure and function

Chromatin is a DNA protein-complex localized inside the eukaryotic nucleus and carries all the genetic and epigenetic information. Huge length of DNA is compacted very precisely into the chromatin to accommodate itself inside the tiny nucleus. Chromatin serves some very basic cellular functions like 1) DNA packaging to accommodate the huge length of DNA inside the tiny cellular space, 2) provides the entire genome a manageable shape and mechanical strength which can non-erroneously passed into the daughter cells through mitosis, 3) compaction also provides sufficient protection against DNA damage, and 4) finally it regulates the DNA accessibility to the other proteins and control basic genetic events like transcription and replication.

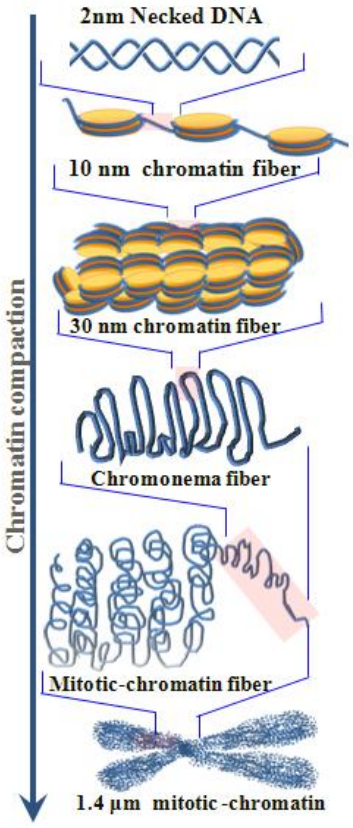

Figure 1.1: Levels of chromatin organization. Necked DNA is packed inside the different types of chromatin fibers through different types of interactions

Genomic DNA is compacted to the chromatin through the help of a group of basic histone proteins. Basic structural unit of chromatin known as nucleosome composed of H2A, H2B, H3 and H4 histone octamer and ~146 bp of DNA. 146 bp DNA wraps around the histone octamer with ~1.7 turns and form the nucleosome core particle [1]. Nucleosomes are connected with each other through the linker DNA and form "string-of-beads" like 11 nm basic chromatin fiber. The chromatin fibers are further compacted through a complex interaction between nucleosomes and the linker histone H1 to form 30 nm chromatin fibers [2]. The 30 nm chromatin fibers are further packed into higher order chromatin structure. The mechanisms behind the compaction are poorly understood. Many non-histone proteins play the crucial role. The interphase chromatin fibers are packed to form a larger chromatin fiber known as "chromonema" fiber [3]. The final chromatin packaging takes place during the mitosis to provide the genomic DNA a sufficient

mechanical strength for smooth transfer of the genome into the daughter cells. Mitotic chromatins are compacted differently from other type of chromatin compaction. The compaction ratio between necked DNA and mitotic chromatin reach ~7000:1 in completely compacted mitotic chromatin [4]. Mitotic chromatin packing mechanism is not fully understood, despite of the fact that many mitotic specific non-histones play a vital role in the compaction.

Throughout the interphase progression, cells need to maintain the chromatin structure in a dynamic manner in order to conduct DNA dependent cellular events. During interphase chromatin exhibit two types of basic higher order structural form, named euchromatin and heterochromatin. Euchromatins are loosely compacted regions enriched with active genes. The major fraction of interphase chromatins are in this structural state. Heterochromatins are highly condensed transcriptionally inactive regions specifically located in the nuclear periphery. Furthermore heterochromatins are of two types 1) constitutive heterochromatin and 2) facultative heterochromatin. Constitutive heterochromatins are constituted with the permanently silenced gene regions characterized by repetitive sequence and generally located in the centromeres, telomeres and a few other regions. Facultative heterochromatins are temporarily inactive for a specific time period or inactive in a certain cell type for example facultative heterochromatin is inactive in female X chromosome but it is active in male.

1.1.1.2 Chromatin structural regulation

All genomic and epigenetic events are directly regulated by the higher order chromatin structure [5]. Dynamic architectures of the chromatin are maintained through structural organization based on different physical interactions like DNA-protein and protein-protein interaction. However synchronization of those physical interactions are still poorly understood. Chromatin structure and functions are also regulated by many epigenetic and non-epigenetic factors like DNA modification, histone post translational modifications (PTMs), histone variants, non-histone protein-chromatin interactions and non-cording RNA interactions [6]. Histones are one of the key components of chromatin and histone tails hanging outside the nucleosome core particles are prime substrates for PTMs due to their easy accessibility. More than eleven types of histone PTMs are reported including phosphorylation at serine and tyrosine residues; acetylation, methylation, ubiquitination, and sumoylation at lysine residue; methylation at arginine residue

and other PTMs like ADP ribosylation, glycosylation, biotinylation and carbonylation [7]. PTMs of histones alter the histone-histone, DNA-histone and histone-protein interactions which directly affect the structural integrity of the chromatin and alter the DNA template accessibility to other proteins which finally affect chromatin dependent biological functions [8-11]. DNA methylation at cytosine also alters DNA-protein interaction and affects the chromatin dependent basic genomic and epigenomic events through regulating the structural integrity of the chromatin [12]. Recently, non-histone protein-chromatin interactions are shown to play a regulatory role in maintaining the proper structural integrity of chromatin and its functions [13-15]. Taking together chromatin biology is controlled by histone PTMs and DNA methylation which in turn are directly regulated through the chromatin associated proteins and protein complexes [16]. Therefore knowledge of chromatin associated proteins and their changes in response to intra- and extra-cellular signals will help to understand the chromatin biology.

1.1.2 Chromatin proteomics

1.1.2.1 Chromatin protein and its importance

Chromatin regulates all DNA dependent basic nuclear events like transcription, replication, genome packaging, maintenance of genome stability and chromatin segregation. To perform these events chromatin reorganized its structure accordingly. It is well-established that chromatin biology is regulated by a group of enzymes and protein complexes that involve in regulation of histone and DNA modification through the induction of modification (“writers”) and the deletion of modification (“erasers”) [17, 18]. Another group of protein (“readers”) involved in this regulatory process by reading the epigenetic codes and conducts the specific functions [17]. Improper coordination between “writers”, “erasers”, and “readers” or their malfunctioning cause deregulation of the chromatin biology and promote pathological events including cancer [19, 20], and many epigenetic diseases [21]. The functions of chromatin associated proteins are highly dependent upon their chromatin association topology, i.e. associated with euchromatin or heterochromatin regions. But chromatin binding topology of the chromatin-interacting proteins is not well understood. The knowledge of the dynamic chromatin associated proteome and their binding topology provides invaluable information to understand the dynamics of the chromatin biology in normal biological conditions and pathological events.

1.1.2.2 Nuclease digestion and chromatin protein extraction

Various acid extraction methods are commonly used to extract basic proteins including histones from chromatin. In addition to acid extraction approach salt extraction is also used to extract chromatin binding proteins from chromatin. The chromatin binding proteins can also be extracted by shearing the chromatin by the mechanical means such as sonication or by the enzymatic means like nuclease digestion. Nucleases are the enzymes which cleave the phosphodiester linkage of the nucleic acid. Nucleases are classified into two major categories endonuclease and exonuclease. They cleave the nucleic acid both in sequence specific or non-specific manner. Non-specific nucleases like micrococcal nuclease (MNase) and deoxyribonuclease I (DNase I) are commonly used for digestion of the whole chromatin. MNase is an endo-exonuclease obtains from *Staphylococcus aureus* and cleaves both DNA and RNA in a nonspecific manner and produces 3´ phosphomononucleotides. MNase digestion produces smallest DNA fragments of ~146-200 bp which are protected by nucleosome core particle [22, 23] (Fig. 1.2a). DNase I is a vertebrate endonuclease that cleaves the phosphodiester bonds between pyrimidine nucleotides and produces 5´ phospho-terminated oligonucleotides with 3´ free hydroxyl group. DNase I preferentially cleaves DNA at GC enrich regions of the promoter and transcription start sites of the active genes known as DNase I hypersensitive site [24-26]. For example DNase I hypersensitive site is located in between –60 to –260 bp of the putative transcription start region of the β-globin gene [27] (Fig. 1.2b). Sometime transcription factor and other protein binding sites are located inside the DNase I hypersensitive regions. Protein binding in those regions prevents DNase I digestion, for example, protective region like Sp1 binding sites at the SV40 early-promoter are protected from DNase I digestion [28] (Fig. 1.2c). Both those two enzymes digest chromatin into mononucleosome or small

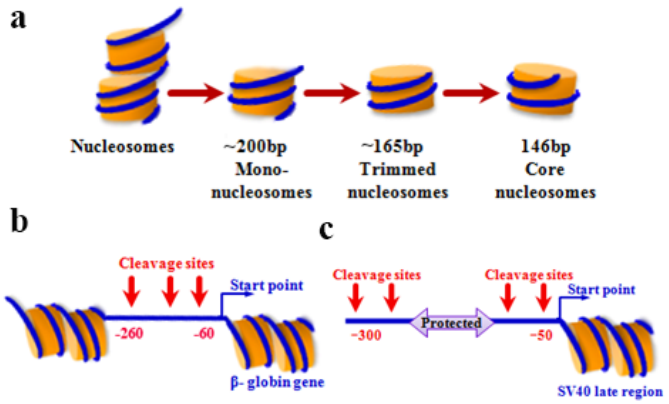

Figure 1.2: Nuclease digestion of chromatin. a: MNase digested various mononucleosomal particles. b: DNase I hypersensitive site located in the β-globin gene. c: Protected region and DNase I hypersensitive site within the SV40 early-promoter region.

oligonucleosome particles which are easily solubilized in the buffer along with the associated proteins that can be easily isolated from the insoluble chromatin fraction.

1.1.3 Mass spectrometry-based quantitative proteomics

In biological and biomedical discovery research quantitative proteomic profiling of multiple biological states is essential to answer various biological and biomedical questions. Mass spectrometry based high throughput quantitative proteomic methods are particularly suitable for discovery-driven research. Both absolute and relative quantitation can be performed by mass spectrometry based quantitative proteomics. Commonly used absolute and relative quantitative proteomic techniques [29-32] are enlisted in the figure 1.3.

For label based methods, labeling can be performed both in protein and peptide levels and among them stable isotope labeling by amino acids in cell culture (SILAC) and isobaric tags for relative and absolute quantification (iTRAQ) are commonly used for relative quantification.

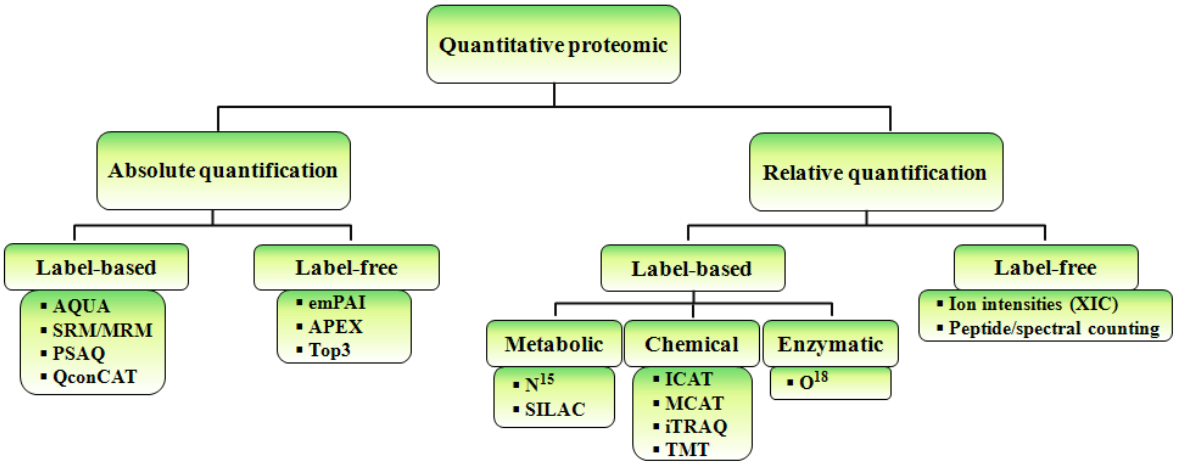

Figure 1.3: Commonly used quantitative proteomic methods. The methods can be classified into absolute quantitation to measure the absolute abundance of protein in a sample, and relative quantitation to measure the relative abundance of the same protein across multiple samples. Each method can be further divided into stable isotope label-based and label-free strategies. AQUA, absolute quantification; SRM, selected reaction monitoring; MRM, multiple reaction monitoring; PSAQ, protein standard absolute quantification; QconCAT, concatemer of standard peptides for absolute quantification; emPAI, exponentially modified protein abundance index; APEX, absolute protein expression; SILAC, stable isotope labeling by amino acids in cell culture; ICAT, isotope-coded affinity tag; MCAT, mass-coded abundance tagging; iTRAQ, isobaric tags for relative and absolute quantification; TMT, tandem mass tags.

SILAC labeling is performed in protein level and quantitative information are acquired from precursor ion in the MS spectrum [33], while iTRAQ labeling is performed in peptide level and quantitative information are collected from fragmented reporter ions in the MS/MS spectrum [34]. Currently, iTRAQ is one of the most well accepted MS/MS based technique for high throughput quantitative proteomic studies. Using this technique we can simultaneously quantify 4 or 8 biological samples in different states together by 4-plex or 8-plex iTRAQ reagents.

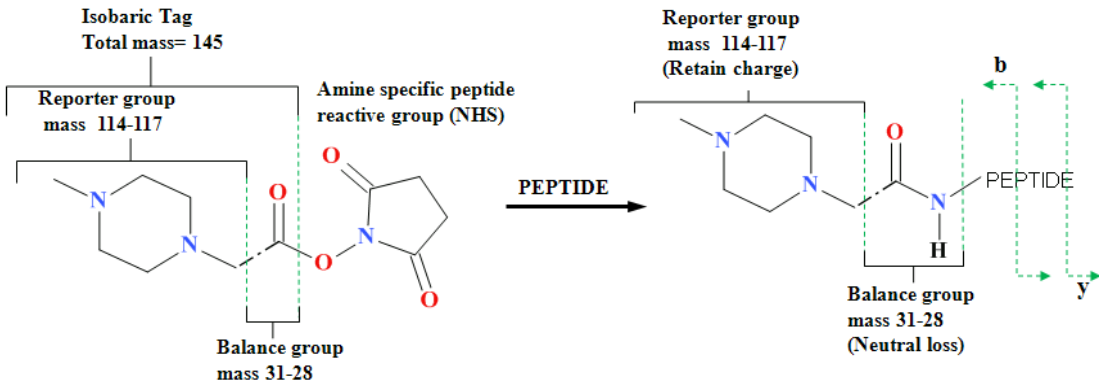

Figure 1.4: Schematic representation of the isobaric tagging chemistry of iTRAQ.

iTRAQ reagents are covalently associated with the amine group of digested peptides and produced amine-derivatized peptides producing unique MS/MS reporter ions by collisionally activated dissociation (CAD) in the low mass regions which is used for quantification (Fig. 1.4) [34]. Due to its peptide labeling property this technique is suitable for all types of post harvesting protein samples. This quantitation technique was successfully applied in our quantitative proteomic studies and I used the similar work flow describe in the figure 1.5 in all iTRAQ-based quantitative proteomic experiments reported in my thesis. The electrostatic repulsion hydrophilic interaction chromatography (ERLIC) based peptide fractionation technique provided good peptides separation that increase the protein identification and quantification quality over commonly used strong cation exchange (SCX) fractionation method[35].

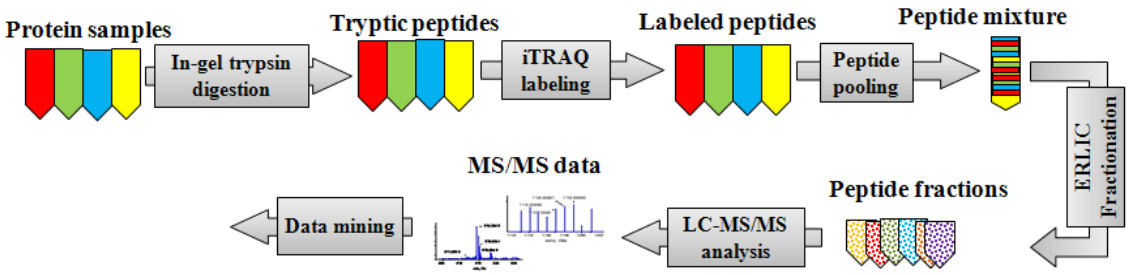

Figure 1.5: Schematic representation of the work flow of a iTRAQ based proteomic experiment.

Comparing to the above described stable isotope label based quantitative method, label free quantitative proteomic methods have relatively low quantification precision. Despite of this disadvantage, label free quantitative techniques have several advantages such as low cost and suitability for unlimited number and any type of samples, and also provided the higher sequence coverage of quantified proteins. Therefore, label free quantification provides high analytical depth and dynamic range [31]. Many approaches are used for the label free quantification including XIC or spectral count and protein abundance based quantification technique like exponentially modified protein abundance index (emPAI) and absolute protein expression (APEX) index. Among them emPAI is the label-free quantification method which I used to achieve protein abundance estimation in my experiments. The algorithm was developed by Ishihama *et al*. [36] and adopted by Mascot™ (Matrix Sciences, UK) to calculate the emPAI value of the Mascot identified proteins. During database search in the Mascot emPAI value for each protein is generated automatically according to an algorithm modified from the original method developed by Ishihama *et al*. PAI is defined as the ratio of number of experimentally observed peptides ($N_{observed}$) and number of observable peptides ($N_{observable}$) for each protein as stated in the Eq. 1. PAI have a liner relationship with the logarithm of protein concentration. Protein abundance estimation is achieved through converting the PAI value into exponentially modified PAI (emPAI) value according to the Eq. 2, which is directly proportional to the protein concentration in a sample. The molar percentages of the proteins in the mixture can also be calculated from the emPAI value according to the equation stated in the Eq. 3 where $\sum$ (emPAI) represents the sum of all emPAI values of the identified proteins. Only peptide with ion score at or above homology or identity threshold is considered for count of observed peptide list. Observable peptide number is defined as the numbers of peptides within the mass spectrometer

scan range obtained from *in silico* digestion of protein sequence. The emPAI-based label free quantitative method was successfully applied to develop the proteomic strategy for studying dynamic release of chromatin associated proteins from the chromatins as described in chapter 2.

$$PAI = \frac{N_{observed}}{N_{observable}} \qquad \textbf{(Eq. 1)}$$

$$emPAI = 10^{PAI} - 1 \qquad \textbf{(Eq. 2)}$$

$$\text{Protein content (mol \%)} = \frac{emPAI}{\sum(emPAI)} \times 100 \qquad \textbf{(Eq. 3)}$$

1.1.4 Cell cycle progression and chromatin proteomics

1.1.4.1 Cell cycle clock

Duplication of mother cells into new daughter cells occurred through a ubiquitous complex cellular process known as cell cycle. Cell cycle is involved in the regulation of various biological events including cell growth and proliferations, organ development, DNA damage repair, and is also involved in many diseases including cancer. Cell cycle is mainly controlled by many regulatory proteins that direct cells through the sequential specific events and finally produce two new daughter cells. Cell cycle consists of two major consecutive events characterized by duplication of the genetic materials via DNA replication and evenly distributed the duplicated genetic material into the new progeny [37]. Generally cell cycle is divided into two stages: mitosis, i.e. the process of nuclear division and

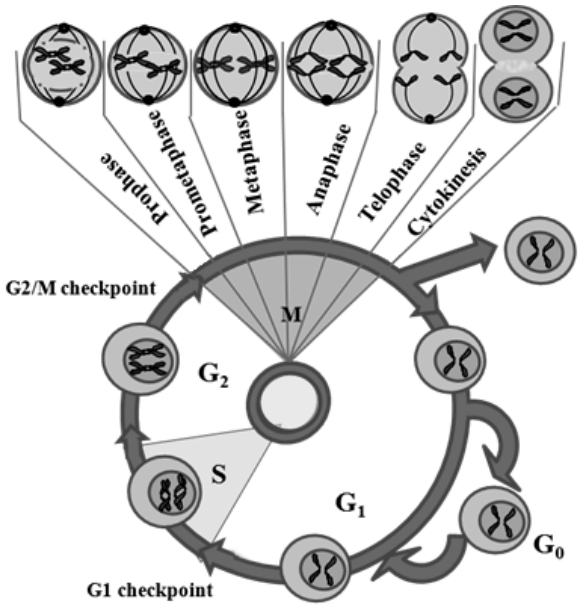

Figure 1.6: Schematic diagram of cell cycle. Cell cycle consists of two stages, interphase and mitosis. Interphase further divided into G_1, S and G_2 phase and mitosis again subdivided into following stages: prophase, prometaphase, metaphase, anaphase, telophase, and cytokinesis. End of each mitosis cells are reentering into the interphase and complete the cycle or exit the cycle and enter into quiescent state known as G_0 phase.

interphase which interlude between two mitosis cycles (Fig. 1.6). According to the cellular events mitosis i.e. M phase is subdivided into prophase, metaphase, anaphase and telophase and also includes the cytokinosis. In interphase, cells grow in size and prepare themselves for mitosis. Interphase is divided into three distinct parts, named as G_1, S and G_2 phases[38]. DNA replication, an important event that reproduces the genetic material in cell cycle, begins at a specific part of interphase known as S phase. S phase preceded through a gap called G_1 during which cells are preparing for DNA synthesis and is followed by a gap known as G_2 during this time cells prepare themselves for mitosis. Sometime cells exit the cell cycle and enter into a quiescent state known as G_0 phase[38]. In G_0 phase cells are either undergo through differentiation or reentered in the cell cycle and proliferate. The four phases, G_1, S, G_2 and M are traditional subdivisions of the standard cell cycle (Fig. 1.6).

1.1.4.2 Cell cycle regulation

Numerous molecular mechanisms are involved in the control of cell cycle events and ensure the appropriate cell division. Among them cyclin dependent mechanisms are the key regulators of the each cell cycle step which ensures the prefect cell division. Cyclins are the regulator of serine/threonine protein kinases family proteins named as cyclin-dependent kinases (CDK). CDK phosphorylates cell cycle specific selected proteins and controls their functions which lead to the cell cycle progression. Different types of cyclins and CDKs are activated during different stages of cell cycle and regulate progression of specific cell cycle phase. Different cyclin-CDK complexes are activated during specific stages of the cell cycle [39]. Simplified schematic representation of the cyclin-CDK complexes during different cell cycle stages is in the figure 1.7. Concentrations of the CDKs are not change throughout the cell

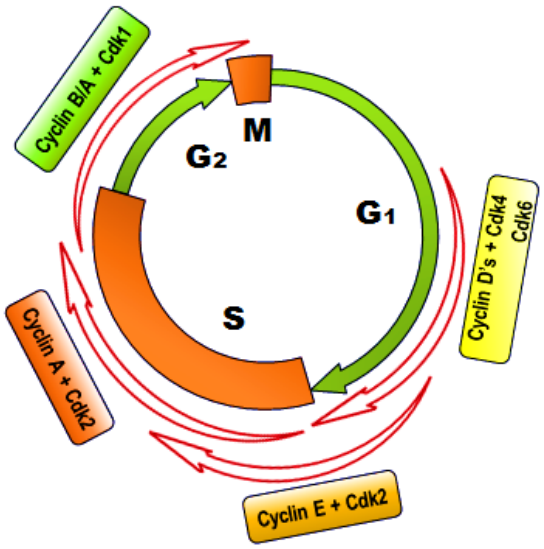

Figure 1.7: Different levels of cyclins and cyclin dependent kinase complexes at different stages of cell cycle. During early G1 CDK activities are very low but during mid G1 Cdk4 and Cdk6 activities are increased due to their increasing association with D-type cyclins (D1, D2, and D3). During G1/S transit activity of cyclin E-Cdk2 complex is increased and continues its activity with cyclin A-Cdk2 complex throughout S phase.G2 to M progression is drive by the sequential activities of cyclin A-Cdk1 and cyclin B-Cdk1 complexes [39] .

cycle but concentrations of the cyclins are specifically varied throughout the cell cycle. Concentration of cyclins finally served as the regulatory factors for the CDK activity. CDK activity also counteracted by numerous numbers of inhibitors known as CDK inhibitor (CKI) and unlike cyclins they also plays the regulatory role during cell cycle progression [40]. Malfunctioning of the cell cycle regulatory control causes cell cycle deregulation which directly associated with cancer.

1.1.4.3 Cell cycle checkpoints

Cell cycle checkpoints are the quality control system for perfect cell division in eukaryotic system. Checkpoints thoroughly examine the completion of each process at the entry point of each new phase. Throughout the cell cycle progression checkpoints are activated and act as a sensor system which recognized the DNA damage or other cellular irregularity. If any abnormality sensed by the checkpoints the cell cycle is immediately halted at that position. Cell used that delay time for the damage repair or errors correction. Farther unrepaired damage or non-rectified error triggers the different signaling pathways through the checkpoints that cause cell death or senescence and prevent the production of defected progeny which may produce cancer cells. Many checkpoints are activated throughout cell cycle progression. The major checkpoints are G_1 checkpoint, post-replicative checkpoint, G_2 checkpoint and metaphase checkpoint. Different types of checkpoint sense different types of cellular defects at different points of cell cycle and cause cell cycle arrest at that specific point. Sense of DNA damage or adverse growth condition during G_1 phase imposed cell cycle arrest at G_1/S transit through G_1 checkpoint (Fig. 1.8). Replication defects and DNA damage during S phase slow down S phase

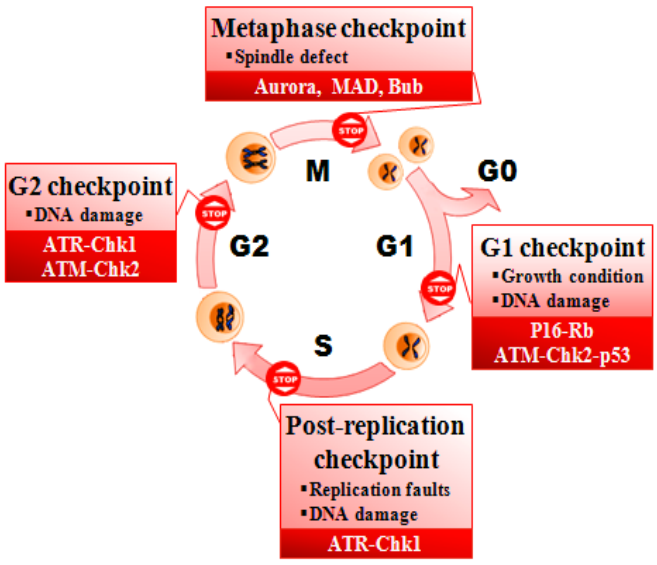

Figure 1.8: Schematic diagram of cell cycle checkpoints. Check points activity during different stage of cell cycle in response to different type of stress and damage. Stress and damage sensing and cell cycle arresting was conducted through different molecular pathways.

progression through post-replication checkpoint, while DNA damage during G_2 phase imposed cell cycle arrest at G_2/M transit by activating G_2 checkpoints (Fig. 1.8). Errors in the mitotic spindle assembly activate the metaphase checkpoints and prevent the mitotic exit (Fig. 1.8). Damage and stress sensing at different checkpoints and cell cycle arresting is conducted through different molecular mechanisms (Fig 1.8). All checkpoint mechanisms act through either p53 dependent or p53 independent pathways. DNA damage response triggers p53 dependent pathways and imposes cell cycle arrest at G_1 and G_2 phases and is also responsible for activation of apoptosis during excessive DNA damage [41]. P53 independent pathways are generally regulated through checkpoint kinases but activation of checkpoint kinases are directly regulated by protein kinases ATM and ATR. During G_1 phase unfavorable growth condition imposes cell cycle arrest through Rb pathway [42]. Mitotic checkpoint detects the defected spindle assembly by the kinetochore proteins such as Mad and Bub. Moreover, aurora kinase also plays an important role in this checkpoint activation [43]. Mutation in DNA damage check point pathways cause genomic instability and abnormal cell survival which lead the cells towards cancer phenotype formation [44, 45]. Knowledge of the cell cycle check points regulation provides better understanding of the cell cycle pathology in cancer and also helps to develop new therapeutic strategy.

1.1.4.4 Cell cycle and cell proliferation

Cell growth is regulated by the cell cycle. Proliferation rate of a cell population is related to cell division rate and growth fraction (number of cells participating in cell division cycle). Cell death rate suggests the dual control of cell cycle and apoptosis in cell proliferation. Therefore cell cycle regulators and checkpoints regulators can influence the cell proliferation. In mammalian cell cycle length of the S, G_2, and M phases are almost constant but length of the G_1 phase is highly variable [46]. The G_1 phase plays as a determining factor for cell proliferation. Entry from the G_1 phase into the S phase is directly regulated through G_1 checkpoint known as restriction point which acts as a rate limiting factor for the cell division rate. The G_1 checkpoint is controlled by Rb pathway [42, 47, 48] and a simplified schematic model of the Rb pathway is represented in the figure 1.9. Interference with the functions of Rb dependent growth regulatory pathway proteins such as p53, p16, and p21 caused cell cycle deregulation which leads to hyper-

proliferation or growth arrest [49-51]. Many other factors like transcription factor AP-1, transcription regulator c-MYC, signaling molecule integrin and ECM proteins are involved in the cell proliferation and regulate the cell cycle through Rb pathway dependent manner [52-55]. Reported evidences suggest that the change in the epigenetic regulator like DNA methylation has direct influence on the Rb pathway through its regulators and causes cell cycle deregulation [56-59]. Balance between proliferation and differentiation is regulated by Rb pathway through controlling chromatin organization, transcriptional and epigenetic regulations [60]. Mutation or amplification of the Rb pathway regulatory genes imbalances the normal regulatory control system and shortens the G_1 phase length which cause uncontrolled cellular growth and cancer [61-64]. Knowledge of the differential chromatin association topology of chromatin proteins is essential for detail understanding of the pathological control of this pathway in cancer.

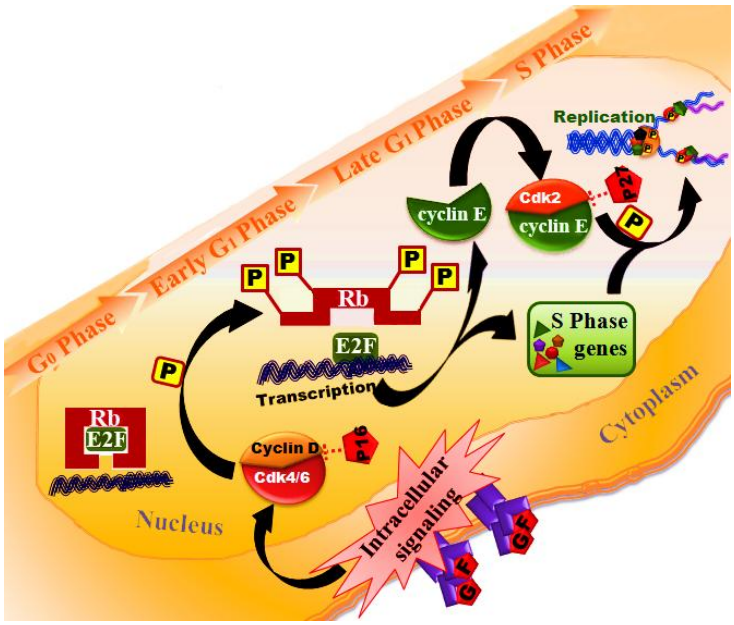

Figure 1.9: Simplified schematic model of Rb pathway mediated regulatory control of G_1 to S phase progression

1.1.5 Chromatin proteomics and hypoxia induced cancer progression

1.1.5.1 Tumor hypoxia and cancer progression

Cancer contributes second highest mortality rate among the non-communicable diseases (NCDs) in global death and 90% of cancer motility is caused by the metastasis [65]. Initially primary cancers are initiated with localized focus and easily eviscerate with proper prognosis but metastasized form of cancers are poorly prognosis and its spreading is unstoppable by radio- and chemotherapy [66, 67]. In the beginning cancer cells are rapidly proliferated and grow up to 1-2mm in size but after that tumor growth is arrested and cells go in to the quiescent forms. To

overcome the situation cancer cells evolve some biological processes including angiogenesis and metastasis [68, 69]. Due to the rapid proliferation cancer mass is expanded rapidly and suffer from insufficient blood supply in the growing regions. Cells within the blood supply limited regions suffering the harsh hostile environment including acidosis and very low or no supply of oxygen and nutrient [70, 71]. In normal tissue oxygen can diffuse up to 100-180μm surrounding of the blood vessel [72]. Tumor surface is full with blood vesicles but due to rapid expansion tumor core become unreachable for blood supply and become hypoxic. Cells in the abnormal physiological environment undergo through evolution and co-opt some defensive measurement for survival and growth maintenance such as 1) induction of angiogenesis to restore blood supplies, 2) shifting metabolic pathway into the glycolysis to compensate oxygen availability, 3) induction of self-sufficient proliferation signals, antigrowth signals resistance and unlimited replication capability to maintain cell growth, 4) induction of new mechanisms to escape from immune system and apoptosis induced cell death, and maintain cell survivability, and 5) induction of tissue invasion and metastasis to migrate into favorable environment and maintain cell survivability [73]. All adaptations co-opt during hypoxia interfere with the normal cell cycle regulation and may convert the normal cancer into immortal metastasized cancer phenotype. Figure 1.10 represents a simplified scheme of hypoxia induced cancer progression. Cancer hypoxia is one of the important and interesting physiological candidates for studying the cancer biology to understand the mechanism of the tumorigenesis.

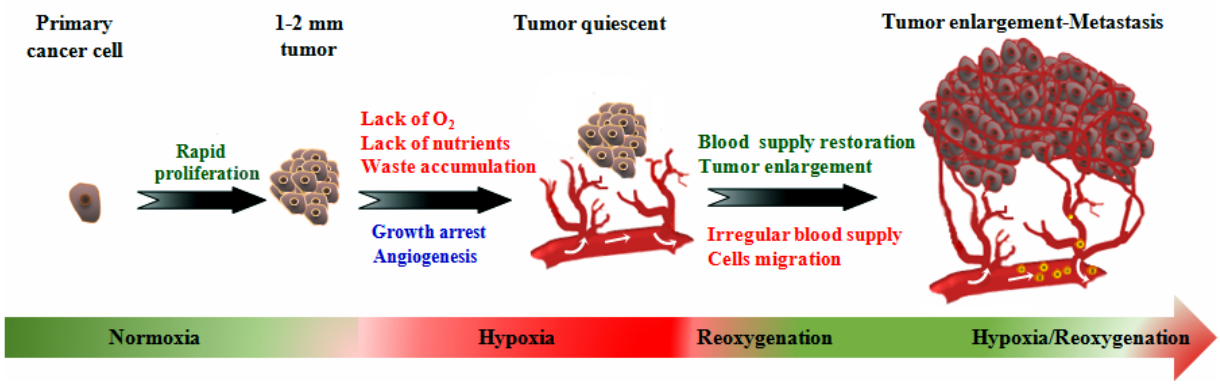

Figure 1.10: Schematic diagram of hypoxia induced cancer progression.

1.1.5.2 Hypoxia and radio and chemo-resistance

Observed clinical evidences and laboratory research indicate that hypoxia complicate the cancer treatment by producing resistance against radiotherapy and chemotherapeutic agents [74-76]. One of the mechanisms behind the radio-resistance is absence of oxygen which reduces oxygen inducing free radical generation leading to cell death [77]. Beside this oxygen factor several biological factors are involved in the radio resistance mechanism [78, 79]. In response to hypoxia immediate cellular response is activation of the transcription factor hypoxia inducible factor (HIF) which is the regulator of the hypoxia induced pathophysiological events including chemo- and radio-resistance [80, 81]. Another important mechanism behind radiation-resistance is alternation of DNA damage sensing and repair mechanisms [82, 83]. Recent experiments show that up-regulation of NHEJ pathway proteins during hypoxia reveal the contribution of DSBs repair in hypoxia inducing radio-resistance [84]. Hypoxia induced chemo-resistance is implemented through different mechanism such as efflux of the intracellular anticancer drugs through transporter protein cascade [80], HIFs induce gene transcription activation [76, 85, 86], cell-ECM interaction [87], and physical factors including abnormal vascular system which reduces drug delivery in the targeted area and contribute in the chemo-resistance [88]. All biological factors involve in radio- and chemo-resistance during hypoxia are directly or indirectly regulated through the chromatin dependent events. Therefore, information of hypoxia evolved chromatome will help us to understand the molecular mechanisms of the hypoxia induce radio- and chemo-resistance.

1.1.5.3 Hypoxia and cell migration and invasion

Cell migration and invasion is the hallmark of cancer metastasis [89]. Tumor invasion and metastasis is very complicated and complex cellular event. It is compose of several complex cellular process such as disintegration of the cell-cell association and translocation from local microenvironment, dissolution of surrounding ECM and translocation into the new microenvironment and continuation of the secondary cancer growth [73]. It is well established that hypoxia induced adaptations not only helps the cells to survive and grow in hypoxic microenvironment but also helps them to migrate into the distal territory through invasion and metastasis. Clinical evidences also suggest that hypoxia is one of the key regulators of invasive

cancer phenotype formation [90]. Cell migration is a very well organized event where cells are piloted by both internal and external stimuli. The mechanical and chemical stimuli are sensed by the different types of receptor including adhesion, chemokine and growth factor receptors that drive the migration process [91-93]. Crosstalk between different mechanical and chemical stimuli like ECM topography, ECM stiffness, external force and presser, autocrine, paracrine, and oxygen tension, regulate the effector factors of cell migration including matrix metalloproteinases (MMPs) secretion, matrix synthesis, growth factor receptors (GFR) and integrin expression [94]. Regulations of these factors during hypoxia are poorly understood and mechanism behind hypoxia induced cell migration and metastasis remains partially explored. Emerging evidences suggest like other hypoxia induced processes HIFs are also involved in the regulation of cell invasion and metastasis through activating several genes but along with HIFs many other transcription regulators also involved in this process [95]. Several epigenetic reorganizers like histone lysine-specific demethylase 4 (KDM4) and histone methyltransferase complex MLL1 play a key role in hypoxia induced cell invasion and migration [96-98]. Knowledge of hypoxia evolved chromatome will provide better understanding of the hypoxia induced cancer metastasis.

1.1.5.4 Hypoxia and cancer steam cell

According to the cancer stem cell hypothesis cancer stem cells (CSCs) are the key driving force behind tumorigenesis and initiation of metastasis. CSCs are characterized by their specific proprieties like self-renewal, differentiation, active telomerase expression, apoptosis resistance, membrane transporter amplification, migration and metastasis [99]. Still now the cancer stem cell biology is not well understood. There is a big question about the origin of the CSCs. Unlike normal stem cell, CSCs also have the self-renewal capability. Recent evidences suggest that self-renewal property of CSCs is regulated through several signaling pathway [100]. Recent evidences also indicate that signaling pathways such as Wnt/β-catenin signaling pathway [101, 102], Hedgehog signaling and Bmi-1 regulated pathway [103, 104], and p16 and Rb pathway [105] are involved in regulation of self-renewal property of the CSCs. Many signaling and regulatory molecules are used as CSCs marker for different types of cancer including CD44, CD133, CD15, or ABC transporter proteins [106]. According to the hypothesis, CSCs are responsible for therapeutics resistance. Recent evidences suggest that the resistance is developed

through several adoptive mechanism co-opt by the CSCs such as alternation of cell cycle kinetics, DNA replication and repair mechanism and cellular transport mechanism and adaptation of unlimited replication capability, and apoptosis resistance [99]. So CSCs are the prime targets for the new therapeutic development for cancer treatment. Available information suggest that hypoxia play an important role in induction and regulation of CSCs [107]. Mechanisms by which hypoxia induces the stemness remain unknown. Emerging evidences reflect involvement of HIFs in regulation of the stemness rather than other factors. Recent evidences demonstrate the regulatory control of HIFs upon notch dependent stem cell pathway through activation of Notch-1 which prevent the cell differentiation and produce the dedifferentiated CSCs phenotype [108, 109]. Unlike Notch-1, HIFs also regulate Oct-4 and c-Myc activation that regulate self-renewal property and proliferation of CSCs [110, 111]. HIFs also activate the genes responsible for cell migration and invasion including VEGFs, LOX, MMPs and CXCR4 in CSCs which ultimately contribute to the metastasis [112-115]. HIFs also responsible for chemo-resistance of the CSCs through activation of ABC transporter genes and reduce intercellular drug accumulation and activate antiapoptotic proteins like Bcl2 to suppress the drug induced apoptosis [116]. Taking all HIFs directed regulatory mechanisms together we represent a schematic diagram in figure 1.11, to demonstrate the effect of HIFs upon CSCs transformation. Beside this, HIFs control many other factors which directly involve in the CSCs transformation during hypoxia but molecular mechanisms behind these events are still ill-defined. Therefore knowledge on hypoxia induced alteration of chromatome might provide valuable information to reveal new regulatory pathways and also help us to develop new therapeutic strategy to target the CSCs.

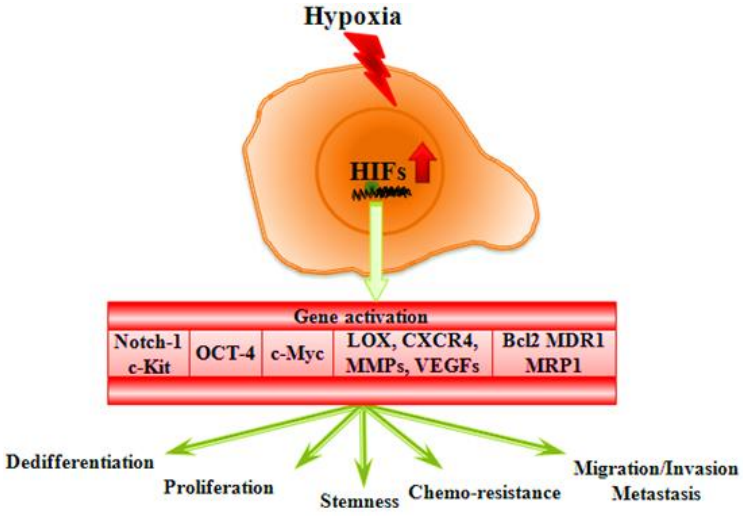

Figure 1.11: Schematic diagram represent the HIFs regulated mechanism of CSCs transformation.

1.1.6 Objectives and the overview of the thesis

Basic genetic events including transcription, replication, and repair are dependent upon DNA accessibility and chromatin integrity. Chromatin integrity is regulated by chromatin-associated proteome which modulate DNA-protein and protein-protein interactions. The chromatin-associated proteome is a dynamic system which changes in response to internal and external stimuli such as internal signal for cell cycle progression and external hypoxia in cancer development. Therefore, knowledge of the chromatome dynamics can provide a better understanding of chromatin biology in developmental stage and disease progression. Cell cycle is a basic cellular event which maintains the existence of the living organism and deregulation of the cell cycle can lead to cancer like disease. All the basic DNA dependent events take place during the cell cycle progression and chromatin maintains its dynamic structural integrity throughout cell cycle progression to perform all genomic and epigenomic events perfectly. Dynamics of chromatin biology during cell cycle progression and its relationship with pathophysiological evolutions including cancer progression are poorly understood. Better understanding of chromatome dynamic changes in both cell cycle and cancer progression would provide novel insight to decipher cancer pathophysiology and progression. Proteomic studies of the chromatome changes in cell cycle and hypoxia-induced cancer progression are still lacking. The objective of my PhD work is to establish a suitable proteomic method to study the chromatin associated proteome and their chromatin association topology on a global basis and then apply this approach to study the chromatome dynamics during cell cycle progression and hypoxia induced tumorigenesis to understand the regulatory control of chromatin biology in cancer pathophysiology.

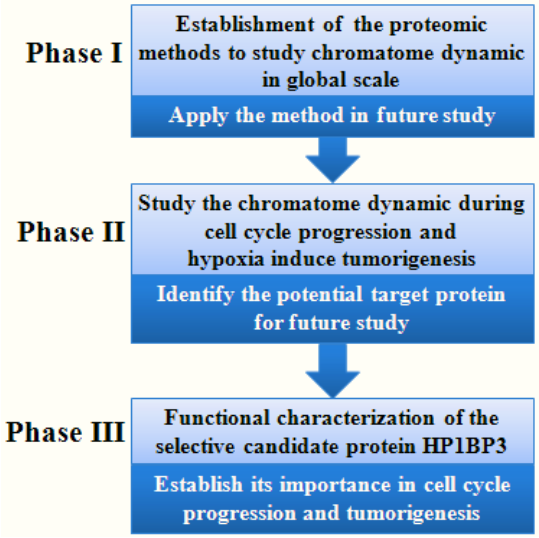

Figure1.12: Schematic work flow of my PhD works

To achieve these objectives my PhD work is divided into three phases as described in the figure 1.12. In the phase I suitable proteomic methods were developed to study the chromatome and their chromatin association topology in a global basis. In this study partial

nuclease digestion based protein extraction approach was adopted for extraction of the euchromatin and heterochromatin associated proteins so that we can study their association topology. In order to achieve this, chromatins were extracted from rat liver tissue and purified by using density gradient based isolation technique. Purified chromatins were partially digested by MNase and DNase I in a time-course basis and differential released proteins were identified and quantified by LC-MS/MS based proteomic approach. Immunofluorescence microscopy approach is also used to study the localization of selective target proteins to confirm the proteomic results. In phase II nuclease digestion coupled with LC-MS/MS based quantitative proteomic strategy was applied to study the chromatome dynamics during interphase progression and hypoxia induced tumorigenesis. To achieve this goal chromatins from different cell cycle phase synchronized cells and from different hypoxia conditioned cells were extracted followed by digestion with MNase and DNase I respectively to extract the euchromatin and heterochromatin associated proteins. iTRAQ based quantitative proteomic approach was used for identification and quantification of the chromatome. Through bioinformatics analysis of the chromatome data sets, one common potential target protein was identified, which showed its dynamic chromatin association both during cell cycle progression and hypoxia induced tumorigenesis. In phase III, functional characterization of the target protein candidate identified from phase II study was performed at molecular and cellular levels. shRNA based knockdown approach was adopted for generating the candidate protein knockdown cell lines that were studied for its functional role in cell cycle progression and tumorigenesis.

Chapter 2

2 Developing quantitative proteomics approach to elucidate the chromatin protein binding topology in the chromatome

Chapter 2

2.1 Summary

Chromatin is a very well organized DNA-protein complex located inside the nucleus and regulates all genomic events including genome transcription, duplication, and packaging and also involve in maintenance of genome stability. Many factors like histone PTMs, DNA methylation and non-histone-chromatin interaction, directly regulate the chromatin structure but a complete picture of chromatin structural dynamics is poorly understood due to lack of information regarding chromatome and their chromatin binding topology. In this study we temporally released the chromatin associated proteins in the relatively open euchromatin regions in the chromatome by MNase and DNase I partial digestion. The released soluble euchromatin binding proteins and the tightly bound heterochromatin proteins in the pellets were quantitatively profiled through emPAI based label-free quantitative approach. This study identified 694 proteins with high confidence and 160 of them are known to be chromatin associated protein. They were functionally classified into the following categories such as histones, non-histones involved in architectural maintenance, proteins involved in DNA replication and repair, transcription machinery, transcription regulation, other chromatin proteins, cell cycle proteins and several novel proteins. A number of the identified proteins were presumed to be novel chromatin associated proteins and their chromatin interaction topologies were characterized for the first time. The result demonstrated that our newly developed proteomic method is capable of comprehensively determining the differential chromatin binding topology of the chromatome and in the elucidation of the dynamics of chromatin biology.

2.2 Introduction

Entire genome is packed inside the chromatin in the form of a DNA-protein complex which regulates all DNA dependent basic genomic and epigenomic events for centrally control all cellular processes. Besides controlling normal cellular events, chromatin deregulation is involved in the pathobiology of cancer and many other diseases [117, 118]. Basic chromatin structure is composed of the array of nucleosomes, composed a histone octamer unit of histone H2A, H2B, H3, and H4 wrapped by 146 bp DNA. Chromatin structure is directly regulated through protein-DNA and protein-protein interactions [1]. Through DNA-protein and protein-protein interaction chromatins are further folded and existed in higher order structural forms.

During interphase, chromatins existed in two different types of higher order structural form, loosely packed transcriptionally active euchromatin and heavily compacted transcriptionally inactive heterochromatin. Biological functions of chromatin are regulated through its higher order structure by controlling the accessibility of DNA template. Many biological factors like PTMs of histones and non-histones, DNA modification and other epigenetic factors are regulated by both protein-protein and DNA-protein interactions, which ultimately regulate chromatin structure and functions [119, 120]. Altered chromatin biology is directly linked with the epigenetic related disorders including Williams-Beuren syndrome, ATRX syndrome, SIOD [121-124]. Knowledge of chromatin associated proteins and their binding topology would provide the better understanding of the molecular mechanisms of those disorders.

Despite of its importance in biology and disease, chromatin proteome is not extensively studied. The First ICAT based quantitative proteomic study of chromatome of human B lymphocyte was performed in 2003 by Shiio *et al.* [125]. Recently study of mitotic-chromatin proteome was performed through mass spectrometric (MS) based proteomic approach by several researchers like Gassmann *et al.* [126] and Uchiyama *et al.* [127]. Chu *et al.* identify and characterized the *C. elegan's* meiotic chromatin associated proteins and established their importance in fertilization [128]. Recently, reported study of mouse chromatome during cardiac disorder reveals the chromatin reorganization principal during pathophysiological condition [129]. Despite these reports of chromatin associated proteomic studies, global chromatin binding topology of the chromatome and its dynamic changes in response to internal signal such as cell cycle progression and external stress such as hypoxia tumor microenvironment are still unavailable which limited our understanding of its function in normal biology and disease initiation and progression.

Recent advance in the field of proteomics studies provided the better understanding in protein-protein interactions and PTMs. Current evidences showed the impact of histone PTMs like acetylation, methylation and phosphorylation in genomic events including transcription regulation and chromatin organization [9, 10, 130, 131] and also in cellular events like cell cycle regulation [132, 133]. Reported evidences established the importance of non-histone Polycomb Group proteins (PcG) in chromatin organization and chromatin folding. During continuation of DNA dependent genomic events, chromatin need to maintain the DNA template accessibility and

it was achieved through dynamic changes of higher order chromatin structure, which is regulated by the chromatin associated proteins. It is well established fact that chromatin structure is regulated through DNA-histone and histone-histone interactions [1] and recent evidence showed that non-histone proteins are also involved in chromatin structural regulation. Du *et al.* studied the interacting proteome of histone H2A.X variant during ionization radiation induced DSBs through FLAG-tagged based pull-down approach [134]. Reported evidences suggested that combination of immunopurification and MS based high throughput proteomic approaches were used for studying the protein-protein interaction in different biological systems including yeast and human cells [135-138]. Advances in MS based proteomic technologies provided the further advancement in proteomic fields in terms of throughput, sensitivity and increase the protein identification and quantification efficiency but establishment of protein-protein interaction of chromatome remains challenging. Shechter *et al.* established histones and non-histone proteins extraction from chromatin by using acid extaraction and salt extraction techiniques which are based upon the principal of differential protein solubility [139]. A relatively new technique termed "mChIP" (modified chromatin immunopurification) was used by several researchers to study the chromatin associated proteome [138].

Non-specific endonuclease MNase and DNase I are commonly used nucleases in DNA digestion studies. Both of them cut the chromatin at the linker regions while DNase I have the specificity for the GC enrich sites of the promoter and transcription start regions of active euchromatin regions [24-26]. Evidences suggested that the DNA-protein interaction take place inside the DNase I hypersensitive sites of the several active genes [140-142], while MNase does not exhibit such specific characteristic which can differentiate active and inactive sites. Loosely packed euchromatin regions are easily distinguished from the highly condensed heterochromatin regions by increasing the nuclease susceptibility. Both MNase and DNase I are commonly used for differentiating active and inactive chromatin territories [140-142]. Therefore, in this study we used both MNase and DNase I for chromatin digestion experiments to probe the chromatin binding topology of chromatome.

Here we adopted nuclease digestion based protein extraction approach to extract proteins form chromatin. Nuclease digestion based approach was not only useful for identification of the chromatin-associated proteome but also very helpful for revealing their chromatin binding

topology. Therefore, the main objective of our study is to reveal the global picture of the chromatome and their chromatin binding topology using the differential protein release from chromatin by MNase and DNase I coupled with LC-MS/MS-based quantitative proteomic approach. In this study we extract and purify the chromatin from rat liver using density gradient based isolation technique and the purified chromatins are partially digested by MNase and DNase I in a time-course basis to reveal the chromatin binding topology. We also applied immunofluorescence microscopy technique to study the localization of some chromatin associated proteins.

2.3 Materials and methods

2.3.1 Reagents

Unless indicated, all reagents used in this study were purchased from Sigma-Aldrich, USA. Mouse monoclonal fibrillarin antibody (ab18380), mouse monoclonal nucleolin antibody (ab13541), mouse monoclonal prohibitin antibody (ab1836), and mouse polyclonal nucleostemin antibody (ab88882) were purchased from Abcam, UK.

2.3.2 Experimental design

All animal experimentations were performed according to the protocols approved by Nanyang Technological University for Biological Studies and Animal Care and Use Committees. Sprague Dawley rats (*Rattus norvegicus*) were purchased from Centre for Animal Care, National University of Singapore, Singapore. At the age of 8 weeks, three rats were euthanized with excess isoflurane anesthesia and subsequently perfused with ice cold PBS in the transcardial fashion. Intact livers were collected, snap-frozen in liquid nitrogen and then stored at –80^{o}C.

2.3.3 Chromatin isolation from rat liver and nuclease treatment

The chromatins were isolated from rat liver according to the following method. Rat liver tissue was minced and suspended into buffer A (10mM HEPES of pH 7.5, 10mM KCl, 1.5mM $MgCl_2$, 0.34M sucrose, 0.1% triton X-100 supplemented with 1mM DTT and protease inhibitor cocktail (Roche Diagnostics, Mannheim, Germany)).Tissue suspension was transferred into the dounce homogenizer and homogenized the tissue with 30 stocks by pestle A. The homogenate

was centrifuged at 2000×g for 3min at 4°C and removed the supernatant. The pellet was re-suspended in to buffer A and re-homogenized with pestle B. Homogenate was pass through 70µm cell strainer (BD Biosciences, USA) to remove tissue debris. Then the filtered homogenate was ultracentrifuged (Beckman Coulter, USA) at 150,000×g for 3h at 4°C, using 2.1M sucrose Cushion (10mM HEPES, pH 7.5, 10mM KCl, 1.5mM $MgCl_2$, 2.1M sucrose supplemented with 1mM DTT and protease inhibitor cocktail). Chromatin pellet was found in the bottom of the tube and other tissue debris was in the top of the cushion. The chromatin pellet was collected and washed once with buffer A and twice with washing buffer (10mM HEPES, pH 7.5 supplemented with 1mM DTT and protease inhibitor cocktail). The chromatin pellet was collected by centrifugation at 20,000×g for 45min at 4°C during every steps of washing.

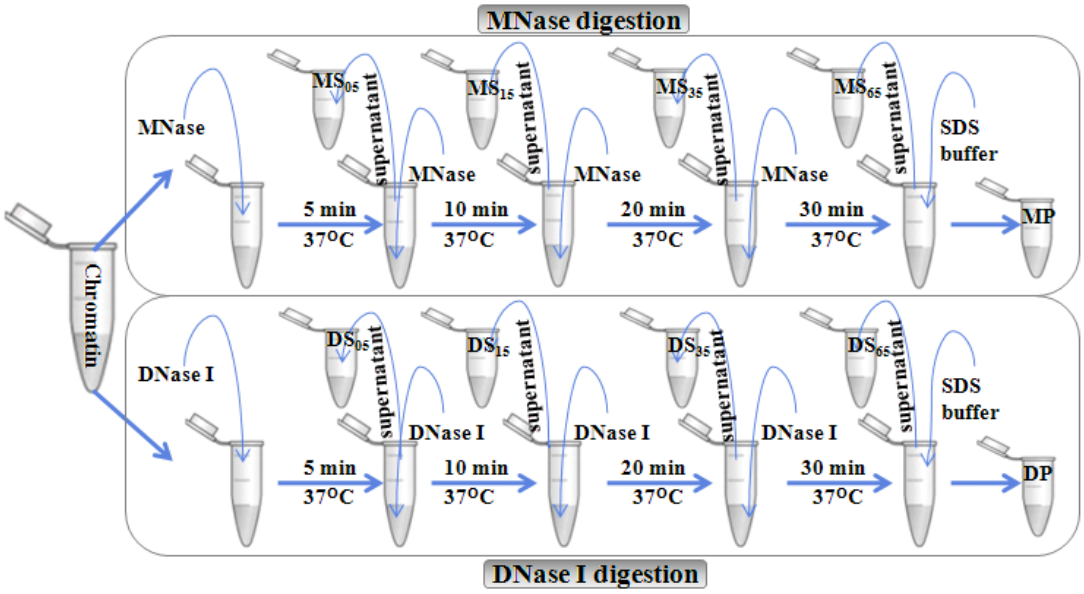

Figure 2.1: Schematic representation of partial nuclease digestion of chromatin. Chromatin extracted from rat liver and digested with 5U of nuclease each time

The purified chromatin pellet was suspended in MNase digestion buffer (10mM HEPES (pH 7.5), 2.5mM $CaCl_2$, 2.5mM $MgCl_2$) and digested with 5U of MNase for 5min at 37°C. Immediately after digestion, supernatant fraction (labeled as M05) was collected by centrifugation at 20,000×g for 10min at 4°C. The remaining pellet fraction was resuspended in digestion buffer and re-digested with another 5U of MNase for another 10min (total 15min) and respective supernatant fraction (labeled as M15) was collected by centrifugation. Similarly, supernatant fractions were collected after digestion for 20min (M35) and 30min (M65). After a

total of 65min of enzyme treatment, the remaining pellet was dissolved in 2% SDS solution, centrifuged and the pellet fraction (labeled as Mp) was used for further experiments. The DNase I digestion was performed in DNase I digestion buffer (10mM tris HCl; pH 7.4, 0.5mM $CaCl_2$, 2.5mM $MgCl_2$) and respective supernatant fractions were labeled as D05, D15, D35, D65 and the pellet fraction Dp as described in MNase digestion methodology. All supernatant fractions collected after nuclease digestions were used directly for further experiment. The entire amount of supernatant and pellet fractions obtained by each digestion step, were used for the proteomic study. The work flow of the whole nuclease digestion procedure is represented in the figure 2.1. The experiments were performed in biological triplicate and the mean of emPAI values with standard deviation were reported.

2.3.4 One dimensional gel electrophoresis and in-gel digestion

The entire amount of supernatant and pellet fractions obtained from partial MNase and DNase I digestion, were separated by 10% acrylamide gel at 100V for 90min. The gels were stained with 0.2% coomassie brilliant blue solution in 40% methanol and 10% acetic acid solution for 45min to visualize the protein bands. After overnight destaining, each sample lane was cut separately into five parts. The gel fractions were then cut into $1mm^2$ small pieces and alternatively washed with 100mM ammonium bicarbonate buffer and 50% acetonitrile (ACN) containing 100mM ammonium bicarbonate buffer to remove the salts and small molecule impurity. The washed gel pieces were dehydrated with 100% ACN and air dried for 15min to complete evaporation of ACN. Sufficient amount of 10mM DTT in ammonium bicarbonate buffer was added into the dried gel pieces and reduced for 30min at 60ºC that followed by alkylation with 55mM iodoacetamide at room temperature for 45min. Gel pieces were alternatively washed with 100mM ammonium bicarbonate buffer and 50% ACN containing 100mM ammonium bicarbonate buffer to remove the DTT and iodoacetamide. Gel pieces were dehydrated with 100% ACN and air dried. Add sufficient amount of digestion solution (10ng/µl sequencing grade modified trypsin (Promega, Madison, WI) in 50mM ammonium bicarbonate solution) and stand for 60min at 4^oC. Carefully removed all excess trypsin solution and add 100µl of 50mM ammonium bicarbonate solution. The digestion was performed at 37^oC for overnight period. Tryptic peptides were extracted with 50% ACN and 5% acetic acid and dried

with vacuum centrifuge (Thermo Electron, Waltham, MA, USA) for subsequent mass spectrometer analysis.

2.3.5 LC-MS/MS analysis

Tryptic peptides were redissolved in 0.1% formic acid and analyzed by LC-MS/MS. LTQ-FT-ultra mass spectrometer (Thermo Electron) coupled with a prominence^{TM} HPLC unit (Shimadzu) was used for this purpose. For each analysis, 100µl of the samples was injected from auto-sampler (Shimadzu) and concentrated in a Zorbax peptide trap (Agilent, Palo Alto, CA, USA). Capillary column (200µm ID×10cm) packed with C18 AQ (5µm particles, 300Å pore size, Michrom BioResources, Auburn, CA, USA) was used for peptide separation. Mobile phase A (0.1% formic acid in H_2O) and mobile phase B (0.1% formic acid in ACN) were used to establish the gradient. A 90min gradient comprised of 3min of 0-5% B; 52min of 5-25% B; followed by 12min of 25-60% B; maintained at 80% B for 8min; finally re-equilibrated at 5% B for 8min, was use for appropriate separation of tryptic peptides. The HPLC was operated at a constant flow rate of 30µl/min and ~500nl/min flow rate at the electrospray tip (Michrom BioResources) during nanospray was archived by used of a splitter. The samples were ionized and injected into MS through an ADVANCE™ CaptiveSpray™ Source (Michrom BioResources). Electrospray ionization technique was used to ionize the peptides and for ionization set the electrospray potential at 1.5kV. The other vital parameters were set at their optimum values to get the best data. Parameter like the gas flow was set at 2, ion transfer tube temperature at 180°C and collision gas pressure was at 0.85mTorr. Positive ion mode was set for data acquisition. Inside the FT-ICR cell a full MS scan was acquired from m/z range 350 to 2000 at a resolution of 10^5 within maximum 1000msec ion accumulation time period. Precursor ion charge state screening was activated and set AGC target value at1e+06 for FT. Ion fragmentation was perform by collision-induced dissociation (CID) technique. The linear ion trap was used for collection of peptides mother ions and also used for measurement of fragment ions. Default AGC setting was used (full MS target at 3.0e+04, MSn 1e+04) in linear ion trap. For CID fragmentation (MS2) only top 10 intense ions which have threshold counts above 500 were selected and this process was performed concurrently with a maximum ion accumulation time of 200msec. After each MS2 scan a MS3 scan was perform for detecting the neutral losses of 98Da for 1+, 49Da for 2+ or 32.7Da for 3+ ions. For this process dynamic exclusion was activated

with a repeat count of 1, exclusion duration of 20sec and ±5ppm mass tolerance. The CID parameters activation Q 0.25; isolation width (m/z) 2.0; activation time 30ms; and normalized collision energy 35% were set to perform optimum CID.

2.3.6 Database searching

Mascot (version 2.2.06, Matrix Science, Boston, MA, USA) search engine was used for all MS and MS/MS data searching. The UniProt Knowledgebase (UniProtKB) rat protein database (33344 sequences) combined with its reversed complements was used for the searches. At first the raw data files were converted into mascot generic file (mgf) format using an in-house program and those mgf files were used for mascot search [143]. For data search, the following parameters were set to get high quality data set. Enzyme limits were set at full tryptic cleavage at both ends and consider maximum of two missed cleavages. Set peptide precursor's ions mass tolerances 10ppm and fragment ions mass tolerance 0.8Da. The # 13C value was set at 2. In protein modification parameter we Set carboxamidomethylation (+57.02) at cysteine residues as fixed modification while oxidation (+15.99) at methionine, phosphorylation at serine, threonine or tyrosine (+79.96) as variable modification. Search data was extraction in mascot.dat file format using parameter seating of significance threshold $p<0.05$ and "Ignore Ions Score Below" parameter 20. However, the selection of proteins for further analysis was based on target-decoy search strategy with cutoff set to ≤ 1% FDR.

2.3.7 Data analysis

We used emPAI-based label free quantification approach for comparison of different conditions. emPAI values were calculated according to the stated Eq 1 to 3 [36]. The N_{obsd} and N_{obsbl} were denoted as the number of observed and observable tryptic peptides per protein respectively. All emPAI values were calculated by Mascot during search. During emPAI value calculation mascot uses only those peptides which were identified with score at or above homology or identity thresholds. After completion of mascot search all peptide/protein lists were exported to csv file format and further processed using in-house scripts for detail analysis.

$$PAI = \frac{N_{obsd}}{N_{obsbl}} \qquad \text{(Eq. 1)}$$

$$emPAI = 10^{PAI} - 1 \qquad \text{(Eq. 2)}$$

$$Normalize\ emPAI_i = \frac{emPAI_i}{\sum_{i=1}^{5} emPAI_i} \qquad \text{(Eq.3)}$$

The physical and chemical properties of enlisted proteins, including molecular weight and isoelectric point were calculated using online Compute pI/Mw tool (http://web.expasy.org/compute_pi) in ExPASy (SIB Bioinformatics Resource Portal) web server. We used Protein knowledgebase (UniProtKB), GeneCards® (Version 3) and Entrez Gene database for classification and functional annotation of enlisted proteins. The temporal release at different time point was calculating by normalization of the emPAI value of each protein in each of the five fractions. The normalization was performed by dividing the emPAI value of each fraction with sum of the five respective fractions of each individual protein as stated in the Eq 3. We clustered the proteins according to their release patterns by using online Gene Pattern software (http://genepattern.broadinstitute.org). We applied Hierarchical clustering and Pearson correlation methods to perform clustering.

2.3.8 HEPG2 Cell culture

Cells were grown in DMEM (Dulbecco's Modified Eagle Medium) with high glucose (4500mg/l) and L-alanyl-L-glutamine (862mg/l), supplemented with 1% Pen-Strep (10000µg/ml streptomycin and 10000U/ml penicillin), and 10% FBS (fetal bovine serum) and incubated in 5% CO_2 containing humidified incubator at 37°C for their optimal growth.

2.3.9 Immunofluorescence analysis

1×10^6 cells were seeded on $20\times20mm^2$ cover slips inside the 6 wells plate and grown until 50% visual confluence. The 50% confluent cells were washed thrice with PBS and fixed by 4% paraformaldehyde treatment for 20min at room temperature (RT). PBS washing was performed twice to remove paraformaldehyde and permeabilized the cells by kept the cells into 0.2% triton X-100 in PBS for 5min at RT. Again cells were washed twice with PBS to remove triton X-100. Nonspecific antibody binding sites were blocked by treating the cells with 4% BSA in TBST (tris-buffered saline containing 0.1% twenn-20) for 1h at RT. For particular protein staining cells were incubated with corresponding primary antibody at 4^oC for overnight. Excess

and nonspecifically bound antibodies were removed by TBST washing. Cells were then incubated with Alex 488-conjugated IgG secondary antibody (1:400) (Invitrogen) for 1h at RT. Again TBST washing was performed to remove excess and nonspecifically bound antibodies. Then cells containing cover slips were air dried for 2h at RT inside dark cabinet. Finally cover slips were mounted on glass slides with Vectashield mounting medium with DAPI (1.5µg/ml) (Vector Laboratories, Burlingame, California, USA). All immunostained samples were examined by Axio Observer.D1 microscope (Zeiss) equipped with 63X/1.25 NA Plan-Neofluar objective (Zeiss). Image J software was used to process and analyze the data.

2.4 Results and discussion

2.4.1 LC-MS/MS based chromatin associated protein profile

To understand the actual mechanism behind DNA packaging into very limited place like nucleus, without compromising with its biological activity, it was necessary to understand the global map of the chromatin associated proteins and their differential chromatin association. It was a well-known fact that interaction between DNA and histones change the accessibility of template DNA for other active molecules [145]. Besides histones, a vast number of proteins interact with chromatin and regulate its structural and functional activities. All DNA dependent biological activities like transcription, replication, DNA repair and epigenetic regulation are principally dependent upon higher order chromatin structure that is dynamically controlled by many chromatin interacting proteins through DNA-protein and protein-protein interaction. Lack of information about the chromatin association topology of chromatin interacting proteins in a global scale, was making it difficult to understand their contribution in the chromatin biology.

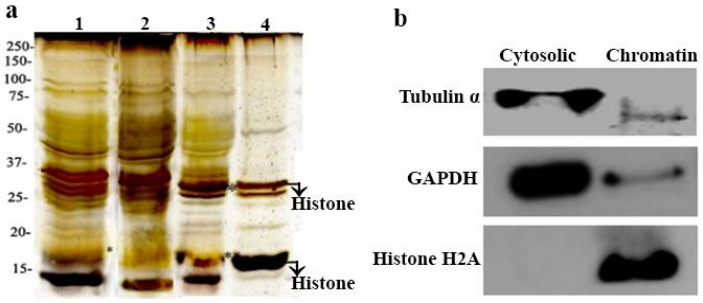

Figure 2.2: Quality control of chromatin enrich fraction. a: Gel picture of different tissue fractions. Samples were resolved through 10% gel and stained with Silver Stain. Lane 1: Whole rat liver homogenate; Lane 2: crude cytosolic fraction; Lane 3: Nuclear enrich fraction; Lane 4: Chromatin enrich fraction. b: Western blot analysis of cytosolic and chromatin fractions [144].

Here we applied partial nuclease digestion with LC-MS/MS based proteomic approaches for the protein identification and reveal their differential chromatin association topology. In this study we isolated chromatins from rat liver and digested them with different nucleases for 65min time period and solubilized supernatant fractions and the undigested pellet fractions were collected and analyzed through LC-MS/MS. Our western blot result showed the purity of our chromatin enriched fraction (Fig. 2.2b) and silver stained gel picture also showed the enrichment of histones in the chromatin fraction (Fig. 2.2a). Our western blot analysis shown tubulin and GAPDH were present in low abundance in the chromatin fraction but chromatin marker histone H2A was present in high abundance thus suggesting higher enrichment of chromatin in the purified fraction (Fig. 2.2b). Gel pictures showed the differential histone distribution among nuclease digested supernatant and pellet fractions (Fig. 2.3a-b).

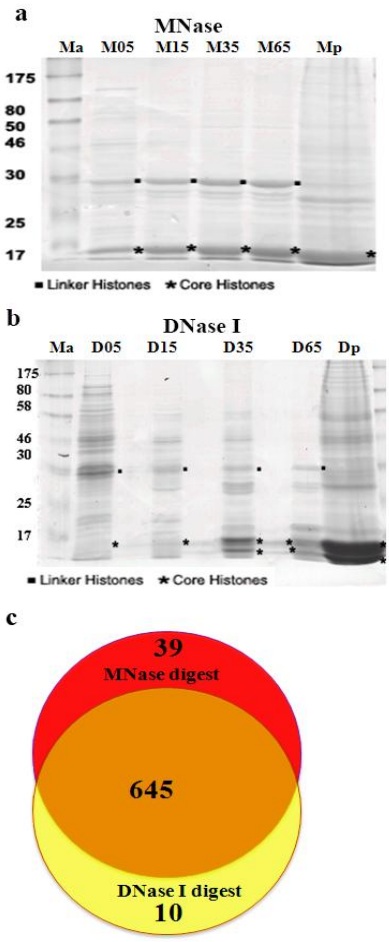

Figure 2.3: MNase and DNase I digested chromatin fractions. a-b, Coomassie stained gels of MNase and DNase I digested supernatant and pellet fractions respectively. c, Overlap diagram of proteins identified in the MNase and DNase I digested chromatin fractions [144].

694 high confident proteins with FDR value of ≤ 1% were identified in our present LC-MS/MS based proteomic study. Further analysis of the data showed among the total 694 identified proteins 10 and 39 proteins were unique in DNase I and MNase digested samples accordingly and 645 proteins were common in both two digestion experiments (Fig. 2.3c). Distribution of identified 694 proteins according to their physical and chemical properties showed comparable distribution pattern with the whole rat proteome enlisted in the UniProtKB database (Fig.2.4a-b) indicating the unbiasedness of our techniques used in this study. Classification of the identified proteins was performed according to their subcellular localization and we found that 58.8% of identified protein have nuclear localization, 35.6% protein do not have nuclear localization and the subcellular localization of 5.6% of the proteins is still unknown (Fig. 2.5a).

Identified nuclear proteins were further classified according to their biological and functional characteristics and 39% of them were found to be chromatin associated proteins, and 26% were involved in RNA processing. The rest of them were localized in nucleus (22%) and ribosome (13%) and involve in many biological events (Fig. 2.5b). The complete purification of any isolated organelle from any tissue sample was very challenging particularly when identification was performed by any unbiased technique like mass spectrometry. In spite of this challenge our western results showed that enrichment of histone H2A in our chromatin fractions, and relatively few cytosolic contaminants (Fig. 2.2b) indicate the high level of chromatin enrichment in the purified fraction.

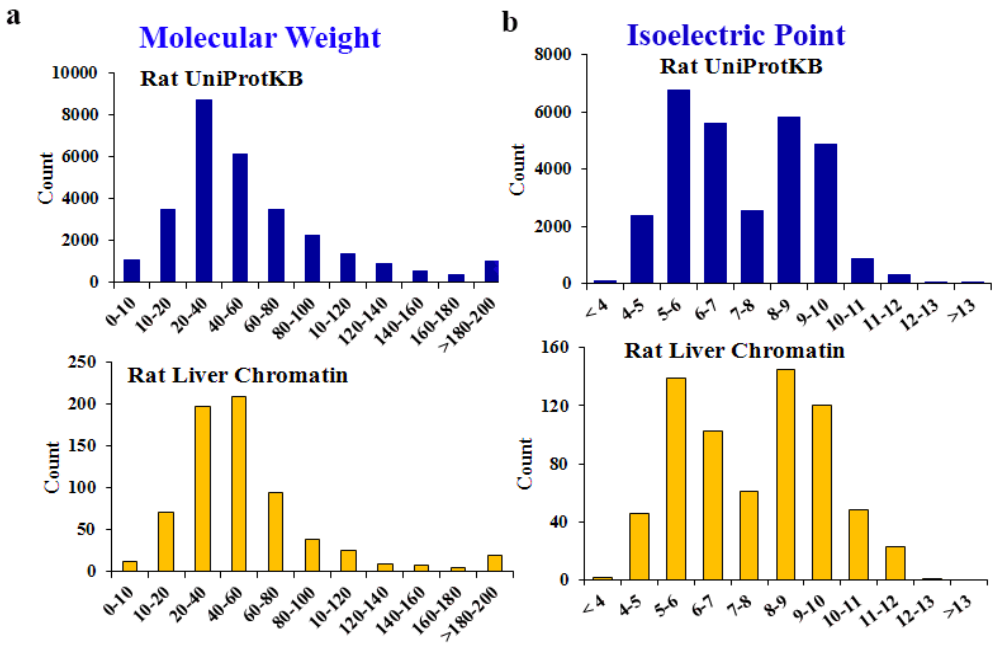

Figure 2.4: Protein distribution according to the physicochemical characteristics. a: Distribution of molecular weight within whole rat proteome and our data set. b: Distribution of isoelectric points within distribution whole rat proteome and our data set [144].

The main objective of our study was to understand the chromatin structure specific association of chromatin interacting proteins as such we used only the known chromatin interacting protein for further analysis. To achieve this goal we shortlisted the proteins on the basis of their chromatin interaction property maintained in the gene ontology (GO) annotations. After applying this specification we filter out the other proteins [128, 138] and enlisted only 160 known chromatin associated proteins for final analysis. The shortlisted data showed that only 16 proteins were unique in the MNase treated samples thus indicates that MNase has the property of

releasing the proteins differentially from different regions of chromatin. Short listed proteins were finally classified according to their biological functions and classification of the proteins revealed that 7% of them were histones, the core component of chromatin and 21% proteins were directly involved in the maintenance of higher order chromatin structure and chromatin remodeling, while other were involved in other DNA dependent biological process like transcription (19%), replication (7%), DNA damage repair (7%), cell cycle regulation (6%) and miscellaneous biological process (28%) (Fig.2.5c). We calculated the percentage of protein release on the basis of total amount of protein solubilized in all five supernatant fractions after DNase I or MNase treatment and we drew the comparison between the protein release pattern upon DNase I and MNase digestion (Fig. 2.7a-d and 2.10a-d). We also did the temporal profiling of protein release pattern during different time of nuclease treatment and on the basis of the temporal release profiles, we categorized different protein clusters as shown in the heat map (Fig. 2.6 and 2.9)

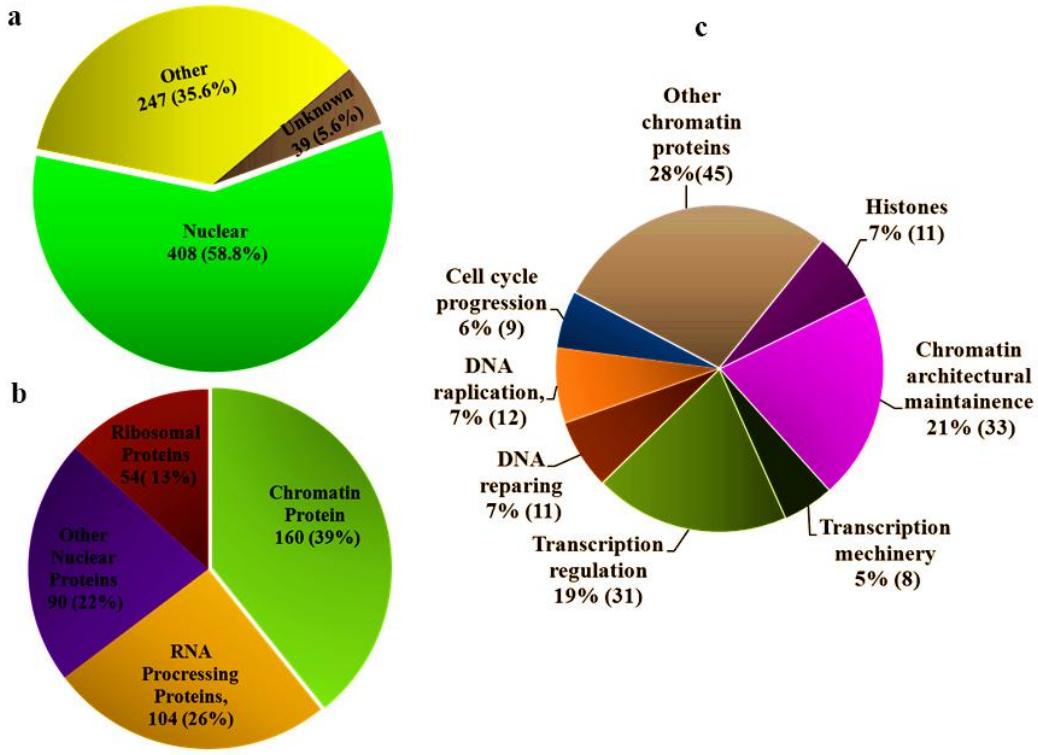

Figure 2.5: Classification of identified proteins based on their localization and biological functions. a: Classification of identified proteins based upon their subcellular localization. b: Biological and functional classification of identified nuclear proteins. c: Classification of chromatin-associated proteins based on their biological function [144].

2.4.2 Temporal release profiles of chromatin associated proteins

Chromatin is a DNA-protein complex regulates all DNA dependent nuclear events. Inside the chromatin DNA was organized in a very compacted form by formation of nucleosome followed by higher-order structures. For biological functioning open DNA template is need so chromatin structural integrity acts as the driving forces for all DNA dependent biological activity. Chromatin structure plays a regulatory role in nuclease cleaving. Nuclease cleaved only accessible DNA templates so proteins release after nuclease treatment provides the crucial information regarding structure integrity of chromatin where they were associated. Transcriptionally active euchromatin regions were openly configured and easily digested by MNase but transcriptionally silenced and heavily compacted heterochromatin regions were practically resistant to MNase cleavage. Whereas endonuclease DNase I have cleavage specificity and specifically cleaved in the GC enrich promoter and transcription start regions of the active genes [24-26]. Unlike MNase, DNase I was also unable to cleave the heterochromatin regions. Site specificity of the nuclease cleavage provides very powerful information regarding chromatin-protein interaction and help to determine the protein binding regions. To map the chromatin-associated proteins and their chromatin association regions we used both DNase I and MNase digestion experiment independently. Our LC-MS/MS based proteomic approach successfully identified the proteins in the supernatant and pellet fractions of digested chromatin and we are able to quantify the protein amount based on their emPAI values. With the help of our proteomic data we create the temporal protein release profile which gives the protein association map of different chromatin regions. Protein release profiles were justified by the release profile of identified histone isoforms, the central component of chromatin.

2.4.3 Temporal release dynamics of histones upon nuclease digestion

Chromatin consisted chains of nucleosome subunits, composed by histone octamer beads inside a 200 bp DNA string. The “beads on strings” structure of nucleosome was formed as a result of electrostatic interaction between positively charged core histones and negatively charged DNA [1]. So core histones play the key role to basic DNA packing inside chromatin and release patterns of histones also provide the information regarding their localization either inside digestible euchromatin or heavily compacted heterochromatin region. Temporal release profiles

of core histones were presented by the Fig. 2.6-2.8. Besides the core histones, another group of histone known as linker histones has a key role in the stabilization of both nucleosome and higher-order chromatin structure. Unlike core histones linker histones were not the stable chromatin component but they were dynamic components of the chromatin structure [146]. Release profiles of the histone H1.0 and H1.2 showed only 11-13% of protein was released after 5min treatment which indicated their strong interaction with linker DNA [147]. Our digestion data also showed that release of histones H1.0 and H1.2 were increasing with treatment time and achieved the maximum peak after 35min treatment and the release patterns were comparable for both MNase and DNase I (Fig. 2.8a-b). Histone H1 was bound with linker DNA located between two nucleosome and pack the chromatin into the zigzagged 30nm chromatin fiber structure due to its association within the packed chromatin region. Release dynamics of different histone isoforms after nuclease treatment showed isoform specific localization of histone H1 which provided the valuable information regarding its functional role during gene regulation but it is unable to provide information regarding its gene regulation mechanism, which was still unclear. Previously it was believed that only linker histones played the key role in chromatin packaging and regulates the higher order chromatin structure. However, recent studies showed that core histones are also directly involved in chromatin compaction and maintenance of higher order chromatin structure [148]. Release profiles of core histones showed that Histone H2A isoform H2A.1 and H2A/1 released in a lower amount after nuclease treatment compare to their unreleased counterpart (Fig.2.8a-b). The release profiles of DNase I and MNase digestion showed DNase I released histone 2A isoforms comparatively higher amount than MNase. But histone H2B isoforms showed differential release profile. Isoform H2B type 1 has shown comparable release profile with H2A isoforms, while another isoform H2B type 1-A remain unreleased after both nuclease treatment and identified in the pellet fraction. Recent studies found that H2B type1-A was the interacting partner of heterochromatin forming protein CBX8. [149]. Both nuclease digestions were unable to solubilize the H2B type1-A isoform due to its

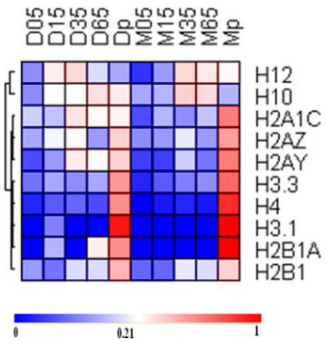

Figure 2.6: Hierarchical clustering of histones according to their release after DNase I and MNase digestion [144].

localization inside the inactive heterochromatin regions where DNA was inaccessible for enzyme cleavage. In the nucleosome

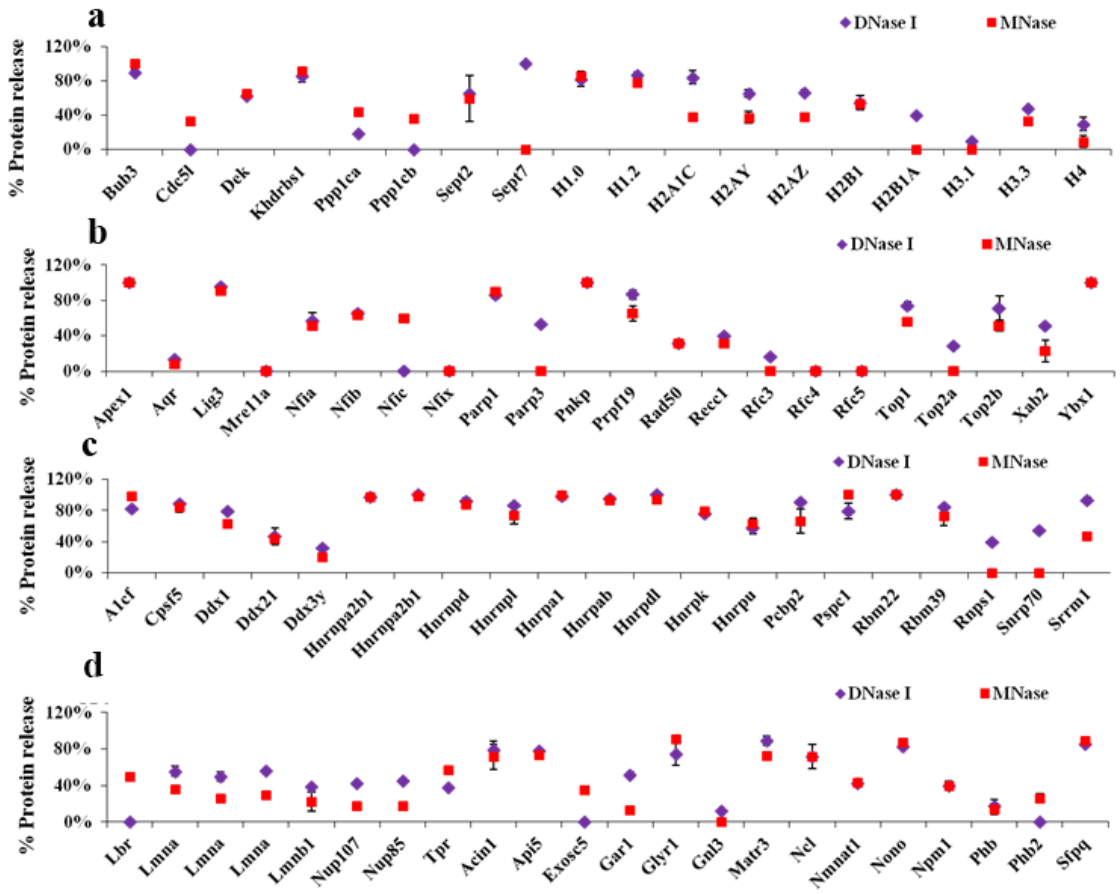

Figure 2.7: Comparison of histone and other chromatin binding protein release pattern by 65min DNase I and MNase treatment. a: Histones and proteins involve in cell cycle progression, b: Proteins involve in DNA replication and repair. c-d: Other chromatin associated proteins [144].

structure, histone H3 and H4 were located at the center portion and H2A and H2B located at the surface. DNA-Protein interaction was much stronger in the central turns of the DNA compare to the peripheral turns around the histone octamers. Our digestion data showed that more than 50% H2A/H2B were released whereas maximum amount of H3/H4 remain unreleased after partial nuclease treatment (Fig.2.7a and 2.8a-b). During nuclease digestion DNA in the peripheral turns were digested due to the loose DNA-protein interaction of the regions caused shorten of DNA length. Collapse of nucleosome structure in the peripheral regions caused release of the H2A/H2B, while core of the nucleosome remain uninterrupted and H3/H4 remain inside the core

particle. Recent evidences shown that core particle component histone H3 isoforms H3.3 was localized in the nucleosomes of the active euchromatin territory while inside constitutive heterochromatin nucleosomes H3.3 isoform was replaced by H3.1isoform [150]. Our nuclease digestion data also showed that H3 isoform H3.3 was released partially after nuclease treatment and release pattern was comparable with other core histones but isoform H3.1 remain unreleased after both DNase I and MNase digestion. In context with available evidences our data also reflect the localization of H3.1 within the heterochromatin regions, and localization of H3.3 isoform within active euchromatin territory.

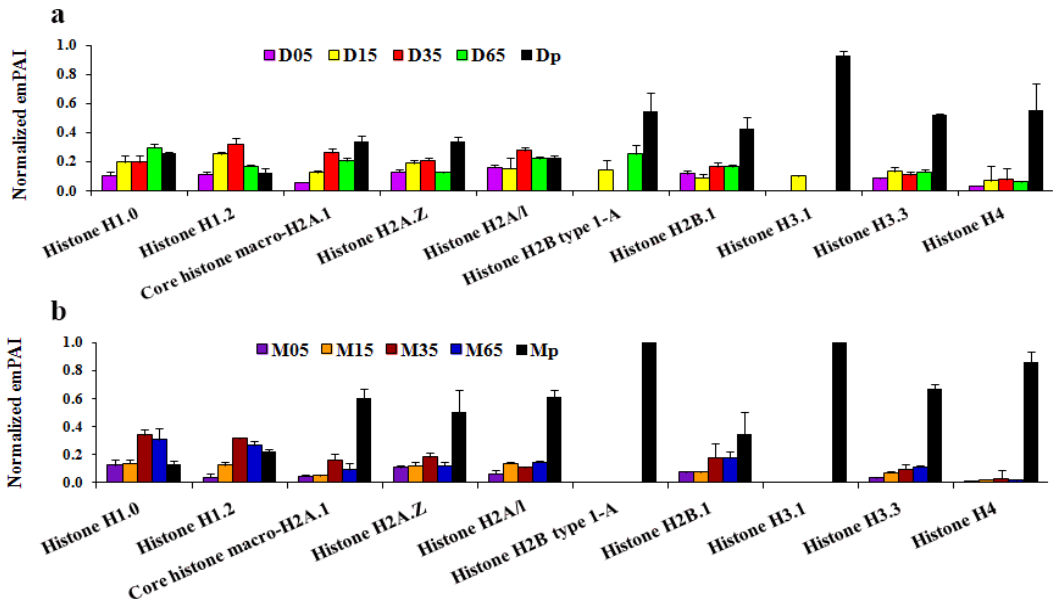

Figure 2.8: Temporal release profile of histones. a: Temporal release of histones by DNase I digestion. b: Temporal release of histones by MNase [144].

2.4.4 Temporal release dynamics of non-histones proteins

Histones are the key proteins for the DNA packaging inside chromatin structure but many non-histone proteins are also involved in the packaging process but their specific functions and mechanism of their function remain unexplored. Our study identified many non-histone chromatin proteins and they showed differential release patterns during chromatin digestion. A global view of their time dependent release profiles generated by DNase I and MNase digestion were presented in the form of a heat map (Fig. 2.9). According to their release patterns during different nuclease treatment proteins formed different clusters and on the basis of the clustering patterns proteins were classified into major five groups (cluster a-e). Proteins in the ‘cluster a’

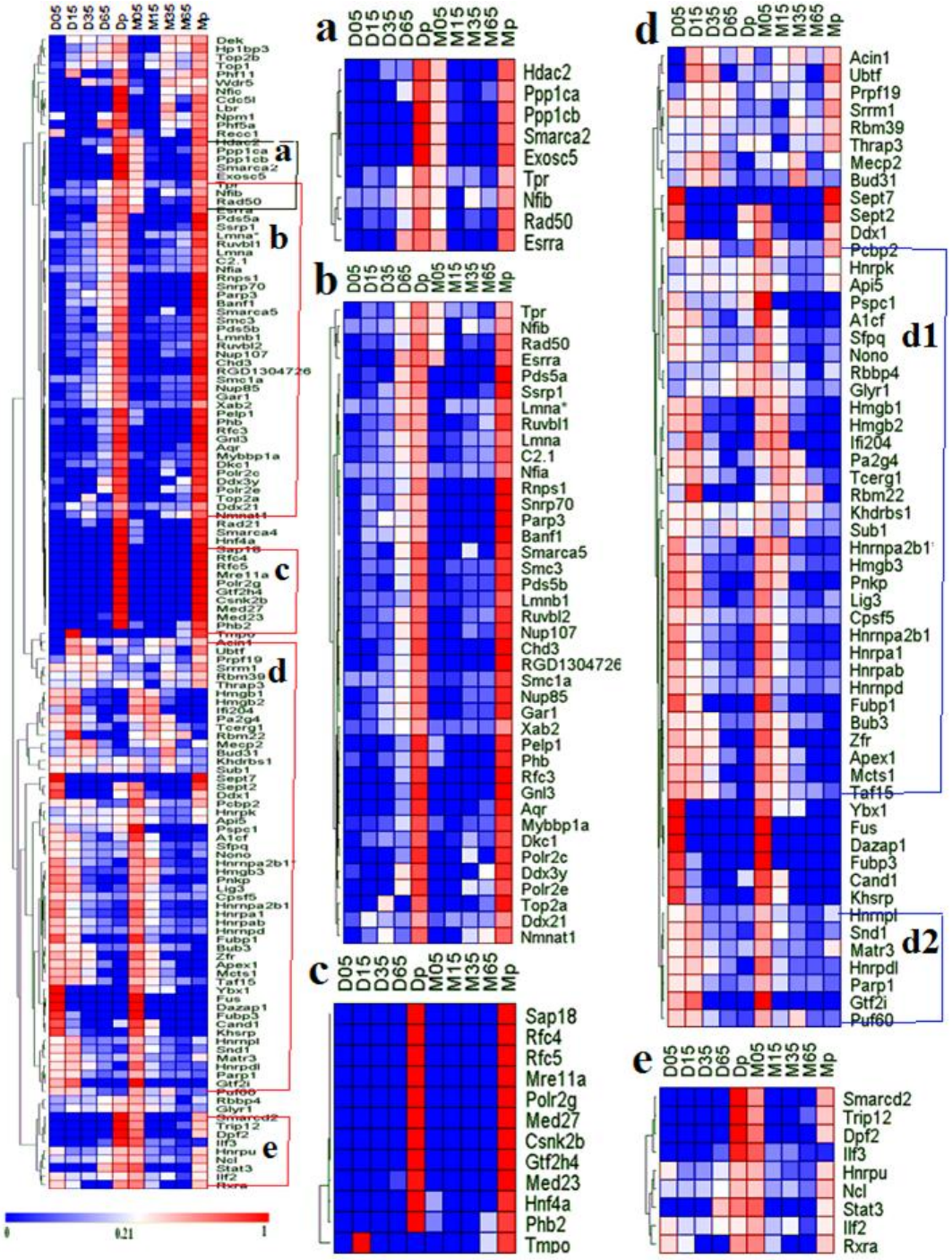

Figure 2.9: Hierarchical clustering of non-histone proteins according to their release after DNase I and MNase digestion. 'Cluster a': proteins released by 5min MNase but not by DNase I treatment; 'Cluster b': proteins released by 65min DNase I but not by MNase treatment; 'Cluster c': Proteins remain unreleased in pellet fraction after both nucleases digestion; 'Cluster d': Proteins with mixed release pattern after both nucleases digestion; and 'Cluster e': Proteins released quickly by MNase while minor quantities released or totally unreleased by DNase I [144].

were partially released by 5min MNase digestion but DNase I digestion unable to release them within 5min. Proteins released only by MNase within 5min time period indicated that they were associated within the loosely compacted active euchromatin territory and DNase I resistance indicating their specific association within the GC reach promoter or transcription start regions, located within the DNase I hypersensitive sites. Due to their binding within DNase I hypersensitive site prevent the DNase I's DNA accessibility and remain unreleased after DNase I treatment. Unlike DNase I, MNase do not have such cleavage specificity so that it can release the proteins quickly. Beside the quick release portions remain unreleased after 65min MNase treatment indicates that proteins in the 'cluster a' also associated with the heterochromatin regions. Proteins clustered inside the 'cluster b' were released in a minor quantity after 65min of DNase I digestion but remain totally unreleased after MNase digestion. Significant amount of unreleased proteins in the pellet reflect their heterochromatin association but delay release of

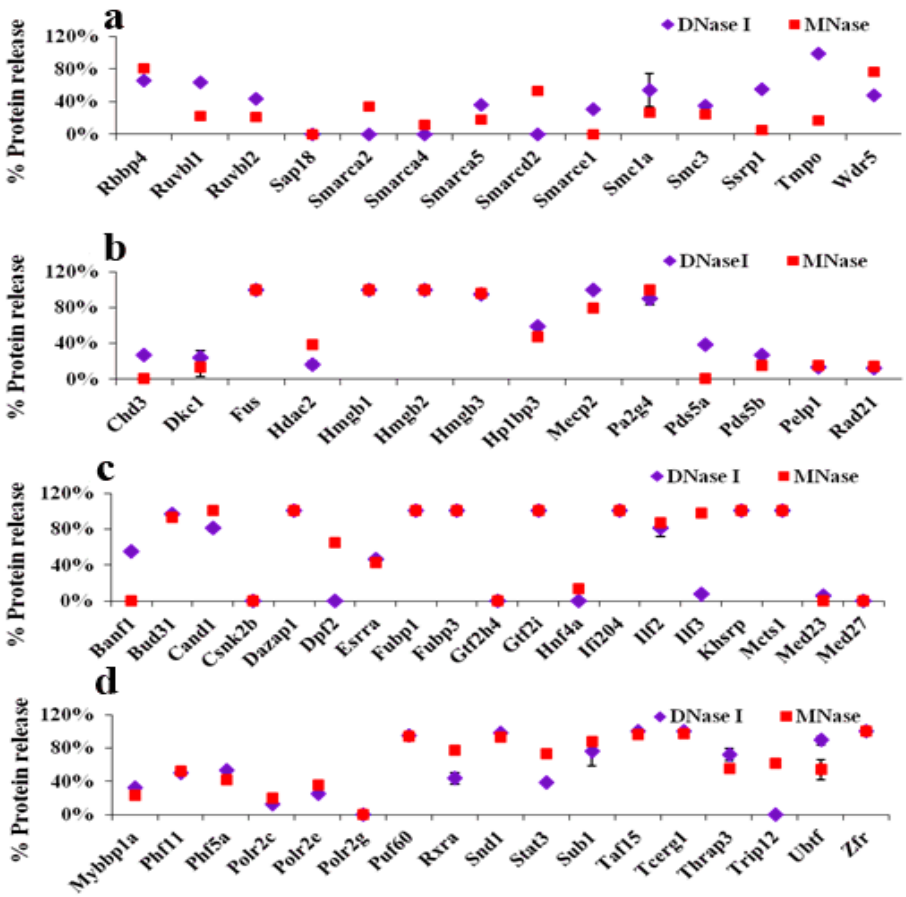

Figure 2.9: Release pattern of Non-histone proteins from rat liver chromatin by DNase I and MNase. a-b: Proteins involved in chromatin architectural maintenance. c-d: Proteins involved in transcription regulation [144].

those proteins suggested their association in the protected rear regions, initially produce resistance during DNA accessibility. Proteins like Csnk2b, Gtf2h, Med23, Med27, Mre11a, Phb2, Polr2g, Rfc4, Rfc5, Sap18, Hnf4a, and Tmpo were grouped in 'cluster c' and their release profiles showed that proteins remain completely unreleased after both MNase and DNase I digestion and identified only in the pellet fractions. Whereas proteins of the 'cluster d' have some sub-clusters like 'cluster d1' and 'cluster d2' and proteins in those two subgroups showed almost complete release after both nucleases treatment and shared the comparable release profiles for both MNase and DNase I digestion. Release profiles of those proteins suggested that they were associated within active euchromatin regions but they were not bound in the GC enriched promoter or transcription start sites. MNase released the proteins of group 'cluster e' in a greater quantity within short time period, while DNase I digestion showed proteins were released in a very low quantity or remain completely unreleased after digestion. Temporal release profiles of those proteins reflect their localization within the active sites specifically in the GC enrich promoter or transcription regions.

Functional analysis showed that 33 identified non-histone proteins were involved in maintenance of higher-order chromatin structure, chromatin remodeling and transcription regulation process. We identified a few proteins like Hmgb1, Hmgb2 and Hmgb3 that belong to the HMG family are important member of this class. HMG proteins were constantly moving within the nucleus [151-153] and their binding with chromatin alter the chromatin structure and functions [154, 155]. HMG proteins were binding with the chromatin in different mode during interphase and mitotic phase of the cell cycle [156]. Temporal release profiles showed HMG proteins were completely released by both MNase and DNase I during digestion (Fig. 2.9b, 2.11a, and 2.11c). Our digestion data suggested that HMG proteins were associated with the loosely compacted euchromatin regions, easily accessible for nuclease cleavage and completely released by MNase and DNase I. Members of the SWI/SNF protein family are integral component of the ATP dependent nucleosome remodeling complexes and regulate the DNA dependent events like transcription, replication and repair through chromatin remodeling [157, 158]. We identify SWI/SNF-family protein Smarca2, Smarca4, and Smarcd2 in our data set. MNase digestion profile exhibited bimodal protein release, either released only after 5min digestion or remain unreleased during further time period of digestion, while DNase I was not able to release these proteins (Fig. 2.10a, 2.11b, and 2.11d). In context of both DNase I and

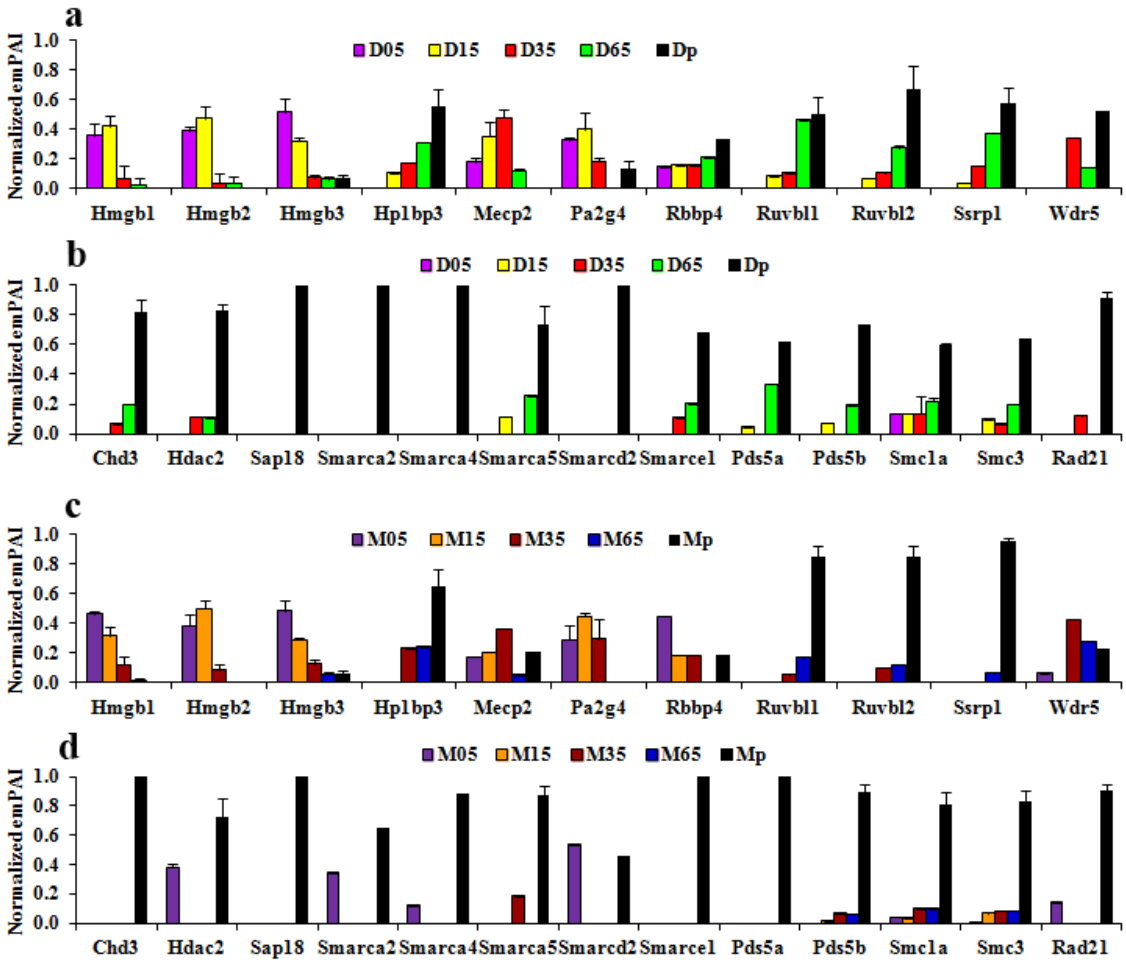

Figure 2.11: Temporal release profiles of non-histones involve in maintenance of chromatin architecture. a-b: Temporal release of non-histones by DNase I. c-d: Temporal release of non-histones by MNase respectively [144].

MNase digestion profiles we suggested that SWI/SNF family proteins were binding with both heterochromatin and euchromatin and also suggested that proteins were specifically bound within the GC enrich promoters or transcription start regions of the active genes, protect the regions from DNase I cleavage. According to overall release profiles of those proteins suggest more than 70% protein was located in the heterochromatin regions and minor fraction of protein was associated in the promoter or transcription start regions of the active gene territory. Unlike SWI/SNF proteins Hdac2, Chd3 and Sap18 were components of many chromatin organization complexes like histone acetylases, deacetylases and chromatin remodeling complexes, which regulate most of the DNA dependent biological activities. Their release profile showed that greater amount of proteins remain unreleased after both nuclease treatment (Fig. 2.10b, 2.11b,

and 2.11d) reflecting highly condensed nuclease resistant heterochromatin regions as a major binding region for these three proteins. We identified two important WD-repeat containing proteins Rbbp4 and Wdr5 that are involved in chromatin modification through histone acetylation and also involved in chromatin assembly. Result showed more than 60% of Rbbp4 and Wdr5 were released by both nuclease digestion (Fig. 2.10a, 2.11a, and 2.11c) indicating their association within the nuclease susceptible loosely compacted chromatin could activate gene transcription through histone acetylation. Our digestion study also showed that major part of the cohesion complex proteins Smc1a, Smc3, Rad21 Pds5a and Pds5b remain unreleased after 65min of nuclease digestion and two comparable release profiles were generated during DNase I and MNase digestion (Fig. 2.9a-b, 2.11b, and 2.11d). Cohesion binding regions of the meiotic chromatin remain intact after DNase I treatment, while other regions were digested [159]. Our digestion data together with this observation suggests that binding of cohesion complex block the nuclease cleavage sites and components of the cohesion complex remain unreleased after nuclease digestion.

During DNA replication, DNA polymerase need the help of other accessory factors and one of the accessory factors is heteropentameric RFC complex that composed of five different size 140, 40, 38, 37, and 36kDa subunits [160]. Larger subunit known as Rfc1 and four small subunits were named Rfc2, Rfc3, Rfc4, and Rfc5 accordingly. In our study we identified Rfc3, Rfc4 and Rfc5 and all of them were identified only in the pellet fraction of both DNase I and MNase digested chromatin (Fig. 2.7b, 2.12a, and 2.12c). Proteomic data reflected that due to large size DNA replication complex protect the replication site from nuclease cleavage and proteins of the replication complex remain unreleased after digestion. Topoisomerases regulate winding and unwinding of the DNA and play a key role during replication and repair. Here we identified few topoisomerases including Top1, Top2a and Top2b in our data set. Digestion data exhibited that three of them were partially released after both nuclease treatment (Fig. 2.7b, 2.12a, and 2.12c). Overall, the release profiles showed more than 60% of topoisomerases Top1 and Top2b were released after nuclease treatment and the rest of the 40% protein remain unreleased and identified in the pellet fractions. Top1 and Top2b were bound within the relaxed chromatin region and unwind the DNA helixes [161] for replication and repair. Due to their binding with the relaxed chromatin both of them were easily released after MNase and DNase treatment. However 40% unreleased Top1 and Top2b (Fig. 2.12a and 2.12c) reflected their

association within the heterochromatin territories in liver tissue and may be their heterochromatin association was necessary for maintaining structural integrity of heterochromatin. Our explanation was supported by the findings, SWI/SNF complex along with TOP1 involved in the ATP independent positive supercoiling of circular DNA and SWI/SNF complex induced positive supercoil formation by destabilizing nucleosome organization in yeast [162]. Unlike Top1 topoisomerase 2 isoforms Top2b and Top2a were not easily released by nuclease digestion only a very small fraction (10-29%) of protein was released after 65min digestion reflected the fact that topoisomerase 2 isoform Top2a was localized in the heterochromatin regions of the liver chromatin.

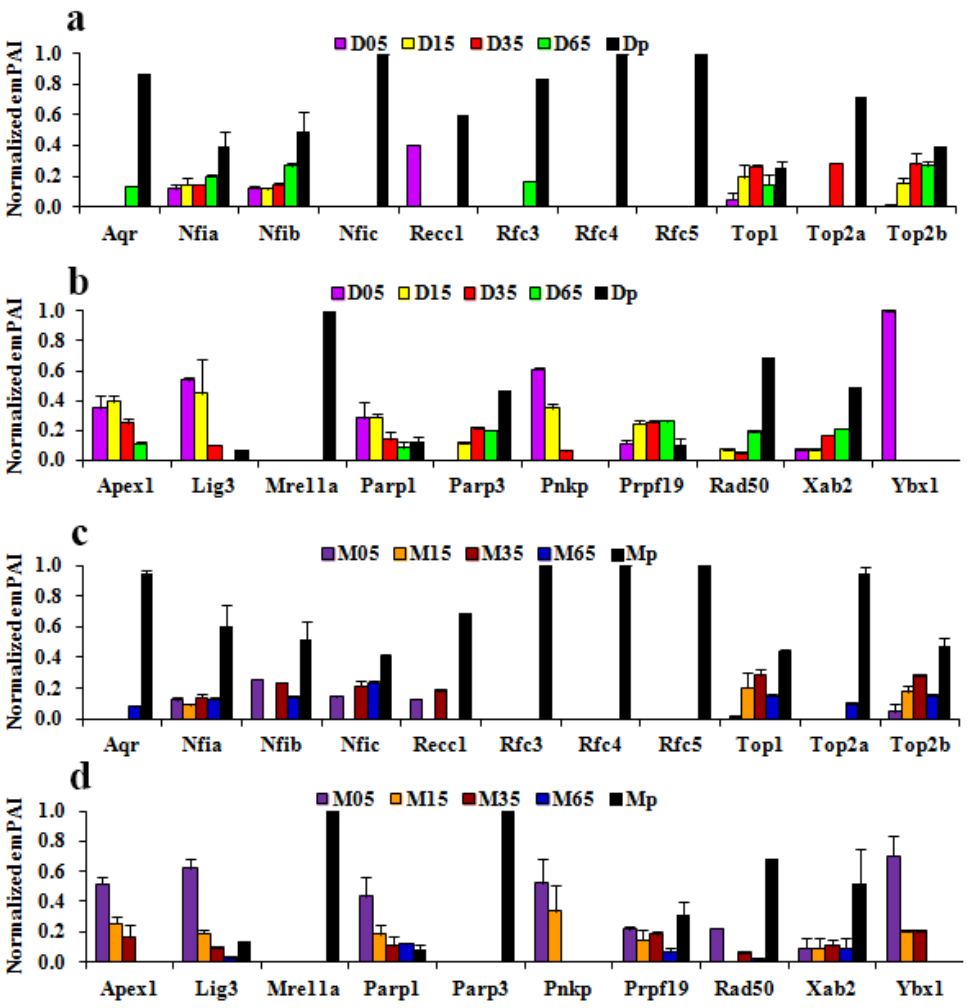

Figure 2.12: Temporal release profiles of proteins involve in DNA replication and repair. a-b: Temporal release of proteins by DNase I. c-d: Temporal release of proteins by MNase [144].

DNA repair sites maintain the relaxed configuration during repair and allow access of the DNA template to repair proteins. Release profiles of DNA repair protein Apex1, Lig3, Parp1, Pnkp and Prpf19 have shown the complete release of the proteins after both nucleases treatment (Fig. 2.7b, 2.12b, and 2.12d) due to their association with the relaxed chromatin region located inside the repair zones. Rad50 and Mre11a were the central constituents of the MRN complex, which maintain the telomeres structure [163, 164]. It was a well-established fact that telomere regions were constructed of repetitive sequence and behaved like heterochromatin regions. MRN components Rad50 and Mre11a exhibited the expected response during nuclease digestion and remain unreleased after digestion (Fig. 2.7b, 2.12b, and 2.12d). NF family proteins are involved in different nuclear events such as transcription and replication and we identified three NF protein including Nfia, Nfib and Nfic (Fig. 2.7b, 2.12a, and 2.12c). In our data set Nfia and Nfib exhibited their partial release during both MNase and DNase I digestion, while, Nfic was only released by MNase. According to the characteristic of NF proteins they generally bind in the promoter regions of active genes. On the basis of the both MNase and DNase I digestion data we suggested Nfia and Nfib preferentially bind in the AT rich promoters and were easily released after DNase I digestion but Nfic specifically bind in the CG enrich region and remain unreleased after DNase I digestion.

In this proteomic based study we identified 31 chromatin interacting proteins which are functionally act as a transcription regulator and figures (Fig.2.13a-f) represented their temporal release profiles during nuclease treatment. Transcription takes place in the loosely compacted euchromatin regions known as active sites and its relaxed structure provided an easy DNA accession for transcription regulator proteins. Our digestion result showed a majority of transcription regulators were identified in the supernatant fractions. Due to the open configuration, active sites were highly susceptible to nuclease attack and proteins associated with these sites were easily released after nuclease digestion. However few transcription regulatory proteins like Csnk2b, Dpf2, Hnf4a, Ilf3, and Mybbp1a and transcription machinery proteins like Polr2c, Polr2e, Polr2g, Gtf2h4, Med23, and Med27 were found in the insoluble pellet fractions (Fig. 2.10c-d and 2.13a-f). Although during transcription progression polymerase and other transcription machinery proteins were bound with the relaxed DNA template and transcribed the DNA but the large size of the transcription complex, protein-protein and protein-DNA interaction make the transcription site inaccessible for other proteins or enzymes. So during

digestion, nucleases did not digest the DNA of the transcription sites due to its inaccessibility and transcription machinery proteins along with the polymerase sub-units remain in the undigested pellet fractions. Few transcription regulator showed differential release patterns during DNase I and MNase digestion of them Ifl3, Trip12, Dpf2 and Hnf4a were released in the

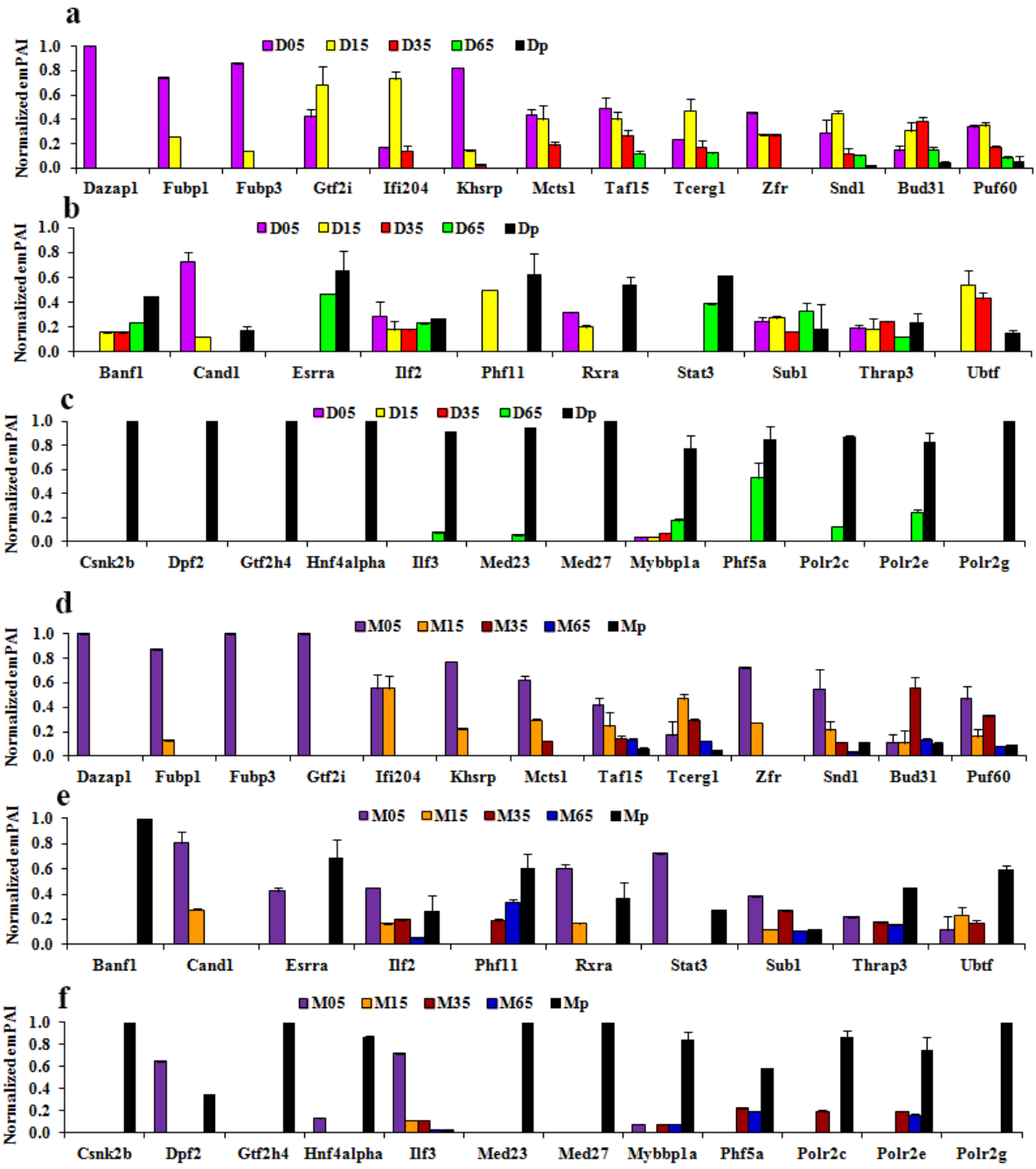

Figure 2.13: Temporal release profiles of transcription regulators and transcription machinery proteins. a-c: Temporal release of proteins by DNase I. d-f: Temporal release of proteins by MNase [144].

supernatant during MNase digestion but remain unreleased after DNase I treatment (Fig. 2.10c-d). Four of them have transcription factor activity and they generally bind with the DNA in a sequence specific manner [24]. Digestion results showed that their binding produce only DNase I resistance. This reflected their specific localization within the GC enrich promoter or transcription starting sites. However, release profiles of transcription regulators Rxra and Stat3 (Fig. 2.10d) showed comparatively larger amount of protein was released by MNase this suggesting their association within both AT and GC enrich promoter regions.

Nuclear matrix associated proteins play a key role during interphase and regulates many chromatin dependent biological functions like chromatin organization, transcription, DNA replication and repair. We identified three matrix proteins in our data set such as Matr3, Nono and Sfpq. Their temporal release profiles showed that 70-80% protein was released after 65min nuclease treatment and release profiles were comparable for both DNase I and MNase digestion

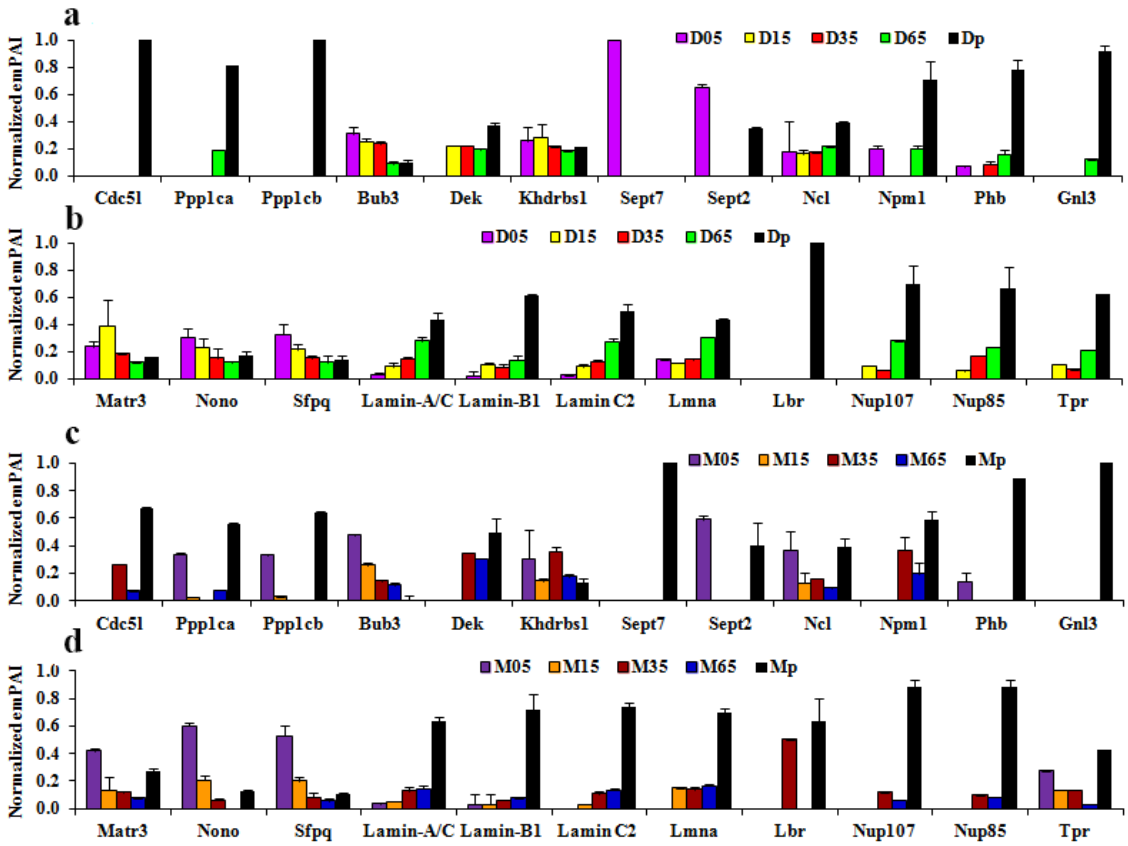

Figure 2.14: Temporal release profiles of miscellaneous chromatin associated proteins. a-b: Temporal release of proteins by DNase I. c-d: Temporal release of proteins by MNase [144].

(Fig. 2.7d, 2.14b, and 2.14d). According to our digestion data 70-80% matrix associated proteins were bound in the loosely compacted euchromatin and regulate the chromatin dependent process. In addition, our proteomic experiment also identified 19 nuclear membrane proteins, and most of them were lamins and porins. They were mainly involved in nuclear transport but they also interact with chromatin and regulate many nuclear events. Identified lamins including lamin A, lamin B1 and lamin C2 showed partial release after both MNase and DNase I digestion, while porins were released in a low quantity after long time nuclease treatment (Fig. 2.7d, 2.14b, and2.13d). Emerging studies suggest involvement of lamins in chromatin organization, transcription and other chromatin dependent events [165, 166]. Due to their localization in the inner nuclear membrane, lamins are interacting with the chromatins which were located very close to the periphery. Our digestion results showed more than 50% of lamins remain unreleased after digestion. This reflects their association with the pericentric heterochromatin, located towards nuclear membrane.

Cell cycle is a very important process through which cells were divided and produce new progeny cells. During cell cycle all genetic information were transferred into the progeny cell through a series of chromatin dependent events. Throughout cell cycle progression different type of proteins were associated with chromatin and regulate the process. In our data set we found few cell cycle regulatory proteins including Bub3, Dek, and Khdrbs1. Their release profiles showed partial protein release but comparatively higher amount of protein released. However proteins like Cdc5l, Ppp1ca, and Ppp1cb were released in a low quantity after 65min digestion or remain completely unreleased. We found Sept7 only in the DNase I digested supernatant fractions (Fig. 2.7a, 2.14a, and 2.14c). Throughout cell cycle progression chromatin exhibited very dynamic structure and going through structural rearrangement for participating in the different DNA dependent events [167]. Differential release of the proteins indicated their differential chromatin binding during cell cycle progression. Mitotic chromatins exhibited highly condensed and compact structural forms which prevent chromatin dependent cellular activities including transcription, replication and DNA repair. Inhibition of the chromatin dependent events could be achieved through histone modifications and alternation in the chromatin associated proteins organization [168].

Overall, digestion data suggested that proteins associated with euchromatin were released quickly after nuclease digestion but proteins associated with heterochromatin remain unreleased after both DNase I and MNase digestion. But proteins released by MNase but remain unreleased after DNase I treatment, were binding within the GC enrich promoter or transcription start regions of the active gene territories. The figure 2.15a-c represents our findings in form of a schematic model.

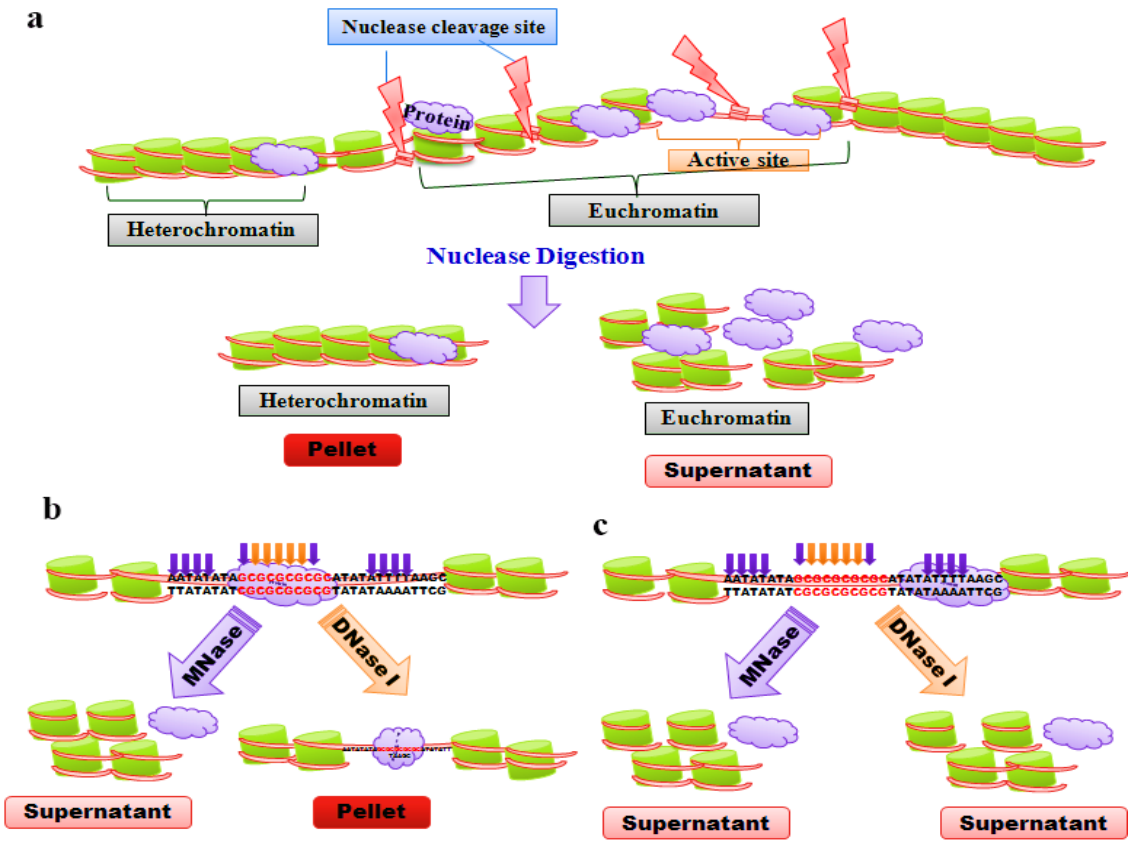

Figure 2.15: Model of protein association and chromatin digestion. a: Nonspecific nuclease digestion. Nucleases cleave the DNA in the linker region (nuclease cleavage site) and easily digested the euchromatin regions and solubilized the euchromatin associated proteins in the supernatant fraction. Highly compacted heterochromatin regions remain undigested and heterochromatin associated proteins remain in the pellet fraction. b-c: The effect of protein binding in nuclease digestion. Specific protein binding in the cleavage site prevent nuclease digestion and proteins remain unreleased after digestion but nonspecific proteins binding in linker region did not prevent nuclease cleavage and solubilized the proteins after digestion.

2.4.5 Novel chromatin associated proteins and immunofluorescence analysis

In our study we identified 39 proteins which do not have specified subcellular localization. We also identified several novel proteins such as Actl6a, Erh, LOC361990, Luc7l, Luc7l2, Mettl7b, Noc2l, Norp, RpoB, Ttc35, Ythdf1, and WD40 repeat-containing proteins Cirh1a, Smu1, Wdr18, Wdr61, Wdr74, and Wdr75. Analysis of their amino sequence in the UniProtKB database showed sequence similarity with known chromatin-associated proteins, suggested that proteins might have chromatin association. Actual functions of the novel protein Erh still not clear but available evidences suggested that it have some cell cycle specific functions. Recent *in silico* protein-interaction study suggest Erh have transcription regulator activity [169] and experimental evidences also revealed the interaction of Erh with H19 [170]. We suggested that identified novel nuclear proteins such as Cirh1a, Erh and Smu1 may have some contribution in regulation of chromatin dependent events. In our data set we observed presence of some chaperone proteins such as Dnajb1, Hsp90aa1, Hspa5, Hspa8, and Trap1, suggesting these proteins could have some interaction with chromatin and purified with chromatin. Recent study elucidate the role of DnaJ homolog PfDnaJA, during apicoplast genome replication/repair [171]. During the ChIP study heat shock protein like HSPA5 and HSPA8 were co-immunoprecipitated with centromeric histone H3 [172] indicating their possible chromatin interaction. WD40 repeats containing proteins have a WD40 domain responsible for protein-protein interaction and due to presence of the WD 40 domain proteins act as a scaffold molecule for many protein complexes. Emerging evidences suggested that WD40 repeats containing proteins were involved in wide range biological process like transcription regulation, RNA processing, signal transduction, and cell cycle regulation. Here we identified few novel WD 40 repeat contending proteins including Wdr18, Wdr61 and Wdr91 which might have some roles in chromatin dependent biological events like known WD40 repeat containing proteins.

We identified several nuclear proteins like prohibitin (Phb), nucleolin (Ncl) and nucleostemin (Gnl3) which participated in many chromatin dependent biological events such as chromatin condensation, telomere maintenance, transcription regulation and mane other [173-175]. Temporal release profiles of Gnl3, Ncl, and Phb showed that partial release of these proteins during both DNase I and MNase digestion and also showed that a greater fraction of proteins remain unreleased compare to released fraction (Fig. 2.7d, 2.14a and 2.14c). In this

study we apply immunofluorescence microscopy approach to confirm their localization in the HEPG2 cell line (Human liver carcinoma cell line) (Fig. 2.16). Microscopy result showed that Phb was co-localized with deeply DAPI stained regions of nucleus. In the context of our nuclease digestion and microscopy experiments we suggest that Phb was associated with the heterochromatin and might be involved in transcriptional modulation by interacting with various transcription factors, including nuclear receptors. However, nuclear protein Ncl and Gnl3 were shown their major localization inside nucleolus but also showed a minor fraction of protein was co-localized with DAPI stained chromatin in the nucleolus surrounding region. In growing eukaryote Ncl is a major nuclear protein which might be involved in the chromatin dependent nuclear events. Microscopic images showed that Ncl was localized in nucleolus during interphase and also showed its co-localization in nucleolus surrounding chromatin territories which also support its partial release after nuclease treatment. Microscopy data confirmed Gnl3 localization inside the nucleolus. Both digestion and microscopy data mutually support each other.

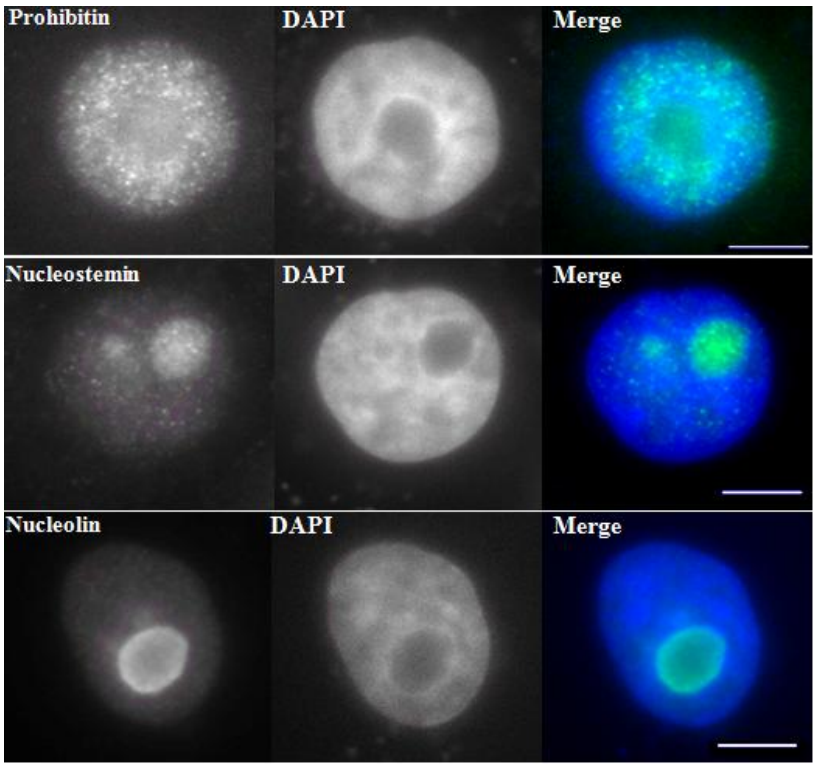

Figure 2.16: Distribution of nuclear proteins in the HEPG2 nuclei. HepG2 cells were plated on glass cover slips and immunostained with respective primary antibodies and Alexa 488 conjugated secondary antibodies (green) and nucleus were counterstained with DAPI (blue). Scale bar 10µm [144].

2.5 Conclusion

Chromatin structure is very dynamic in nature in the interphase nuclei. Whole chromatin biology is maximally regulated by protein chromatin interaction and hence knowledge on chromatin associated protein network could elucidate the dynamics of chromatin biology and improve our understanding of the chromatin's regulatory role in the cell nucleus. We have developed an analytical method to study chromatome dynamics using two nucleases, DNase I and MNase, to differentially release chromatin bound proteins that were analyzed by LC-MS/MS and quantified using label free emPAI-based quantification method. We identified 694 proteins with high confidence and among them, 160 proteins have known chromatin association. Their differential releases from the chromatin by nucleases elucidated their structure specific chromatin binding. Classification of the high confidence dataset revealed that histones and non-histone proteins are involved in chromatin architectural maintenance, replication, DNA repair, transcription, cell cycle progression, and other chromatin dependent processes. Further, we also validated the localization of few proteins by immunofluorescence microscopy analysis. This newly developed proteomic method provides the necessary tools for studying chromatome changes in cell cycle and hypoxia induced cancer progression as described in subsequent chapters.

Chapter 3

3. Proteomic and functional studies of chromatome dynamics in cell cycle progression

3.1 Summary

Chromatin, a key component of eukaryotic cells composed of DNA and proteins, plays a key regulatory role by controlling accesses to the DNA templates that carry genetic instructions for all cellular functions. The chromatin-associated proteome actively modulates chromatin structure to regulate the important biological and pathological events like development, growth, ageing, cancer and other disease progression. Cell cycle is the basic biological event necessary for cell division, and maintenance of the organism existence. All important genetic events like replication, DNA repair and recombination, transcription, chromatin segregation, and genome packaging were conducted during cell cycle and very dynamic chromatin structure is maintained throughout cell cycle for completion of the genetic events. A global picture of chromatome is essential to understand the chromatin dynamics during cell cycle progression. Handfuls of chromatin proteomic studies were reported as of now and chromatin binding topology of the chromatome during cell cycle progression remains unknown. Here partial MNase digestion and iTRAQ based high throughput quantitative proteomic approach was applied for identification and quantification of the chromatin-associated proteins during interphase progression. In the present study 481 proteins were identified at high confidence level and involved in chromatin dependent events like chromatin organization, DNA replication and repair, transcription regulation and many others. The quantitative data revealed their dynamic interactions with chromatin during interphase progression. Our findings also suggested the dynamic chromatin association of the novel chromatin protein HP1BP3 during the different stages of interphase. The detailed functional studies uncover its regulatory role in transcription regulation by maintaining the heterochromatin integrity during the G_1-S progression, which regulate the length of G_1 phase and control cell proliferation. The present study also uncovers the other functional roles of HP1BP3 in maintenance of nuclear transport and nuclear size.

3.2 Introduction

Eukaryotic cells divide through a sequential series of events known as cell cycle. Cell cycle consists of two major consecutive events characterized by duplication of the genome via DNA synthesis and evenly distributed in the duplicated genome into the two new daughter cells through nuclear division known as mitosis. In between two mitotic cycles intermediate phase

known as interphase consist of DNA synthesis step known as S phase and two gaps G_1 and G_2 before and after S phase accordingly when cells are prepared for the DNA synthesis and mitosis.

In cell cycle progression, various chromatin dependent genetic events such as transcription, replication, genome repair, genome packaging, and chromatin segregation take place at various stages. A majority of these genomic events occur during the interphase progression. To perform those basic genetic and epigenetic events DNA template accessibility by chromatin associated proteins are vital for successful completion of these events. The DNA accessibility is achieved by maintaining the dynamic chromatin structure throughout interphase [176, 177]. Genomic and epigenomic regulations share equal importance in the regulation of basic cellular events. Similar to genetic information, epigenetic information is transferred as it is into the daughter cells after every cell division and also transferred from one generation to the next generation. Cell cycle is the fundamental process which plays a vital role in this transmission process [178]. Epigenome replication is less accurate compare to genome replication. Induction of new epigenetic marks or removal of old marks took place during epigenome replication [178, 179]. Alterations in the epigenome are responsible for cell differentiation, which plays an important role in developmental biology [180] and also induce many unprogrammed events which are responsible for evolution of disease including cancer [181-183]. Epigenetic inheritances are directly controlled by the various factors including DNA and histone modifications, histone variants, non-histone chromatin proteins, nuclear RNA and higher-order chromatin structure [184-187]. During interphase chromatins are structured in two distinct forms; euchromatin (loosely compacted active regions) and heterochromatin (highly compacted silent regions) that are continuously interchanged according to the necessity of the DNA template accessibility. During the metaphase chromatins are further compacted into a heavily condensed structure which prevent DNA dependent basic biological events and maintain proper structural integrity for non-erroneous transference of genome copies into the progeny cells [188, 189]. During interphase progression, loosely compacted euchromatin structure is essential for conducting the major genetic and epigenetic events [190-193] Whereas heterochromatin structure is vital to prevent aberrant DNA access that could evolve unwanted genetic and epigenetic events during interphase and disrupt the cell cycle progression [194-196].

Imbalance in the chromatin structure dependent regulatory system causes deregulated cell cycle, responsible for evolution of cancer like diseases [197, 198].

The structural dynamics of interphase chromatin is regulated by the protein-DNA and protein-protein interactions, through various epigenetic regulators like protein PTMs, DNA modifications and many others [6]. During the cell cycle progression chromatin dynamic is regulated through key chromatin component protein histone isoforms [199, 200]. Rather than histones other non-histone chromatin interacting proteins also play an important role in the regulation of chromatin biology. Unlike histone their regulatory role still not well understood. Recent study regarding chromatin associated non-histone proteins like HMGNs, topoisomerase II α, RNA polymerase III and heterochromatin protein 1 revealed their functions in regulation of the structural dynamics of chromatin [156, 201-204]. Global picture of the chromatin-associated proteins and their association dynamics during different cell cycle stages might provide the valuable information regarding dynamic regulation of chromatin biology during interphase progression. But insufficient proteomic information keeps the dynamic regulation of chromatin during interphase in a less-understood format. Proteomic study of the chromatome on a global basis is less extensive and a few studies are reported including *C. Elegans* meiotic chromatin proteome [128], yeast replicative chromatin proteome [205], and human mitotic chromatin proteome [127]. Few researchers also conducted the proteomic study to identify the ATM kinase dependent alternation of DNA damage response complex [206]. Proteomic study of post-meiotic genome associated factors was also reported very recently [207].

Partial nuclease digestion coupled with LC-MS/MS based proteomic strategy as described in the chapter 2, was applied here with minor modification to study the chromatome dynamics during cell cycle progression. Briefly, our experimental planning involves partial MNase digestion of different chromatin samples extracted from cells synchronized at different interphase stages and release the chromatin associated proteins. It is very useful tool for profiling chromatin association topology of the chromatin proteins during interphase progression but also for understanding chromatin dynamics throughout the cell cycle progression. All those valuable information regarding changes in chromatin proteome during different stages of cell cycle might serve as a very strong explanatory tool for proper understanding of the altered biology of cancer and many other diseases. Therefore the goal of our present study is to understand the global

picture of the chromatin associated proteins and their association dynamics during interphase progression and also understand their contribution in chromatin biology throughout interphase progression. To achieve this objective, partial MNase digestion coupled with iTRAQ based quantitative proteomic strategy was used for both identification and quantification of chromatome (chromatin proteome) during the cell cycle progression. The present biochemical and biological studies also revealed the regulatory functions of novel proteins including KDM1A and HP1BP3 and their contribution in chromatin-, cellular-, and patho-biology.

3.3 Materials and methods

3.3.1 Reagents

Unless indicated, all reagents used in this study were purchased from Sigma-Aldrich, USA. Antibody against Tubulin α (sc-5286), GAPDH (sc-32233), Ku-70 (sc-17789), and Ku-80 (sc-5280) were purchased from Santa Cruz Biotechnology, Inc., USA. Histone H2A (ab13923), Histone H4 (ab10158), and HP1BP3 (ab98894) antibodies were purchased from Abcam, UK. Antibody against actin (MAB1501) was purchase from Millipore, USA and the ECL system was purchased from Invitrogen, USA. All cell culture media and supplements were purchased from Gibco® (Life Technologies, USA).

3.3.2 Experimental methodology

3.3.2.1 293F cell culture and Cell cycle synchronization

The 293F cells (Invitrogen) were cultured in Free Style 293 expression medium (GIBCO™, Invitrogen). 3×10^5 viable cells/ml were seeded into the 125ml vented, sterile PETG flask (NALGENE) and incubated at 37°C in a shaking incubator containing 5% CO_2 with 120rpm. The cells were sub-cultured once their density was reached at 2×10^6 cells/ml. Cell density of 1×10^6 cells/ml was used for cell cycle synchronization experiment. Double thymidine blocking was used to synchronize the cells in G_1/S-phase. For double thymidine blocking, cells were first treated with 2.5mM thymidine for 18h and released them into the fresh culture medium for next 8h followed by another 18h thymidine treatment. Finally G_1/S phase synchronized cells were harvested, PBS washed and stored at –80^{o}C for farther studies. The cells were synchronized

at G_2/M phase and G_0/G_1 by thymidine-nocodazole blocking. Cells were first treated with 2.5mM thymidine for 24h and released into drug free fresh medium for 3h. After 3h, nocodazole was added at a concentration of 200ng/ml and the treatment was continued for 16h. G_2/M synchronized cells were harvested after 16h nocodazole treatment. For G_0/G_1 synchronization, cells were released in fresh medium after 16h nocodazole treatment for next 6h. After 6h, cells were harvested, PBS washed and stored at –80^{o}C.

3.3.2.2 Propidium iodide staining and flow cytrometry analysis

2×10^6 viable cells were harvested and washed twice with multivalent cation free ice cold PBS. Cells were re-suspended in 0.1ml ice cold PBS. For ethanol fixing, 0.1ml cell suspension was added drop wise into 0.9ml 95% ethanol (cooled at–20^{o}C) and stored the cell suspension for overnight at –20°C. Ethanol fixed cells were collected by centrifugation at 2000×g for 2min at 4^{o}C and washed twice with ice cold PBS. 400-500 µl of propidium iodide staining solution was added and stained the cells for 15min at 37°C. Finally DNA content of the cells was measured by flow cytometer (BD FACS Calibur™, BD Biosciences, California, USA) and CELLQUEST program was used for the analysis.

3.3.2.3 Chromatin isolation and digestion

Chromatin isolation was performed according to the protocol as described in the previous chapter with minor modification. 7×10^7 cells were suspended into nuclei extraction buffer A (10mM HEPES of pH 7.5, 10mM KCl, 1.5mM $MgCl_2$, 0.34M sucrose, 0.1% triton X-100, 1mM DTT and protease inhibitor cocktail) and kept on ice for 30min. The suspension was dounced (50 strokes) with large clearance pestle A. The homogenate was centrifuged at 2000×g for 3min at 4°C. Supernatant fraction was removed carefully and collected the pellet fraction. The pellet was then re-suspended in nuclei extraction buffer B (10mM HEPES of pH 7.5, 10mM KCl, 1.5mM $MgCl_2$, 0.34M sucrose, 0.1% NP-40, 1mM DTT and protease inhibitor cocktail) and re-dounced (30 stocks) with pestle B. Homogenate was loaded on the top of the 2.1M Sucrose Cushion (10mM HEPES, pH 7.5, 10mM KCl, 1.5mM $MgCl_2$, 2.1M sucrose,1mM DTT and protease inhibitor cocktail) and ultra-centrifuged at 1,50,000×g for 3h at 4°C using SW41 rotor and Optima™ L-100XP ultra (Beckman Coulter). After ultra-centrifugation, sticky white cell debris was restrained in the middle interface of the two liquid layers and chromatin fraction was settling

down in the bottom of the tube. Supernatant including debris were removed carefully and chromatin pellet was collected from bottom of the tube. The chromatin pellet was washed twice with washing buffer (10mM HEPES, pH 7.5, 1mM DTT and protease inhibitor cocktail) and each time chromatin pellet was collected by centrifugation at 20,000×g for 45min at 4^{o}C. All reagents used for chromatin extraction, were pre-chilled at 4^{o}C prior to start the experiment. All biological replicates were pulled together before chromatin extraction.

Purified chromatin pellet was taken and suspended in 50µl of MNase digestion buffer (10mM HEPES (pH 7.5), 2.5mM $CaCl_2$, 2.5mM $MgCl_2$). 20U of MNase was added and digest the chromatin pellet for 60min in a 37^{o}C water bath with occasional vortexing. Immediately after 1h digestion, 1mM EDTA solution was added to stop the digestion and the supernatant fraction (S) was collected by centrifugation at 20,000×g for 30min at 4^{o}C. The remaining undigested pellet was dissolved in 2% SDS solution (P). G1-S, G1/S-S and G2/M-S supernatant fractions were obtained from G_1, G_1/S and G_2/M phase chromatin. Pallet fractions of the corresponding chromatins were labeled as G1-P, G1/S-P and G2/M-P. Protein content of the chromatin digests were measured by using 2-D Quant Kit (Amersham Biosciences, USA).

3.3.2.4 In-gel Digestion

75µg of protein from each sample was taken for in-gel digestion. Protein samples were loaded and separated in the 12.5% polyacrylamide gel. Electrophoresis was performed at 80V for 15min to entrap the proteins into the gel. Entrapment of the protein molecules inside the gel immobilized the protein molecules and increases the trypsin digestion efficiency which ensures complete protein digestion. Each sample lane was cut separately into small pieces and alternatively washed with 25mM triethylammonium bicarbonate (TEAB) in 75% ACN and 25mM TEAB buffer to remove the salts and other impurities such as DNA fragments. After washing, the gel pieces were dehydrated with 100% ACN. ACN was completely removed by air drying. Reduction was carried out by using 5mM tris 2-carboxyethyl phosphine hydrochloride (TCEP) in 25mM TEAB buffer for 30min at 60ºC followed by alkylation with 10mM methyl methanethiosulfonate (MMTS) in 25mM TEAB buffer at for 45min at RT. TCEP and MMTS were removed by alternative washing with 25mM TEAB in 75% ACN and 25mM TEAB buffer. The gel pieces were again dehydrated and dried. Sequencing grade modified trypsin (Promega

Corporation, WI, USA) solution in 25mM TEAB (10ng/ml) was added into the dried gel pieces and samples were digested overnight at 37ºC. Tryptic peptides were extracted with 50% ACN and 5% acetic acid and dried by using vacuum centrifuge (Fendrop, USA) for subsequent iTRAQ labeling.

3.3.2.5 iTRAQ Labeling

The iTRAQ labeling of tryptic peptides, derived from supernatant and pellet fractions of the G_1, G_1/S, and G_2/M synchronized cell samples, were performed by using iTRAQ reagent multiplex kit (Applied Biosystems, USA) according to the manufacturer's protocol. The tryptic peptides were labeled with respective isobaric tags (Table 3.1) at RT for 2h.After completion of labeling, all labeled peptides were pooled together and vacuum centrifuged to dryness. Then iTRAQ labeled peptides samples were desalted by using Sep-Pak Vac C18 cartridges (Waters, Milford, MA). Desalted samples were again dried by vacuum centrifuged and subsequently used for the chromatography fractionation.

Table 3.1: iTRAQ labels for different conditions

Condition	iTRAQ label
G1-S	**113**
G1/S-S	**114**
G2/M-S	**115**
G1-P	**117**
G1/S-P	**118**
G2/M-P	**119**

3.3.2.6 Electrostatic Repulsion-Hydrophilic Interaction Chromatography (ERLIC)

iTRAQ labeled peptides were then reconstructed into 200µl of sample loading buffer (10mM ammonium acetate in 85% ACN and 1% Formic acid) and fractionated using PolyWAX LP™ column 20 (4.6×200mm^2, 5µm particle size, 300Å pore size) (PolyLC, USA) on a 21 Prominence™ HPLC unit (Shimadzu, Japan) at flow rate of 1ml/min. The 60min HPLC gradient comprised of 100% buffer A (10mM ammonium acetate in 85% ACN and 0.1% Acetic acid) for

5min; 0-28% buffer B (30% ACN and 0.1% Formic acid) for 40min; 28-100% buffer B for 5min followed by 100% buffer B for 10min. The chromatograms were recorded at 280nm. The collected fractions were combined according to their chromatogram, concentrated and dried using vacuum centrifuge.

3.3.2.7 LC-MS/MS Analysis

The ERLIC fractionated iTRAQ labeled peptides were reconstituted into HPLC grade water containing 0.1% formic acid accordingly for LC-MS/MS analysis. The mass spectrometric analysis was performed using a Q-STAR Elite mass spectrometer coupled with online nano flow HPLC system (Applied Biosystems, CA, USA). The peptides were separated using nano-bored C18 column with a picofrit nanospray tip (75µm ID×15cm, 5µm particles, New Objectives, MA, USA). The flow rate was maintained at 300nl/min. All LC-MS/MS analysis were performed in triplicate. All MS data were acquired in the positive ion mode with a selected mass range of 300-2000 m/z. Peptides having charge of +2 to +4 were selected for MS/MS. Top three abundant peptide ions above a 5 count threshold, were selected for MS/MS and dynamically excluded for 30s with 30mDa mass tolerance. Smart information-dependent acquisition (IDA) was activated with automatic collision energy and automatic MS/MS accumulation. The fragment intensity multiplier was set at 20 and maximum accumulation time was set at 2s. The peak areas of the iTRAQ reporter ions reflected the relative abundance of the proteins in the samples.

3.3.2.8 Mass Spectrometric Data Analysis

The data acquisition was performed with Analyst QS 2.0 software (Applied Biosystems/ MDS SCIEX). The identification and quantification of the proteins were performed by using Protein Pilot 3 Software (Applied Biosystems, Foster City, CA). The Paragon algorithm in the Protein Pilot software was used for the peptide identification and further processed by ProGroup algorithm where isoform-specific quantification was adopted to trace the differences between expressions of various isoforms. The defined parameters were as follows (i) Sample Type, iTRAQ 8-plex (Peptide Labeled); (ii) Cysteine alkylation, MMTS; (iii) Digestion, Trypsin; (iv) Instrument, QSTAR Elite ESI; (v) Special factors, None; (vi) Species, None; (vii) Specify Processing, Quantitate; (viii) ID Focus, biological modifications, amino acid substitutions; (ix) Database, The UniProt Knowledgebase (UniProtKB) human protein database (Downloaded on

12 March 2010, including 95624 sequences and 36307192 residues), its reversed complement were combined and used for the searches and the corresponding reverse sequence (decoy for FDR estimation); (x) Search effort, thorough. The peptide for quantification was automatically selected by Pro Group algorithm with criteria 1) the peptide having measurable iTRAQ reporter area 2) the peptide was identified with good confidence 3) the peptide was not shared with another protein identified with higher confidence to calculate the reporter peak area, error factor (EF) and p-value. The resulting data set was auto bias-corrected to get rid of any variations imparted due to the unequal mixing during combining different labeled samples.

3.3.2.9 Western blot analysis

Protein content of all protein samples were measured prior to western blot analysis. Cell lysates were prepared by sonicating the frozen cells in the lysis buffer (1% SDS in 10mM tris-HCl (pH 7.4)) and protein concentration was measured by the Bradford method. For whole chromatin samples, chromatin extracts were sonicated and dissolved in 2.5% SDS in 10mM tris-HCl (pH 7.4) and protein content of the samples were measured by using 2-D Quant Kit. Equal amount of protein from each samples were used for western blot analysis. Protein samples were resolved on 10% polyacrylamide gel and transferred into the nitrocellulose membrane. Immunoblottings were performed by using antibodies against respective proteins and ECL system (Invitrogen) was used for detecting the probed proteins.

3.3.2.10 Preparation HP1BP3 knockdown cell phenotypes

Knock down experiment was performed by using shRNA mediated knockdown strategy. RNAintro GIPZ Lentiviral shRNAmir Starter Kit (Catalog #: RHS4287, Thermo Scientific, USA) was used for the knockdown experiments. All pGIPZ clones were grown in the 100µg/ml ampicillin containing 2X LB broth (low salt) media (2% peptone, 1% yeast extract, 0.5% sodium chloride and ampicillin 100µg/ml) at 37^{o}C. Plasmids were extracted using plasmid extraction kit (Axygen, USA). Transfection of GIPZ Lentiviral shRNAmir of non-silencing and HP1BP3 shRNAs into 293T and A431 cells were performed by using Turbo-Fect Transfection Reagent (Thermo Scientific, USA). For transfection, 1×10^{6} cells were seeded on each well of a 6-well plate in 10% FBS containing DMEM growth medium and incubated for 24h at 37^{o}C. 4µg of GIPZ Lentiviral shRNAmir DNA was diluted into 400µl of serum-free DMEM medium. 6µl

Turbo-Fectin reagent was added into the diluted DNA with immediate vortexing and incubated it for 15-20min at RT. The old culture medium was replaced by 1.6ml fresh serum free DMEM medium and Turbo-Fectin/DNA mixture was added drop-wise. Gently rocked the plate for proper distribution of the complexes and incubated the plate for next 4h at 37^{o}C in 5% CO_2 containing incubator. After 4h, 2ml of growth medium containing twice the amount of normal serum was added to the cells and incubated for another 24h. The transgene expression was analyzed by observing the GFP expression under fluorescent microscopy. After 48h of transfection, transfected cells were trypsinized and seeded in the 6cm plate in 2µg/ml puromycin and 10% FBS containing DMEM medium for stable transfection selection. Cells were culture in puromycin containing medium for next 15d with occasional replacement of old puromycin containing medium with fresh medium. After 15d, each colony was cultured separately and their transgene expression level was analyzed by western blotting to confirm the knockdown efficiency. Finally highest knockdown phenotype was used for future experiment.

3.3.2.11 Chromatin compaction measurement

Chromatins were extracted from the respective cells according to the above protocol and suspended into the MNase digestion buffer (50mM tris-Cl (pH 7.9) and 5mM $CaCl_2$). Each chromatin suspension was divided into three equal volumes. 0U, 5U, and 10U of MNase were added into the respective tube. Digestion was performed for 10min at 37^{o}C and digestion reaction was terminated by adding equal volume of 2X TNESK solution (20mM tris-Cl (pH 7.4), 200mM NaCl, 2mM EDTA, 1% SDS, and 0.2mg/ml proteinkinase K) with overnight incubation at 37^{o}C. DNA fragments were extracted by Phenol-chloroform extraction technique and DNA content was measured by NanoDrop 2000 UV-Vis Spectrophotometers (Thermo Fisher Scientific, USA). Equal amount of DNA from each sample was loaded and resolved on 1% agarose gel for 2h at 80V. Gel images were taken by Gel Doc™ EQ system (Bio-Rad, CA, USA) and the DNA finger printing patterns upon MNase digestion was analysis from the images.

3.3.2.12 Quantitative proteomic profiling of HP1BP3 depleted cells

Quantitative proteomic profiling was performed by using iTRAQ based quantitative proteomic approach. Three biological replicates were pooled together and pooled cells were lysed by sonication. Equal amount of mock and HP1BP3 depleted cell lysates were trypsin

digested, labeled with 4-plex iTRAQ reagent 114 and 115 respectively and fractionated by the ERLIC fractionation technique as describe in previous section. The mass spectrometric analysis was performed using a Q Exactive mass spectrometer coupled with online nano HPLC system (Thermo Scientific; USA). The data acquisition was performed with Xcaliber 2.2 software (Thermo Scientific; USA). The identification and quantification of the proteins were performed using Proteome Discoverer 1.3.0.339 (Thermo Fisher, MA) coupled with Sequest search engine using following parameters like cysteine alkylation, MMTS as static modification and oxidation and deamidation as dynamic modification; full trypsin digestion as digestion parameter, 10ppm and 0.02Da were set as precursor mass and fragment tolerance. The UniProt Knowledgebase (UniProtKB) human protein database (Downloaded on 12 March 2010, including 95624 sequences and 36307192 residues) was used as search database and cut-off set at peptide level with less than 0.5% FDR. The resulting data set was auto bias-corrected to get rid of any variations imparted due to the unequal mixing during combining different labeled samples. All LC-MS/MS analysis were performed in duplicate.

3.3.2.13 Cell proliferation assay

3×10^3 viable cells were seeded in each well of 96-well plate and 10% FBS containing DMEM was used as culture medium. The plate was incubated for 24h at 37^oC in 5% CO_2 containing incubator. After 24h incubation, old culture medium was replaced with fresh culture medium containing 0.5mg/ml MTT reagent and the plate was again incubated for 2h at 37^oC. After 2h, medium was completely removed and 150µl DMSO was added to dissolve the purple formazan crystals. The optical density of formazan was measured at 570nm and 630nm was used as reference wavelength, by using a micro-plate reader (Tecan Magellan™, Switzerland)

3.3.2.14 Cell cycle phase duration measurement

Cells were synchronized at the G_1/S transit using double thymidine block approach. Cells were treated with 2.5mM thymidine for 18h and then released in the fresh medium for 8h followed by another thymidine treatment for 18h. G_1/S synchronized cells were released in fresh medium to restart the cell cycle. Cells were collected at different time point within 0-12h time period after released from G_1/S block. Cells were then fixed and stained with propidium iodide accordingly as described in the previous section. DNA content was measured by flow-cytometry.

100μM Tranylcypromine hydrochloride ((±)-trans-2-Phenylcyclopropylamine hydrochloride (2-PCPA)) was used for inhibition of KDM1 activity. To study the KDM1 inhibition effect on cell cycle progression G_1/S synchronized cells were released in the fresh cell culture medium containing 100μM 2-PCPA and cells were collected within 0-12h time period. Fresh medium was used as a control because 2-PCPA was a water soluble compound. A similar study was conducted to determine the effect of HP1BP3 depletion upon cell cycle. For this purpose, both mock and HP1BP3 depleted phenotypes were used for comparison.

3.3.2.15 Clonogenic assay

500 viable cells were seeded on each well of the 6-well plate, into 10% FBS containing DMEM medium and incubated for 12d at 37°C in a 5% CO_2 incubator. At 13^{th} day, medium was removed and cells were washed with PBS. Cells were then fixed with 95% ethanol and stained with 5% crystal violet solution for 15min at RT. The excess crystal violet was removed by extensive PBS washing. Washed plate was completely dried in air. The colony formed /500 cells were counted and recorded. For quantification crystal violet was dissolved in 2ml 0.5% triton X-100 solution and optical density was measured at 595nm.

3.3.2.16 Immunofluorescence analysis

0.5×10^6 cells were seeded on top of a $20\times20mm^2$ cover slips inside the 6-wells plate and grown up to 50% visual confluence. The 50% confluent cells were washed thrice with PBS and fixed with 4% paraformaldehyde for 20min at room temperature (RT). Excess paraformaldehyde was removed by washing the cells twice with HBSS. Cell membranes were stained with 1mg/ml Alex 594-conjugated wheat germ agglutinin (WGA) (Invitrogen, USA) for 10min at RT. Excess WGA was removed by PBS washing. Cells were then permeabilized by treating them with 0.2% triton X-100 in PBS for 5min at RT. Triton X-100 was removed by PBS washing. Then cells containing cover slips were air dried for 2h at RT inside a dark cabinet. Finally cover slips were mounted on a glass slides with DAPI (1.5μg/ml) containing vectashield mounting medium (Vector Laboratories, Burlingame, California, USA). Immunostained samples were then examined by Axio Observer D1 microscope equipped with the 63X/1.25 NA Plan-Neofluar objective (Zeiss, Germany). ImageJ software was used for images processing and analysis.

3.4 Results and discussion

3.4.1 Mass spectrometric identification and quantification of the chromatin proteome

To study the chromatin association topology of chromatin interacting proteins, 293F cells were cultured and synchronized in different stages of cell cycle (G_1 phase, G_1/S phase and G_2/M phase) by double thymidine and thymidine-nocodazole block (Fig. 3.1). The chromatin fractions were extracted from the synchronized cells and partially digested with MNase to liberate euchromatin binding proteins. Heterochromatin and matrix associated chromatin interacting proteins remained in the undigested pellet fractions. Complete purification of specific portion of an organelle like chromatin which is strongly interconnected with other part of the organelle, is very challenging when mass spectrometry or other non-biased techniques were used for identification. Western blot analysis showed that tubulin α was present in very high amount in the cytosolic fraction, while it was much lower in chromatin fraction (Fig. 3.2a). In western blot analysis the key chromatin component, histone H2A is shown to be present only in the chromatin fractions indicating higher chromatin enrichment in the extracted fractions (Fig.3.2a). Proteins were in-gel digested by trypsin. Tryptic peptides were labeled with iTRAQ reagent, pooled and separated using ERLIC fractionation and run in the QqTOF instrument. The peptides spectra were searched by ProteinPilot 3 software for both identification and quantification. UniProtKB human protein database was used for searching to identify and quantify the proteins.

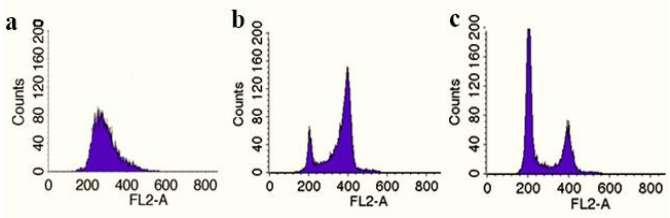

Figure 3.1: Different phase synchronized the cells. a, Double thymidine treated G1/S phase synchronized cells. b, Thymidine and nocodazole treated G2/M phase synchronized cells. c, G1 phase synchronized cells collected 8h after release from G2/M.

In this study, total ~0.12 million spectra acquisition were done from the three technical replicates with total 84 LC-MS/MS runs. After ProteinPilot search, total 681 high confidence proteins were identified with unused score above 2 (99% confidence) and FDR below 1%. Among them, 481 proteins were enlisted which were identified with more than one unique peptide (95% confidence). According to Uniprot database 332 of them have evidence at protein

level and rest of them have only evidence at genetic or transcript level, indicating the chromatome is relatively understudied. The identified proteins were classified according to their subcellular localization reported in the Uniprot and Nextprot database (Fig. 3.2b). Classification indicated that majority of the identified proteins (74%) were localized inside the nucleus and 7%

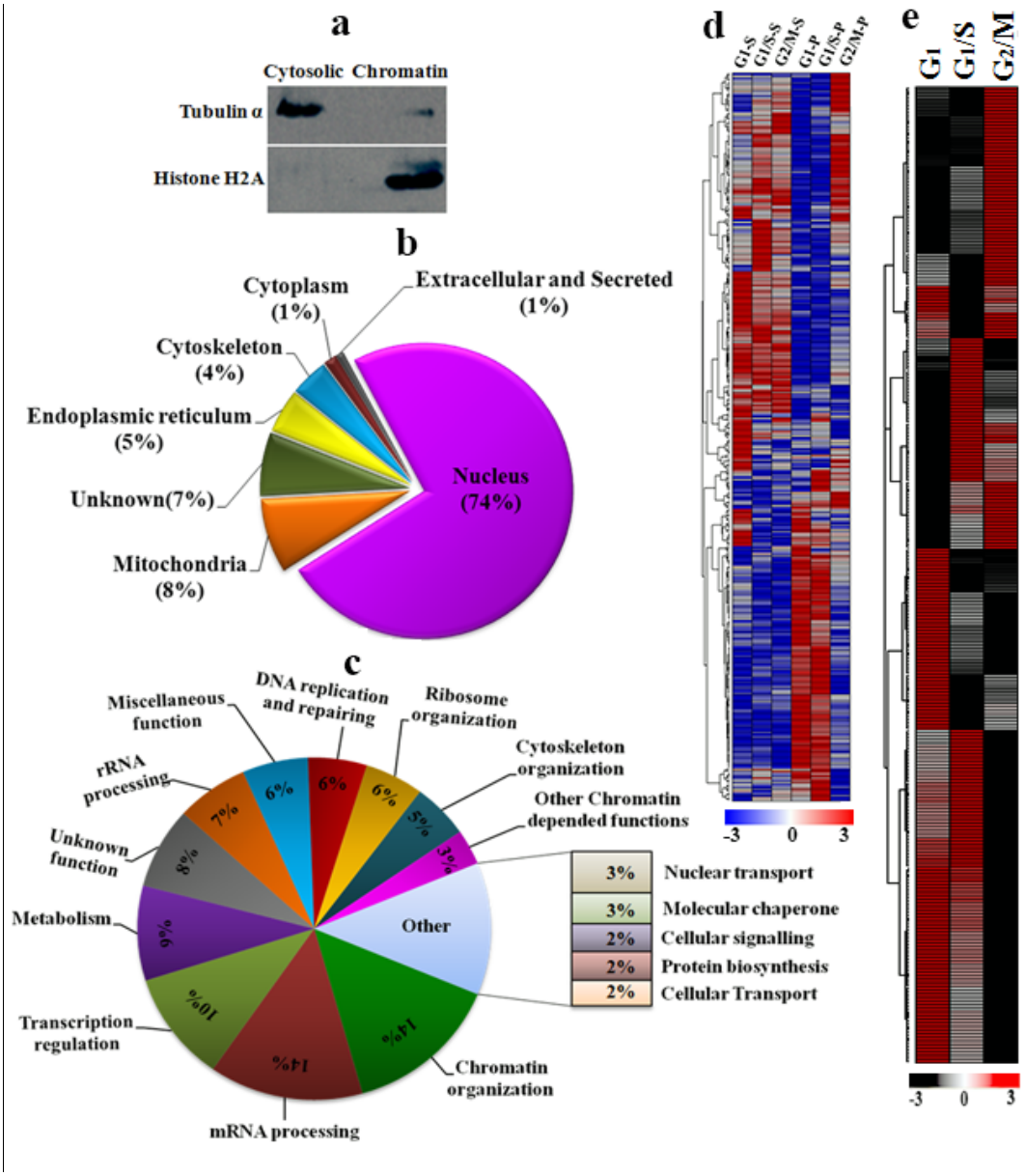

Figure 3.2: Characterization of identified proteins. a: Western blot of tubulin α and histone H2A in cytosolic and chromatin fraction indicating enrichment of chromatin. b: Classification of identified proteins according to their subcellular localization. c: Functional classification of identified proteins. d: Heat map represent the relative protein abundance in the different interphase chromatin digests. e: Heat map represent the relative protein abundance in the different interphase chromatin digests. Supernatant fractions G1-S, G1/S-S and G2/M-S and undigested pellet fractions G1-P, G1/S-P and G2/M-P were obtain from partial MNase digestion of G_1, G_1/S and G_2/M phase chromatin.

of identified proteins have no specified subcellular localization. The rest of the proteins were localized in mitochondria (8%), endoplasmic reticulum (5%), cytoskeleton (4%), cytoplasm (1%) and extracellular region (1%). The identified proteins were also classified according to their biological functions (Fig. 3.2c). The classification showed most of them were involved in various nuclear events like chromatin organization (14%), transcription regulation (10%), DNA replication and repair (6%), other chromatin depended functions (3%), nuclear transport (3%), mRNA processing (14%), and rRNA processing (7%). 8% of identified proteins do not have any define cellular functions. The rest of the proteins were involved in other cellular events such as ribosome organization (6%), cytoskeleton organization (5%), metabolism (9%), molecular chaperone (3%), cellular signaling (2%), protein biosynthesis (2%), cellular transport (2%) and other (6%).

Table 3.2: Data analysis of identified proteins in different interphase chromatin digests.

	Number of proteins with significant change in iTRAQ ratio (p-value <0.05)					
Sample	**G1/S-S**	**G2/M-S**	**G1-P**	**G1/S-P**	**G2/M-P**	**Total number of unique protein***
iTRAQ ratio	**114:113**	**115:113**	**117:113**	**118:113**	**119:113**	
Total	148	117	245	233	153	334
Ratio>1.3	63	44	108	107	65	219
Ratio<0.75	59	45	131	121	72	209

*The number of unique proteins with at least one ratio with p<0.05

The G_1 phase supernatant (G1-S) was used as denominator for the relative quantification of respective conditions. Proteins having significant iTRAQ ratio (P value <0.05) at least in one condition, were chosen and narrowed down the quantified protein list at 334, which was used for the farther analysis. iTRAQ ratio above 1.3 and below 0.75 were considered as cutoff value for the abundance change. Quantitative proteomic data showed total 219 proteins were increased and 209 proteins were decreased their abundance in the different chromatin digests (Table 3.2). Proteins were clustered according to their abundance levels in different chromatin digests. Pearson-correlation was used for the hierarchical clustering of the quantified proteins, which indicates the differential chromatin association topology of the chromatin interacting proteins during the interphase progression (Fig. 3.2d). The relative chromatin-association of the identified

proteins were determined by adding iTRAQ ration of corresponding pellet and supernatant fractions and cluster analysis was performed to understand their chromatin association patterns (Fig. 3.2e).

Chromatin is a protein-DNA complex that acts as a master controller of DNA dependent cellular events. DNA-protein as well as protein-protein interactions play a major role in the regulation of chromatin structure and functions. Throughout interphase higher order chromatin structures are very dynamic in nature and alternatively formed two types of structure, loosely compacted euchromatin and highly condensed heterochromatin. Our partial MNase digestion data showed that easily accessible euchromatin regions were digested by MNase and released the associated proteins, while highly condensed heterochromatin regions remain undigested with associated proteins and proteins were identified in the pellet fractions. Partial MNase digestion of different interphase chromatins showed the differential release pattern as shown in the figure 3.2d. Differential chromatin association patterns of the chromatome during different stages of cell cycle were presented in the heat map (Fig. 3.2e).

3.4.2 Interphase progression and DNA repair

DNA repair is the only defense mechanism to maintain the genomic integrity throughout life time. During DNA repair process, cells repair DNA lesions caused by both endo- and exogenous factors and maintain the genomic integrity. Any sign of genomic instability cause cell cycle delay or arrest by activating check point signaling pathways. Different types of repair mechanisms are activated during different stages of cell cycle to repair the damaged DNA lesions and maintain the steady cell cycle progression. Many DNA repair proteins were identified during this study and these proteins were clustered according to their abundance in different chromatin digests. Cluster analysis showed four distinct protein clusters (cluster a-d) (Fig. 3.3). Proteins in ‘cluster c’ showed that their chromatin associations were relatively increased during early G_1 phase and proteins in ‘cluster b’ and ‘cluster d’ showed their relatively higher chromatin association during G_1/S phase. One of the important DNA repair mechanisms is mismatch repair (MMR) systems essentially involved in the replication induced base mismatches correction which plays a key role in the maintenance of genetic stability [208].

MMR system is composed with many proteins and protein-complexes such as MutSα or MutSβ, MutLα, RPA, EXO1, RFC, HMGB1, PCNA, polymerase and ligase I [209]. MRM is progressing back to back with replication [210] and 8-oxoguanine containing lesions are corrected through MSH2/MSH6-dependent manner during replication [211]. Our experimental data showed heterodimer MutSα complex components MSH2 and MSH6 were cluster in 'cluster c' indicating their association during G_1/S transit and their release data indicated that higher amount of MSH2 and MSH6 were present in G_1/S phase pellet fraction (Fig. 3.4b). Another MMR protein RFC4 also showed its higher abundance in G1/S-P fraction (Fig. 3.6c). Our proteomic results reflected that MMR proteins were loaded into the chromatin during G_1/S transit. DNA double strand breaks (DSBs) caused by both end- and exogenous factors occurred frequently during cell cycle progression. DSBs induce genome instability is stabilized by non-homologous end joining (NHEJ) and homologous recombination (HR) pathways dependent manner. DNA-dependent protein kinase (DNA-PK) plays a key role during NHEJ based DSBs repair pathway. DNA-PK is a holoenzyme complex compose of DNA binding Ku70/Ku80 heterodimer and catalytic (DNA-PKcs) subunit and interaction between DNA-Ku complex and N-terminal of DNA-PKcs activated kinase activity of the enzyme [212]. Euchromatin DSBs are repaired by NHEJ during both G_1 and G_2 phase but heterochromatin DSBs were repaired only during G_2 phase by HR pathway [213, 214]. Recent studies also showed HR pathway dependent DSBs repair also activated during S phase [215]. We identified the DSBs repair proteins in 'cluster b'. Our iTRAQ based proteomic data and western blot analysis showed Ku70 and Ku80 were highly down-regulated in the pellet fractions

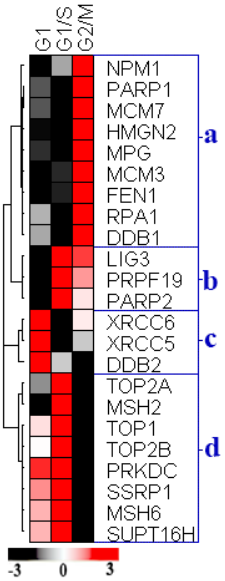

Figure 3.3: Chromatin association of DNA repair proteins in different stages of interphase. Proteins are clustered into four clusters. 'cluster a', proteins association was comparatively increase within G_2/M phase chromatin; 'cluster b', proteins association was comparatively increased in G_1/S phase chromatin but decreased greatly during early G_1 phase; proteins association was comparatively increased in G_2/M phase chromatin; 'cluster c', proteins association was comparatively increased in early G1 phase chromatin; 'cluster d', proteins association was comparatively increased in late G_1 phase (G_1/S) chromatin but greatly decreased during early G_2/M phase.

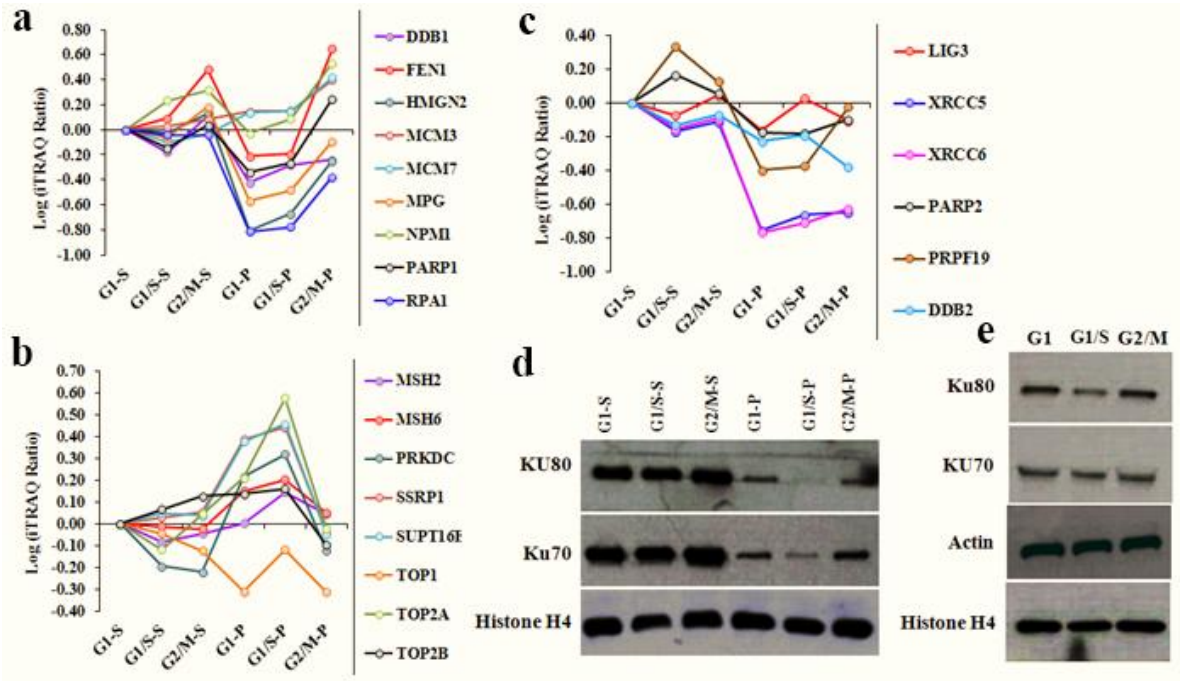

Figure 3.4: Differential release of DNA damage repair proteins from different interphase chromatins during MNase digestion. a-c: iTRAQ ratio represent the relative abundance of protein present in different chromatin digests. Supernatant and pellet fractions were obtain from partial MNase digestion of G_1, G_1/S and G_2/M phase chromatins. d: Western blot represent the concentration of Ku70, Ku80 and Histone H4 in different chromatin digests. e: Western blot represent the protein excrescent level of Ku70, Ku80, histone H4 and actin during G_1,G_1/S and G_2/M phase of cell cycle.

indicating their binding within the euchromatin regions (Fig. 3.4c). Proteomic results showed relatively lower amount of DNA-PK subunits were present in the G1/S supernatant fraction (Fig. 3.4b). Western blot analysis also shown DNA-PK subunit Ku70 and K86 were present in a relatively lower amount in both G_1/S phase supernatant and pellet fractions (Fig. 3.4d). Western blot analysis of whole cell lysate shown expression level of Ku70 and Ku80 were down-regulated during G_1/S transit (Fig. 3.4e). In the context of our experimental data we suggested that NHEJ pathway proteins are loaded into the chromatin throughout the interphase. During early G_1 and G_2 phase, both their expression and chromatin loading were increased due to activation of specific DSBs repair pathways during specific period of cell cycle. Proteins in 'cluster a' shown their higher chromatin association during G_2/M phase indicated their involvement in G_2 specific DNA repair. FEN1 endonuclease removed the 5′ overhanging DNA flaps during replication and repair process. Mutation of this protein causes cell cycle arrest at G_2 and cell death due to lack of its DNA repair ability [216]. FEN1 is localized at telomere regions

after replication and through HR repair pathway it is involved in maintenance of the telomere structure [217]. In this study relatively higher amount of FEN1 was identified in both G_2/M phase supernatant and pellet fractions (Fig. 3.4a). Due to its localization within nuclease resisted telomere regions, protein remains unreleased after partial MNase treatment and found comparatively higher concentration in the pellet fractions. Another two DNA repair protein MPG and DDB1 were released in higher amount after partial MNase treatment and specifically identified with higher abundance in the G_2/M phase supernatant fraction (Fig. 3.4a) indicates their involvement in G_2 phase specific euchromatin lesions repair.

3.4.3 Chromatin organization and transcription regulations during interphase phase progression

Most of the chromatin dependent biological events were performed during interphase. Differential chromatin association of chromatin organizer and transcription regulator non-histone proteins during the interphase progression might provide the picture of the higher order structural and regulation of corresponding biological events. In the present study 62 proteins were identified, which were involved in the chromatin organization and transcription regulations. Cluster analysis of those proteins showed their differential chromatin association levels during different interphase stages. Proteins produced three distinct clusters (cluster a-c) and each cluster was divided into two sub-clusters (Fig. 3.5) according to their relative abundance which indicates their differential chromatin association level. Proteins in ‘cluster a’ showed their higher chromatin association during early G_1 phase when compare to the G_1/S (late G_1) and G_2/M phases (Fig. 3.5) indicating their higher transcription regulation activity during early G_1 phase. Similarly, proteins grouped in ‘cluster b’ clustered specifically increased their chromatin association in G_1/S arrested cells reflecting their specific activity during the late G_1 phase and might involve in G_1/S specific chromatin dependent cellular events. Release profiles of these proteins are represented in figure 3.6a-f. During the G_1-S phase progression influence of the external growth factors activated a huge number of genes which are essential for the S phase progression due to their direct or indirect involvement in DNA synthesis [218]. Recent evidences suggested that transcription regulator protein ILF2 and IFL3 are vital for cell growth and their depletion inhibit DNA synthesis and reduce cellular growth [219]. Here in this study we found that chromatin association of the transcription factors including ILF2, ILF3, PA2G4, PUF60,

DDX5, and HNRNPK ('cluster b2') were increased in G_1/S arrest cells and digestion results exhibited that proteins were present in a greater quantity in all supernatant fractions compare to the pellet factions (Fig. 3.6d). Their association within nuclease susceptible active euchromatin regions caused their easy released after MNase treatment. Proteomic data also suggested that chromatin association of transcription machinery proteins including POLR2A and POLR2B were increased during G_1 and G_1/S phase (Fig. 3.6b-c) which indicate the global transcription activation [220] during G_1-S phase progression justify our proteomic findings. Cyclin D1 is a G_1 cyclin, regulate G_1 phase progression and its expression was modulated through chromatin remodeling factor SNF2H and C/EBP family CCAAT binding protein [221]. Proteomic data showed that chromatin association of CCAAT binding protein CEBPZ and ATP-dependent chromatin remodeling complex protein SMARCA5 were increased during G_1 phase. Release profiles showed higher concentration of proteins in the pellet fractions and chromatin association of CEBPZ was

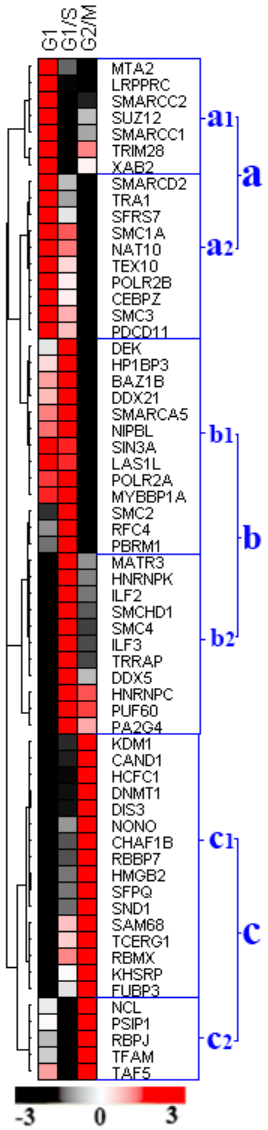

Figure 3.5: Chromatin associations of chromatin organization and transcription regulations during different stages of interphase. Proteins are cluster in to three distinct cluster 'cluster a-c' and each cluster divided into two sub-clusters. 'Cluster a': Proteins association was comparatively increase in early G_1 phase chromatin whereas in sub-clusters 'cluster a1' and 'cluster a2' proteins association was comparatively increase in early G_1 phase but decrease greatly during G_1/S and G_2/M phase respectively. 'Cluster b': Proteins association was comparatively increase in early G_1/S phase chromatin whereas in sub-clusters 'cluster b1' and 'cluster b2' proteins association was comparatively increase in G_1/M phase but decrease greatly during G_2/M and early G_1 phase respectively. 'Cluster c': Proteins association was comparatively increase in early G_2/M phase chromatin whereas in sub-clusters 'cluster c1' and 'cluster c2' proteins association was comparatively increase in early G_2/M phase but decrease greatly during G_1 and G_1/S phase respectively.

decrease in G_1/S phase compare to the early G_1 phase (Fig. 3.6b). Experimental findings suggested that CEBPZ associated with chromatin during early G_1 phase and repress cyclin D1 expression. Gradual reduction of its chromatin association to words S phase increased cyclin D1 expression, which maintains the G_1 phase progression. Due to their repressor activity its binding regions might produce resistance to nuclease cleavage and remain unreleased after partial MNase treatment.

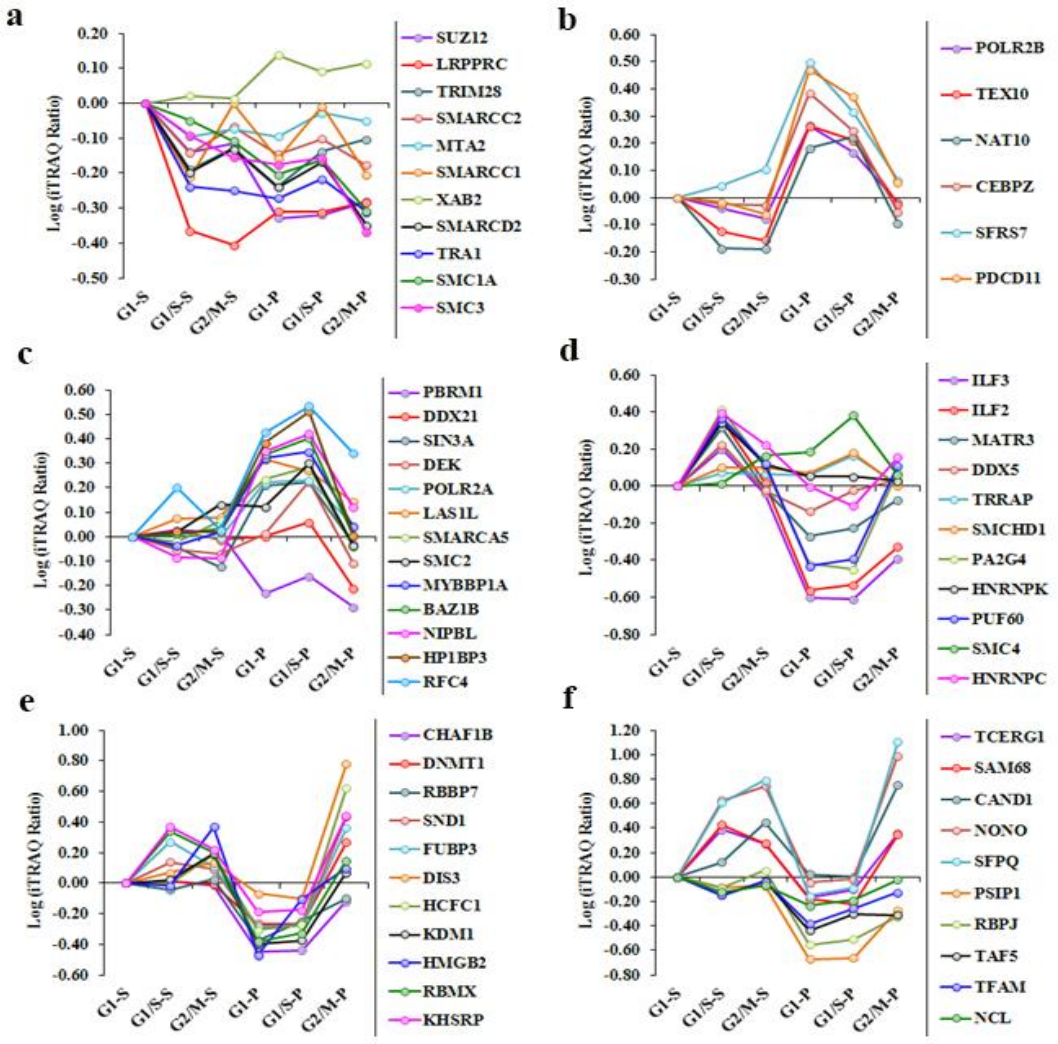

Figure 3.6: Differential release of chromatin organizer and transcription regulator proteins from different interphase chromatins during MNase digestion. a-b: Differential chromatin association pattern of the 'cluster a' proteins. c-d: Differential chromatin association pattern of the 'cluster b' proteins. e-f: Differential chromatin association pattern of the 'cluster c' proteins. iTRAQ ratio represent the relative abundance of protein in the different chromatin fractions. Supernatant fractions G1-S, G1/S-S and G2/M-S and undigested pellet fractions G1-P, G1/S-P and G2/M-P were obtain from partial MNase digestion of G_1, G_1/S and G_2/M phase chromatin.

Proteins in the 'cluster b1' like SMARCA5, HP1BP3, NAT10, BAZ1B, TEX10, SIN3A, LAS1L, and MYBBP1A increased their chromatin binding during G_1 phase compare to the G_2/M phase. Chromatin binding of these proteins were gradually increased during G_1 phase progression and reached the maximum level during late G_1 phase (G_1/S phase) (Fig. 3.6c). Data also showed that maximum amount of proteins were remain unreleased after partial MNase digestion and protein abundance was increased in early G_1 and G_1/S phase pellet fractions compare to G_2/M pellet and all supernatant fractions (Fig. 3.6c). The release profiles indicated that proteins were mainly associated within the nuclease resist heterochromatin regions and remain unreleased after partial MNase treatment. Our western blot analysis also showed that chromatin association of HP1BP3 was increased during early G_1 phase and G_1/S transit compare to G_2/M phase (Fig. 3.7a-b). Emerging evidences suggested that chromatin association of transcription repressor, MYBBP1A is essential for both maintenance of heterochromatin integrity and transcription regulation [222]. According to our proteomic data we suggested that proteins in the 'cluster b1' might regulate transcription activation by maintaining heterochromatin integrity during G_1-S progression and prevent unwanted gene expression [223], which is essential for smooth and steady G_1-S progression.

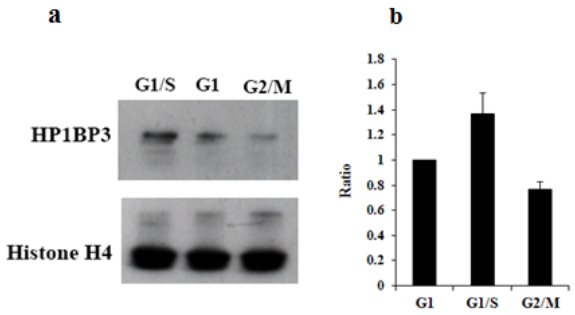

Figure 3.7: Western blot analysis of HP1BP3 in different interphase chromatins. a: Chromatin association of HP1BP3 during G_1, G_1/S and G_2/M phase. b: Relative association level of HP1BP3 with G_1, G_1/S and G_2/M phase chromatin.

Proteins clustered in 'cluster c' were specifically increased their chromatin associations during G_2/M phase compare to early G_1 and G_1/S phase chromatin reflect their chromatin association which might be essential for G_2/M phase progression. Differential release patterns of these proteins in figure 3.6e-f provide their dynamic chromatin association patterns during interphase progression. Reported evidences suggested that HCF-1 and other proteins of this family are involved in both activation and repression of cell cycle regulator genes [224]. Our iTRAQ based proteomic results showed that HCFC1 was present relatively in higher abundance in both G_2/M phase supernatant and pellet fractions as compared to other conditions (Fig.3.6e)

indicates its association with both euchromatin and heterochromatin which could modulate G_2/M specific transcriptions. DNMT1 methylates the CpG islands and maintains its hyper-methylation status, which is essential for maintaining the heterochromatin structure [225]. Proteomic result showed that DNMT1 was present in much higher concentration in G_2/M phase pellet fraction (Fig. 3.6e) indicating its involvement in the maintenance of heterochromatin integrity during the G_2/M phase. Unlike DNA methyl transferease DNMT1, histone demethylase KDM1 and non-histones HMGB2 increased their chromatin association in the G_2/M arrested cells. Digestion data showed that higher amount of protein released after MNase digestion and protein abundance was relatively higher in G_2/M phase supernatant fraction (Fig. 3.6e) reflected their localization within the euchromatin territory during G_2/M phase. Lysine-specific histone demethylase KDM1 is one

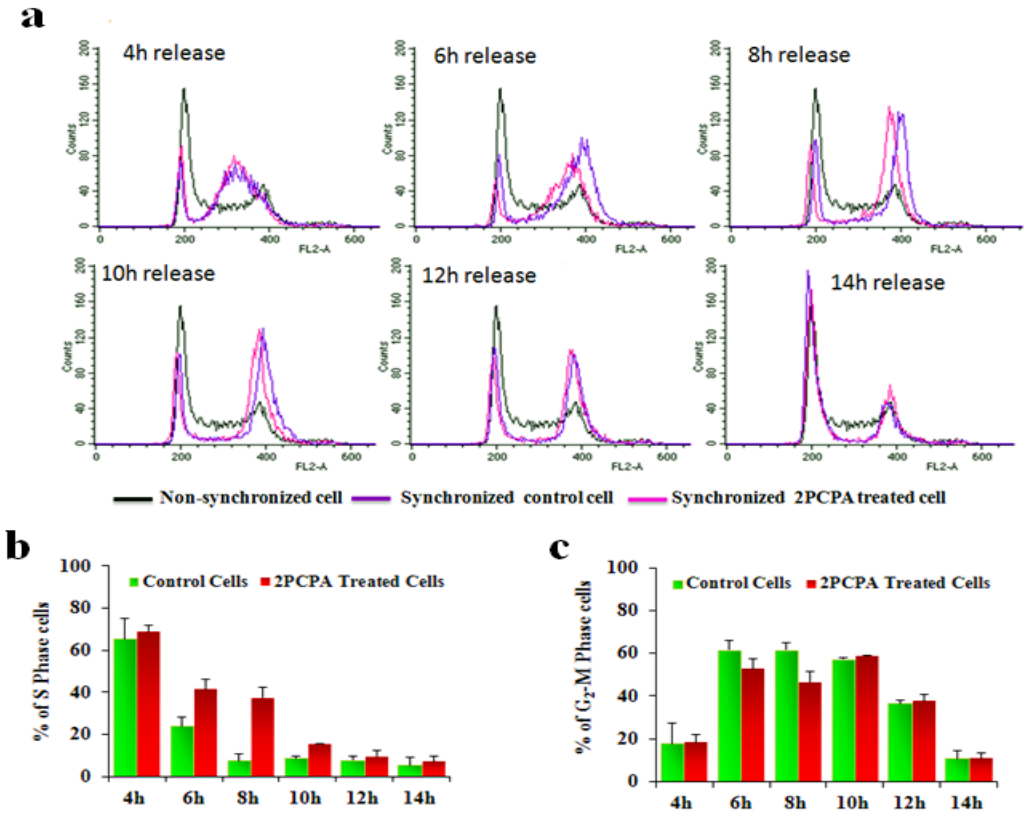

Figure 3.8: Effect of KDM1 inhibition on cell cycle progression. a: Histogram representations of DNA content of cells within 4-14h time period after release from double thymidine block. b-c: % of S phase and G_2-M phase cells present into the total population of cells during 4-14h time period after release from double thymidine block.

of the key enzymes responsible for the histone demethylation specifically at the H3K4 and H3K9 position. Demethylation of methylated histone, KDM1 modifies the epigenetic code and regulates gene expression [226, 227]. To understand its cell cycle specific role, KDM1 was inhibited by using 2PCPA. KDM1 inhibited 293T phenotypes were not exhibit cell cycle arrest but showed delay progression of the S/G_2 transit (Fig. 3.8a-c). Both proteomic and biochemical data revealed that KDM1 mediated histone demethylation is essential for maintenance of the chromatin integrity and gene expression during G_2 phase. Chromatin association pattern of non-histone HMGN2 was comparable with KDM1, suggested that HMGN2 could involve in the regulation of G_2 specific gene expression which is essential for proper G_2 progression. Proteins 'cluster c2' showed that transcription factors and regulator proteins including PSIP1, RBPJ, TAF5, TFAM and NCL were relatively increased their chromatin loading during G_2/M phase (Fig. 3.5). Their release profiles showed that respectively high concentrations of proteins were present in the supernatant fractions in respect to pellet fractions indicate their association in the active sites (Fig. 3.6f). But significant difference was not found in between supernatant fractions reflected that their chromatin association topology is not significantly changed during interphase progression (Fig. 3.6f).

Our proteomic data provided information regarding chromatin binding topology of the chromatin associated proteins and also help to explain their possible functional roles during the cell cycle progression. Here in the present study, proteomic and western blot data showed that this novel chromatin interacting protein HP1BP3 was gradually increased its chromatin association during G_1-S phase progression. Proteomic results suggested its dynamic heterochromatin association during interphase progression. Further bioinformatics analysis revealed that HP1BP3 protein is conserved in higher vertebrate. Bioinformatics analysis also revealed that HP1BP3 had three conserved 'histone-H1' like domains. HP1BP3 still is not functionally characterized. Emerging evidences suggest that it might have some involvement in chromatin organization [228]. Based on our data mining of the rich dynamic cell cycle proteomic data generated in the discovery phase, we have identified a testable hypothesis that HP1BP3 is likely a key protein regulating the chromatin template in G_1 phase by inter-converting euchromatin and heterochromatin to active or silent specific genes. Based on the hypothesis, HP1BP3 was chosen as a candidate protein for details functional study.

3.4.4 HP1BP3 novel regulator of heterochromatin structure

To study the functions of HP1BP3 during the cell cycle progression, HP1BP3 expression has been knockdown by using corresponding shRNA (Fig. 3.9). Reported evidences suggested that HP1BP3 might have involvement in chromatin structural regulation. Structural studies of HP1BP3 showed that the middle region of the protein from residue 153 to 237 has three 'histone-H1' like domains which provide the linker DNA binding property [228]. Structural information also suggested that histone-H1' like domains of HP1BP3 have AKP (Ala-Lys-Pro) helix motif which neutralized the linker DNA segments through electrostatic interaction and formed a chromatosome like structure with reconstituted mononucleosomes [228]. Structural evidences also recommended that HP1BP3 directly interacts with heterochromatin binding protein 1 (HP1) through PXVXL (Pro255–Leu259) motif [228]. Our proteomic data found its maximal presence in the undigested chromatin fractions indicates its heterochromatin specific localization. Evidence of its direct interaction with HP1 justifies our proteomic findings. To study its depletion effect on chromatin structure, mock- and HP1BP3 depleted chromatins were extracted and digested with different amount of MNase for 10min.

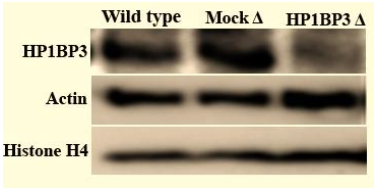

Figure 3.9: HP1BP3 knockdown in 293T. Western blot showed the HP1BP3 expression level in wild type: mock depleted: and HP1BP3 depleted 293T stable cell line.

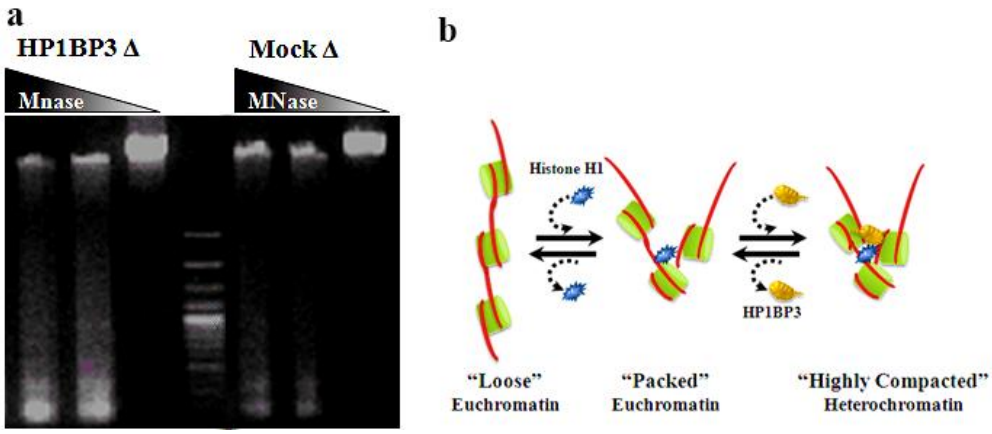

Figure 3.10: Effect of HP1BP3 depletion on higher order chromatin structure. a: MNase figure printing of Mock and HP1BP3 depleted chromatin. Chromatins were digested with different concentration MNase (0U, 5U, and 10U) and then separated by 1% agarose gel. b: Model of HP1BP3 mediated heterochromatin packing.

amount of MNase for 10min. Digestion results showed that HP1BP3 depleted chromatins were more susceptible to MNase digestion compared to mock depleted phenotype (Fig. 3.10a). DNA of the highly condensed heterochromatin regions is inaccessible to other interacting proteins or enzymes and remains undigested during nuclease digestion. Digestion result suggested that HP1BP3 depletion convert indigestible heterochromatin into a MNase digestible chromatin. Evidence with our experimental data and available structural data we hypothesized that HP1BP3 is essential for the chromatin packing inside heterochromatin and depletion of HP1BP3 causes destruction of heterochromatin structure due to unfolding of the chromatin as shown in the model (Fig. 3.10b).

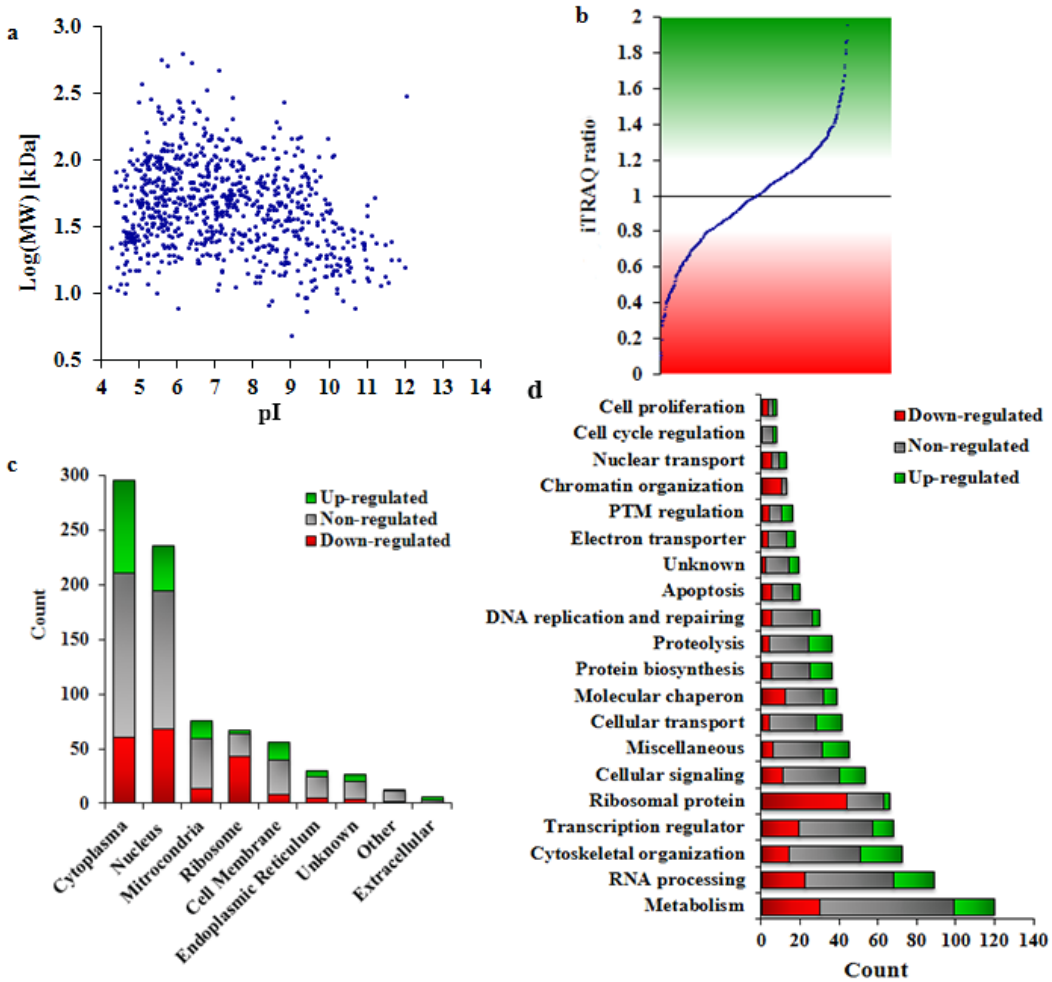

Figure 3.11: HP1BP3 depletion and protein expression. a, Distribution of molecular weight (MW) and isoelectric point (pI) identified proteins. b: iTRAQ ratio represent the differential protein expression of HP1BP3 depleted cells. c: Classification of identified proteins according to their sub-cellular localization with their differential expression. d: Classification of identified protein based upon their cellular function with their differential expression.

3.4.5 Effect of HP1BP3 depletion upon protein expression

Our experimental data showed that HP1BP3 plays a key role in the maintenance of higher order chromatin structure. Any change in higher order chromatin structure affects the transcription regulation which was reflected by the alteration of many cellular events [229]. Alternation in transcription level is reflected in the protein expression level. To study this altered protein expression levels we used iTRAQ based quantitative proteomic approach to identify the differentially expressed proteins in HP1BP3 depleted cells. Our iTRAQ experiment identified total 1651 high confidence proteins with FDR less than 1%. Among them we enlisted 815 proteins which were identified with more than one unique peptide. Distribution of molecular weight and isoelectric point of the identified proteins (Fig. 3.11a) indicated that our technique was equally promising for each and every kinds of protein identification. We set the cutoff values for regulated proteins, iTRAQ ratio above1.2 for up-regulation and below 0.8 for down-regulation. We identified 378 proteins which were expressed differentially in HP1BP3 depleted cells (Fig. 3.11b). Among the 378 differentially expressed proteins 178 were up-regulated and 210 were down regulated in HP1BP3 depleted cells. The identified proteins were classified according to their sub-cellular localization and also basis of their biological functions (Fig. 3.11c-d). Quantitative proteomic data suggested that HP1BP3 not only maintain the heterochromatin integrity but also regulate protein expression through controlling gene transcription.

3.4.6 HP1BP3 novel regulator of cell proliferation

Cell growth is influenced by both external and internal factors including nutrients, extracellular environment, gene expression, protein modification and many other factors. The proper coordination between all external and internal factors is essential for maintenance of the healthy cell growth [230]. Our MTT assay showed HP1BP3 depletion increase cell proliferation by 39% (Fig. 3.12a). 18% increment in clonogenicity was observed in HP1BP3 depleted cells during colonogenic assay (Fig. 3.12b-c). There was no significant difference between mock and HP1BP3 depleted cells during cell cycle analysis. To study the change in any specific phase length we synchronized the cells in G_1/S phase by double thymidine treatment and released them from G_1/S arrest. We observed HP1BP3 depleted cells were pass the G_1/S transit and progress

through S phase which is relatively faster than mock depleted cells (Fig. 3.12d-e). Recent evidence revealed that G_1 and G_1/S phase has a major contribution in cell proliferation regulation [231, 232]. Higher order chromatin structure also involve in the regulation of cell proliferation by controlling cell cycle progression [233]. Our experimental data suggested that HP1BP3 plays a significant role in G_1-G_1/S specific transcription regulation by maintaining the heterochromatin interiority. Depletion of HP1BP3 caused imbalance in transcription regulation which promotes quicker G_1/S transit and shortening the total cycle time and increases cell proliferation.

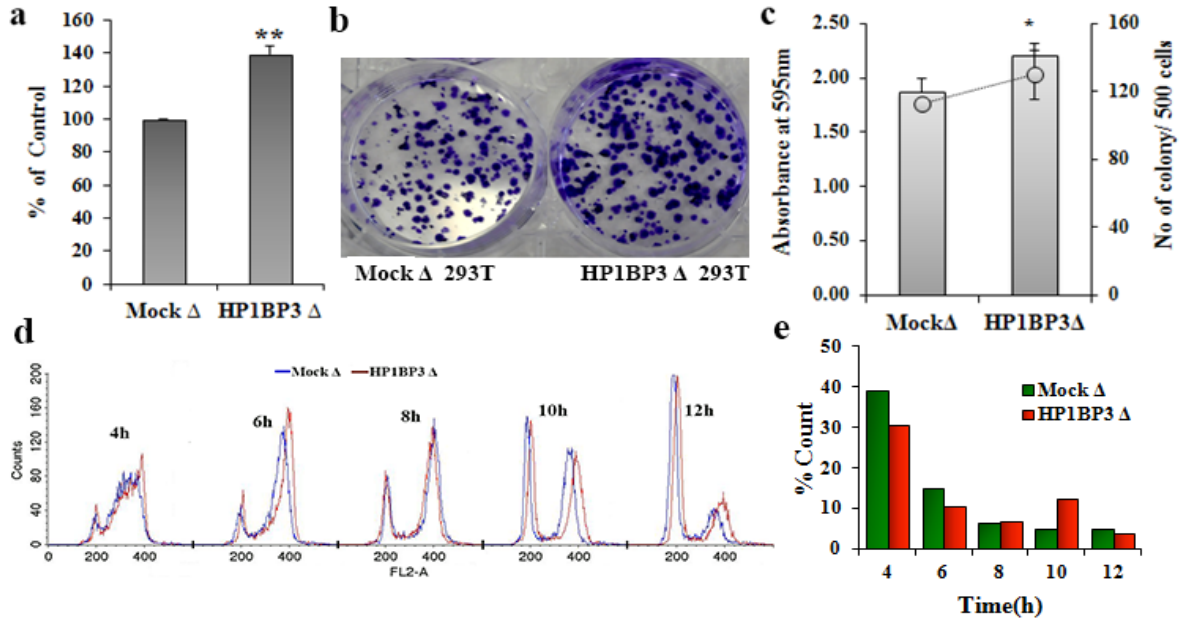

Figure 3.12: HP1BP3 and regulation of cell proliferation. a: MTT assay result represent the relative amount of viable cells in mock and HP1BP3 deleted samples. b: Mock and HP1BP3 depleted cell colony stained with crystal during colonogenic assay. c: Graph represents the both number colonies formed by both mock and HP1BP3 depleted cells and corresponding absorbance value represent the amount of crystal violet needed for stain the colony. d: Progression of cell cycle after release from double thymidine block with in 4h-12h time period. e: S phase cells present in the cell sample collected within 4-12h time points after thymidine withdrawal.

3.4.7 HP1BP3 novel regulator of nuclear size

Our data showed that depletion of HP1BP3 have no impact upon cell size. Both mock and HP1BP3 depleted cells produce identical size distribution profile during FACS based size measurement (Fig. 3.13c). We found that nuclear size distribution of HP1BP3 depleted cells was

different from mock deplete cells and nuclear size was increased in HP1BP3 depleted cells (Fig. 3.13a-b, and d). Nuclear size mainly depends upon cell size [234] and also modulates through other biological factors. But actual reason behind the size regulation was poorly understood. Here we found that HP1BP3 depleted nuclei were larger in size while cells size was comparable with mock depleted cells. Our findings also showed depletion of HP1BP3 caused unpacking of heterochromatin. Experimental data suggested that depletion of HP1BP3 induces both chromatin decondensation and nuclear size increment together. But reported observations and evidences indicated that chromatin condensation and nuclear size modification occurred independently though they happened simultaneously [235]. Reported evidences also showed that nuclear size is

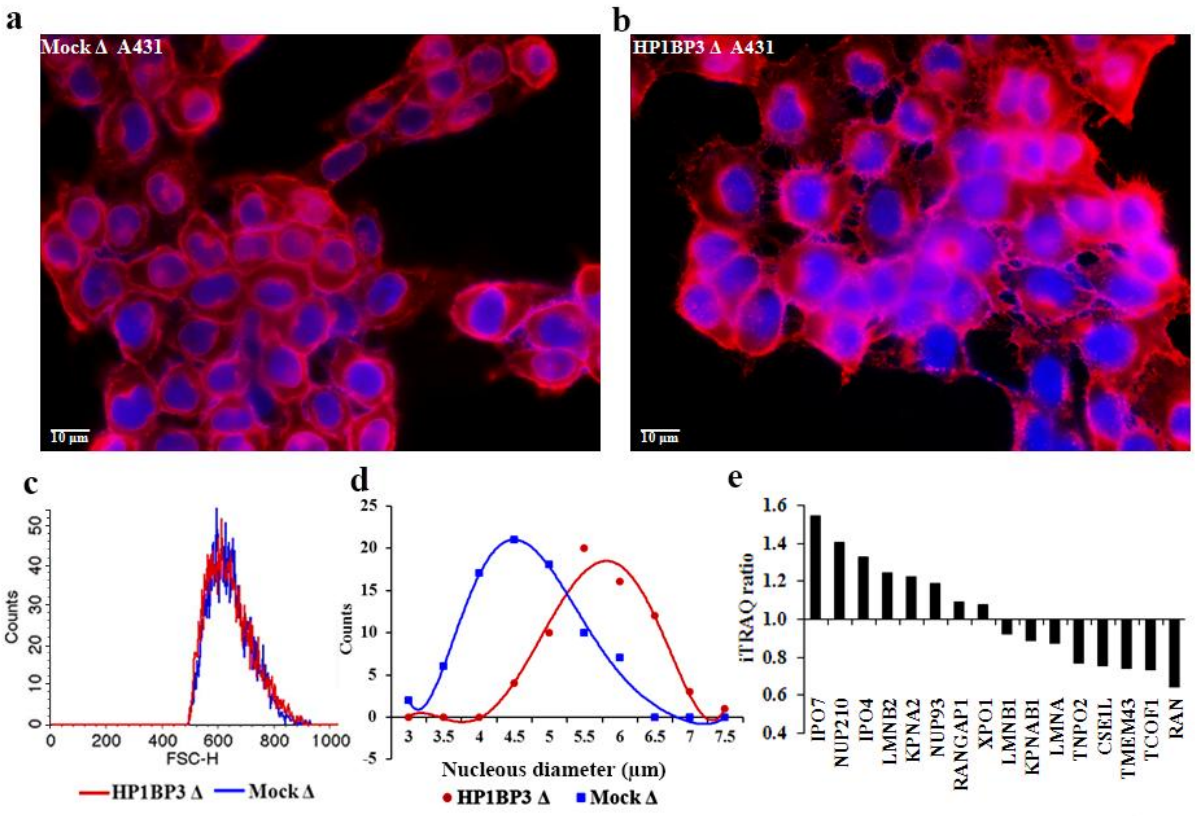

Figure 3.13: Effect of HP1BP3 depletion on cellular and nuclear morphology. a-b: Images of Mock and HP1BP3 depleted A431 cells respectively. Cells were plated on glass cover slips and cell membranes were stained with Alexa 594 conjugated WGA (red) and nucleus were counterstained with DAPI (blue). Scale bar 10µm. c: Relative comparison of mock and HP1BP3 depleted A431 phenotypes cell size: measured by flow-cytometer. d: Size (represented by nucleus diameter) of the distribution of mock and HP1BP3 depleted A431 phenotype. e: Differential expression levels of nuclear transport proteins in HP1BP3 depleted phenotype: protein levels were quantified through iTRAQ based quantitative proteomic technique and iTRAQ ratio represent the relative abundance of proteins.

regulated by the nuclear transport system and increasing nuclear import causes increment in nuclear size [236]. Our proteomic finding showed that many nuclear transport proteins were expressed differentially in the HP1BP3 depleted cells (Fig. 3.13e). Data also showed that proteins involve in the nuclear import like IPO7, NUP210, IPO4, and KPNA2 were up-regulated, while key nuclear export proteins including CSE1L and RAN were down-regulated in HP1BP3 depleted cells (Fig. 3.13e). Taking the experimental findings together, we hypothesized that depletion of HP1BP3 caused unpacking of the heterochromatin and alter protein expression. Alternation in the nuclear transporter expression might up-regulate nuclear import and down-regulate nuclear export, leads to increment in cargo load inside the nucleus and as a result nucleus size is expanded to accommodate cargo overload.

2.5 Conclusions

Throughout cell cycle progression chromatin structure was regulated in a dynamic manner to maintain basic cellular events. Structural integrity of the chromatin was maintained through chromatin-protein interaction. Hence knowledge on chromatin associated protein network and their interaction dynamics during cell cycle progression might be enlightening our understanding about chromatin biology and its regulatory role in essential cellular events during normal and pathophysiological conditions. In this study we used combination of partial MNase digestion and iTRAQ based high throughput quantitative proteomic approach for identification and quantification of the chromatin-associated proteome during interphase progression. Here we identify 481 high confident proteins and most of them were involved in the regulation of genomic events such as genome packaging, DNA replication and repair, transcription regulation and many other. The quantitative data reflect the picture of their dynamic interactions with chromatin during interphase progression. We also identified the dynamic chromatin association of the novel protein HP1BP3 during different stages of interphase. Further data mining and analysis lead to a testable hypothesis that HP1BP3 is likely a key switch regulating the chromatin template in G_1 phase by inter-converting euchromatin and heterochromatin to activate or silent specific genes. The HP1BP3 functions were further studied by knockdown the gene using shRNA and more biochemical and proteomics studies. Depletion of HP1BP3 cause reduction in chromatin compaction and increase MNase susceptibility which alters the protein expression levels of phenotypes and also increase the nuclear size. HP1BP3 depletion may activate many

silenced genes in the heterochromatin regions to generate highly proliferative cell phenotypes by enhancing G_1/S transit. Taking all experimental observations and evidences together we hypothesize that HP1BP3 regulate gene transcription by maintaining the heterochromatin integrity which regulates the length of the G_1 phase and maintain a steady cell cycle progression.

Chapter 4

4 Studies of hypoxia induced cancer cell chromatin changes to identify key regulator for cancer malignant progression

4.1 Summary

Cancer metastasis is one of the leading causes of non-communicable diseases (NCDs) induced global mortality. Hypoxia is one of the key factors of the oncogenesis and also responsible for therapeutic resistance. Most of the hypoxia induced molecular events are directly or indirectly influenced by a group of transcription factors called hypoxia-inducible factors (HIFs). Chromatin dependent events are the key driving forces behind hypoxia induced pathophysiological events so the knowledge of chromatin dynamics is essential to understand the molecular mechanism of tumorigenesis. To study the dynamics of chromatin biology during hypoxia we apply partial DNase I digestion coupled with iTRAQ based quantitative proteomic technique to profile the chromatome during normoxia, hypoxia and reoxygenation conditions. We identify 1446 proteins with high confidence in this study in which 819 proteins were regulated their chromatin association topology in a hypoxia dependent manner. They were involved in the regulation of chromatin dependent genomic events including chromatin organization, transcription regulation, and DNA repair. Our proteomic data also revealed the different hypoxia perturbed pathways including DNA repair pathways. Applying data mining and comparing cell cycle chromatome dynamics we identified a novel chromatin organizer protein HP1BP3 which may be a key regulator in hypoxia induced tumor malignancy. Its functional characterization reflected that HP1BP3 mediated heterochromatinization was activated during hypoxia, which is involved in the transformation of cancer cells into aggressive cancer cell phenotype through increasing cell survivability, radio- and chemo-resistance, and stemness. Taking all the experimental observations from both chapter 3 and 4 together we suggested that HP1BP3 mediated heterochromatinization will be the potential target for new cancer therapy.

4.2 Introduction

Tumor hypoxia is the hallmark of rapidly growing solid tumor. To overcome this abnormal physiological condition cancer cells co-opt some defensive responses such as induction of angiogenesis, adaptation of glycolysis, self-renewal and unlimited replication capability, apoptosis resistance, invasion and metastasis [73], which ultimately convert the cancer cells into an immortal aggressive malignant cancer phenotype. Clinical and experimental evidences also

suggested that hypoxia complicates the cancer treatment through induction of resistance against radio- and chemo-therapy [74-76]. Recent evidences also demonstrated the role of hypoxia in cancer stem cells (CSCs) formation [107]. Overall its importance in tumorigenesis making hypoxia perturbed molecular pathways a prime target for study to understand oncology [237].

It is a well-established fact that hypoxia adopted mechanisms are directly or indirectly regulated through hypoxia-inducible factors (HIFs) [238]. During hypoxia HIFs activity is directly regulated through epigenetic factors like DNA methylation, histone modification, chromatin remodeling factors and regulatory RNAs [238, 239]. Epigenetic regulators control the hypoxia induced pathophysiological events through both HIFs dependent and HIFs independent manner. Emerging evidences showed that the hypoxia directly interfere with the chromatin structure through histone modifications and chromatin remodeling dependent manner [240]. Moreover, chromatin remodeling protein SWI/SNF is involved in activation of specific gene transcription in a hypoxia dependent manner [241]. Evidences also suggested that histone deacetylases HDAC3 and HDAC4 mediated epigenetic reprogramming play a crucial role in cell survival and angiogenesis during hypoxia [242]. Recent study also revealed role of glycoprotein hormone erythropoietin (EPO) in epigenetic reprogramming during hypoxia and suggested its involvement in alternation of histone H3 acetylation and trimethylation pattern but its own expression was epigenetically regulated through DNA methylation in cancer cells [243]. Experimental evidence also highlighted that during hypoxia histone lysine demethylases (KDMs) played a regulatory role in the transcription regulation via epigenetic reprogramming and is a prime target for cancer therapy [244]. DNA methylation mediated epigenetic reprogramming during hypoxia also well evidenced [245, 246]. Beyond the DNA and histone modification many other chromatin-associated non-histone proteins play important role in epigenetic reprogramming but during hypoxia role of the non-histone proteins are not well understood. Knowledge of chromatin association dynamics of chromatin associated proteins might provide better understanding of the chromatin biology during hypoxia, is help us to understand the genetic and epigenetic regulation of the hypoxia perturbed biological events. Quantitative proteomic study regarding hypoxic cancer cell chromatome is less extensive and for the first time, we report proteomic based study of cancer cell chromatome during hypoxia induced cancer progression.

We performed partial DNase I digestion of different chromatin samples, extracted from different hypoxic and reoxygenated A431 cells to liberate the chromatin associated proteins. Quantitative proteomic profiling of both liberated solubilized fractions and undigested unreleased fractions showed differential chromatin association topology of the chromatin associated proteins during hypoxia and reoxygenation conditions which help us to understand the dynamics of the chromatin biology during hypoxia and reoxygenation. Chromatin proteome information also provides a basic understanding between alter epigenomic regulation and cancer progression during hypoxia and reoxygenation. Hence the aim of our present study was to quantitative profiling of the chromatome during hypoxia and reoxygenation conditions to understand the global changes in the chromatin biology and identify novel candidate proteins which are involve in the regulatory processes responsible for the tumor progression. To achieve our goal we used partial nuclease digestion coupled with iTRAQ based relative protein quantitation approach to study the chromatome changes during hypoxia and reoxygenation conditions. We also used various biological and biochemical approaches to perform functional studies of important candidate protein like HP1BP3 to establish its contribution in the cancer biology.

4.3 Materials and methods

4.3.1 Reagents

Unless indicated, all reagents used in this study were purchased from Sigma-Aldrich, USA. All antibodies and other reagents were purchased from corresponding companies as describe in chapter 3. All cell culture media and supplements were purchase from Gibco® (Life Technologies, USA).

4.3.2 Experimental methodology

4.3.2.1 A431 cell culture and hypoxia model

We used A431 squamous carcinoma cells as a model cell line and to mimic the hostile microenvironment we used hypoxia model. The A431 cells were purchased from ATCC and maintain in DMEM medium supplemented with 10% FBS and Pen-Strep (10000µg/ml

streptomycin and 10000U/ml penicillin). For each experiment 2×10^6 cells were seeded on 10cm dish into 10% FBS and antibiotic containing DMEM medium, incubated at 37^{o}C in 5% CO_2 containing humidified incubator. After reaching 30-40% confluence, cells were washed five times with PBS and once with serum free DMEM medium to remove the serum completely. Finally 10ml serum free DMEM medium was added and incubated the cells in different environmental condition including normoxia (Nx) (21% O_2, 5% CO_2) and hypoxia (Hx) (< 0.1% O_2, 5%CO_2) for intended time periods. For induction of hypoxic condition cells were put into hypoxia chamber and oxygen inside the chamber was removed by flashing the chamber with hypoxia gas (5% CO_2 and 95% N_2) for 10min at a constant flow rate of 15l/min and air locked the chamber. Chambers were then incubated at 37^{o}C for next 48h and 72h. Wet tissue papers were put inside the chamber to maintain the humidity. For normoxic condition, cells were incubated at 37^{o}C in 5% CO_2 for 72h. For reoxygenation (Rx), cells were first incubated in hypoxia condition, as stated for 48h time period. After completion of the hypoxia phase old medium was replaced with fresh medium and incubated in normoxic condition for the next 24h. After intended time period, cells were washed with cold PBS, harvested and used for the next experiments.

4.3.2.2 Chromatin isolation and digestion

Chromatin isolation was performed accordingly as described in previous chapter. 7×10^7 A431 cells were used for chromatin extraction for each condition. Purified chromatin pellet was taken and suspended in 50µl of DNase I digestion buffer (10mM tris HCl (pH 7.4), 0.5mM $CaCl_2$, and 2.5mM $MgCl_2$). 20U of DNase I was added and digested the chromatin pellet for 60min at 37^{o}C with occasional vortexing. Digestion was stopped by adding 1mM EDTA solution and incubated the digestion mixture at 4^{o}C for 10min. Supernatant fractions(S) was collected by centrifugation at 20,000×g for 30min at 4^{o}C. The remaining undigested pellet was dissolved in 2% SDS solution, the so-called pellet fraction (P). Nx-S, Hx48-S, Hx72-S and Rx-S supernatant fractions were obtained from normoxic, 48h hypoxic, 72h hypoxic and reoxygenated chromatin. Corresponding pellet fractions were Nx-P, Hx48-P, Hx72-P and Rx-P. Protein content of supernatant and pellet fractions was measured by using 2-D Quant Kit.

4.3.2.3 In-gel Digestion and iTRAQ Labeling

150µg of protein from each sample was taken for in-gel digestion. The in-gel trypsin digestion was performed as described in the chapter 3. Tryptic peptides derived from supernatant and pellet fractions of the normoxic (Nx), 48h hypoxic (Hx48), 72h hypoxic (Hx72) and reoxygenated (Rx) A431 chromatins were labeled with iTRAQ reagent according to the protocol described in the chapter 3. iTRAQ labels used for each condition were described in the table 4.1.

Table 4.1: iTRAQ labels used for labeling the peptides obtain from different conditions

Condition	Nx-S	Hx48-S	Hx72-S	Rx-S	Nx-P	Hx48-P	Hx72-P	Rx-P
iTRAQ label	113	114	115	116	117	118	119	121

4.3.2.6 Fractionation and LC-MS/MS analysis of iTRAQ labeled peptide

iTRAQ labeled peptides were fractionated into 28 fractions by using ERLIC based fractionation technique as described in chapter 3. LC-MS/MS analysis of ERLIC fractionated peptides were performed by using Q-STAR Elite mass spectrometer (Applied Biosystems, USA). Similar instrument settings and experimental methods were used for this experiment as described in the chapter 3.

4.3.2.4 Mass Spectrometric Data Analysis and bioinformatics

Database searching was performed using ProteinPilot 3 software (Applied Biosystems, Foster City, USA) as described in the chapter 3. Bioinformatics analysis of proteomic data like molecular weight and pI (isoelectric point) values were calculated as described in the material method section of the previous chapters. Uniprot and Nextprot databases were used to classify the identified proteins. Cluster analysis of our protein data set was performed using online Gene Pattern software (http://genepattern.broadinstitute.org) as describe in previous chapters.

4.3.2.5 Western blot analysis

Western blot analysis of different hypoxia and reoxygenated A431 chromatin samples and other cell lysates were performed using corresponding antibodies as described in previous chapters.

4.3.2.6 Propidium iodide staining and flow cytrometry analysis

2×10^6 viable A431 cells were harvested from each condition and stained with propidium iodide as described in previous chapter. Cell cycle analysis was performed by using flow cytometer as described in the chapter 3.

4.3.2.7 Preparation HP1BP3 knockdown cell phenotypes

HP1BP3 depleted and mock depleted A431 phenotypes were prepared by using RNAintro GIPZ Lentiviral shRNAmir Starter Kit (Thermo Scientific, USA) as described in the chapter 3. Both A431 phenotypes were used here for different biological and biochemical experiments.

4.3.2.8 Chromatin compaction measurement

Chromatins were extracted from the 48h normoxic and hypoxic A431 cells and digested with different concentration of MNase and finger printing of the digested chromatin was performed as described in the chapter 3.

4.3.2.9 Cell proliferation assay and clonogenic assay

All MTT based cell proliferation assays were performed as described in previous chapter. All clonogenic assays were conducted accordingly by using previously described protocol. To determine the clonogenicity of the A431 phenotypes during hypoxia, we used 48h normoxia and 48h hypoxia treated cells for normoxia and hypoxia condition. For reoxygenation, initially cells were incubated in hypoxia for 24h and then oxygenated for 24h.

4.3.2.10 Cell adhesion assay

24-well plates were coated with different cell adhering molecules like collagen, fibronectin and laminin. The adhering molecules were dissolved in PBS at a concentration of 2µg/ml. Wells were coated with corresponding adhering molecule at 4^oC for overnight time period. Cells were seeded on each coated well at a density of 2×10^5 cells\well in DMEM medium and incubated for 1h at 37^oC. After 1h incubation, old medium was removed and wells were washed twice with PBS to remove the non-adhering cells. Adhere cells were fixed by using 95%

ethanol for 10min at RT. Ethanol fixed cells were stained with 0.5% Crystal violet solution at RT for 20min. The excess dye was removed by extensive PBS washing (at least 5 times).The plates were turned upside down and kept at that position for overnight to complete drying. Next day, 0.8ml of 0.5% triton X-100 solution was added to dissolve the crystal violet and absorbance was measured by using a micro plate reader (Tecan Magellan^{TM}, Switzerland) at 595nm. For normoxia and hypoxia conditions, cells were incubated in normoxia and hypoxia conditions for 48h prior to adhesion assay. For reoxygenation, cells were first incubated in the hypoxia for 24h followed by incubation in the normoxia condition for another 24h prior to assay.

4.3.2.11 Scratch-wound assay

Scratch-wound assay was performed to measure cell migration during different physiological conditions. Cells were seeded at a density of 1.5×10^6 cells/well in 10% FBS containing DMEM medium in 6-well plate and incubated at 37^{o}C in 5% CO_2 for 24h. After 24h, scratches were made by using sterile 10µl pipette tip in the middle of the well. Cells were washed thrice with PBS and twice with serum depleted medium prior to incubation in serum free conditions. Images of initial scratch areas were captured by a Nikon Eclipse TE2000-U. Cells were then incubated in hypoxia condition for next 48h. After 48h, images of the same scratch areas were recaptured. Cells were then reoxygenated for another 24h at 37^{o}C and picture of same scratch areas were recapture after 6h and 24h of reoxygenation. Wound closure was determined which reflect the cell migration.

4.3.2.12 Trans-well assay

Trans-well assay was performed using 24-well trans-well plate with polycarbonate filter fitted insert (8 µm pore size, Costar®, Corning, USA). 4×10^4 cells were seeded in 100µl serum free DMEM medium in each upper chamber and lower chambers were filled with 600µl of 2.5% FBS containing DMEM medium. The trans-well plates were incubated for 48h at 37^{o}C inside 5% CO_2 containing incubator. After 48h, upper chamber was taken out and washed two times with PBS. The non-migrated cells were located in the inner side of the membrane and they were removed by wiping with a cotton swab. Migrated cells were located outer side of the membrane and cells were then fix with 3.7% formaldehyde solution for 2min at RT and stained with 0.5% crystal violet. Excess dye was removed from membrane by extensive PBS washing. Image of the

membrane was taken by using Nikon Eclipse TE2000-U microscope. Finally the membrane was carefully cut and extracted the crystal violet by immersing the membrane into 0.5% triton X-100 solution. Absorbance of crystal violet was measured at 595nm wavelength and determined comparative change in cell migration. To study the effect of hypoxia and reoxygenation, A431 cell phenotypes were incubated in the normoxia and hypoxia conditions for 48h and for reoxygenation incubated the cells in hypoxia for 24h followed by 24h reoxygenation.

4.3.2.13 Radiation-resistance and Chemo-resistance assay

Cells were seeded at a density of 2×10^5 cells/well in 10% FBS containing DMEM medium on a 6-well plate. The plates were incubated for 24h at 37°C in 5% CO_2. After 24h, old culture medium was removed and washed with PBS and serum depleted media. Final add serum free medium and plated were incubated at 37^{o}C inside 5% CO_2. The cells were exposed to total dose of 10Gy (gray) radiations. For radiation treatment we used BIOBEAM 2000 gamma irradiation device (Gamma-Service Medical GmbH, Germany). Radiation treated cells were then incubated at 37^{o}C in 5% CO_2 for the next 24h. After 24h incubation, old culture medium was replaced with 0.5mg/ml MTT containing fresh medium and plate was incubated at 37^{o}C for 2h. After 2h, the culture medium was removed completely and 2ml DMSO was added to dissolve the formazan crystals. The optical density was measured at 570nm with reference wavelength at 630nm by using micro plate reader. For chemo-resistance assay 1×10^4 cells were seeded in each well of 96-well plate in 100µl DMEM medium supplemented with 10% FBS and plates were incubated for overnight at 37°C in 5% CO_2. Next day, doxorubicin was added at a concentration range of 0-1600ng/ml and treatment was continued for next 24h. At the end of the treatment drug containing medium was replaced with MTT (0.5mg/ml) containing fresh medium and plates were incubated at 37^{o}C for another 2h. Finally medium was removed and formazan crystals were completely dissolved in 100µl DMSO and optical density was measure at 570nm with reference wavelength at 630nm.

4.3.2.14 Sphere formation assay

Sphere formation assay was performed to determine the self-renewal property of the cancer cells. For sphere formation assay A431 phenotypes were cultured in a suspension culture in B27, 20ng/ml EGF (epidermal growth factor), 10ng/ml FGF (fibroblast growth factor) and

pen-strep supplemented DMEM/F12 (1:1) medium. In the first day of the assay, cells were seeded in the ultra-low attachment flat bottom 24-well plate (Costar®, Corning, USA) at a density of 500 viable cells per well. Plates were incubated for next 10d at 37^{o}C in 5% CO_2. After 10d, numbers of formed tumorspheres were counted and image of the each tumorsphere was captured by Nikon Eclipse TE2000-U microscopy and determined their diameter. To study the effect of hypoxia and reoxygenation, A431 phenotypes were incubated in normoxia and hypoxia condition for 48h and for reoxygenation cells were first incubated in hypoxia condition for 24h and then reoxygenated for the next 24h. The normoxic, hypoxic and reoxygenated cells were then used for the assay. Cells were seeded at a density of 100cells/well and cultured as suspension culture for next 10d. After 10d, formed spheres were counted and image of the spheres were taken.

4.4 Results and discussion

4.4.1 Mass spectrometric identification and quantification of the chromatin proteome

The main cause of tumor formation and malignancy is a cellular dysfunction that results from accumulation of genetic and epigenetic abnormalities. In case of cancer progression hostile microenvironment plays an important role. Tumor microenvironment is a harsh environment with lack of nutrient and oxygen supply but tumor cells might overcome hypoxia and nutrient depletion and retained their growth through inducing angiogenesis and systemic metastasis. To study the chromatin structure specific association of different chromatin associated proteins during hypoxia and reoxygenation conditions we cultured A431 cells in different environmental conditions such as 48h normoxia (Nx), 48h and 72h hypoxia (Hx48 and Hx72), and 48h hypoxia followed by 24h reoxygenation (Rx). Chromatins were extracted from different normoxic, hypoxic and reoxygenated cells and partially digested with DNase I to extract euchromatin binding proteins but heterochromatin and matrix associated chromatin proteins remain unreleased in the pellet fractions. MNase and DNase I showed comparable release profile during chromatome study in chapter 2 but DNase I digestion gave a little more information due to its cleavage preference in GC enrich regions and so here in this study we used DNase I for digestion. Complete purification of chromatin like organelle which is extremely interlinked with other organelles, was most challenging and proteomic study of those samples were further

challenging when a non-biased technique like mass spectrometry was used for proteomic identification. Western blot data reflected high concentration of GAPDH was present in the cytosolic fraction, while it was present in much lower concentration in the chromatin fraction. Western blotting also showed that key chromatin protein histone H4 was present in very high concentration only in the chromatin fraction (Fig. 4.1a), which indicating higher enrichment of

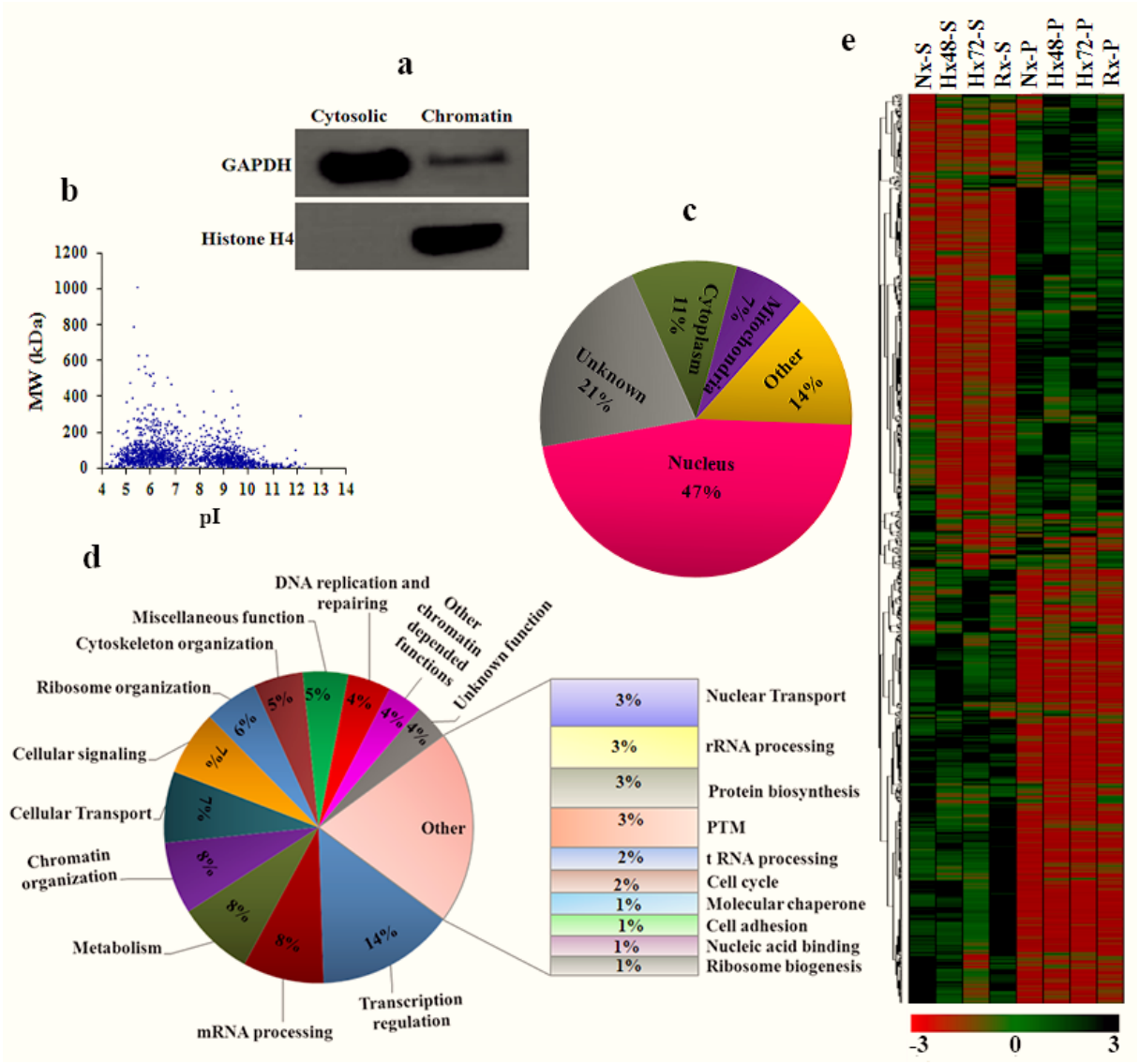

Figure 4.1: Characterization of identified proteins. a: Western blot of GAPDH and histone H4 in cytosolic and chromatin fraction indicating enrichment of chromatin. b: Physicochemical property of identified protein represented by molecular weight (MW) and isoelectric point (PI) distribution. c: Classification of identified proteins according to their subcellular localization. d: Functional classification of identified proteins. e: Heat map represent the relative protein abundance in the different chromatin digests.

chromatin in the purified fraction. Proteins obtained from partial chromatin digested fractions were tryptic digested through in-gel digestion technique and tryptic peptides were labeled with iTRAQ reagent accordingly. Labeled peptides were pooled and separated through ERLIC fractionation and run in a nano-HPLC coupled QqTOF instrument for identification. Mass spectrometry spectra of the peptides were searched using ProteinPilot 3 software following the UniProtKB human protein database for identification and quantification of the respective proteins.

In this study we acquired 1.79×10^5 non-empty spectra from a total of 84 LC-MS/MS runs from three technical replicates. Distribution of physiochemical parameters like molecular weight and isoelectric point of identified proteins (Fig. 4.1b) showed well distribution of these parameters. This indicates that proteomic technique used for this experiment was suitable for all types of protein identification. After ProteinPilot search we identified a total of 1828 high confident proteins with unused score above 2 (99% confidence) and FDR less than 1%. Among them 1446 proteins were identified with more than one unique peptide (95% confidence) and were shortlisted for further analysis. Identified proteins were classified according to their major subcellular localization following Uniprot and Nextprot databases and found that majority of the identified proteins (47%) mainly located in the nucleus where as a significant number of proteins (21%) do not have any specified subcellular localization (Fig. 4.1c). We also classified the proteins according to their biological function and analysis pointed out that major fraction of the identified proteins involved in different nuclear events including transcription regulator (14%), chromatin organization (8%), DNA repair and replication (4%), other chromatin dependent events (4%), mRNA processing (8%), rRNA processing (3%), nuclear transport (3%), cell cycle (2%), and ribosome biogenesis (1%) and remaining of them involved in other cellular events (Fig. 4.1d).

In this iTRAQ based proteomic quantification we used 48h normoxic supernatant fraction (Nx-S) as a denominator for relative quantification of respective samples. Proteins with significant iTRAQ ratio ($p\text{-value}<0.05$) at least in one condition were selected for farther analysis and obtained 819 proteins in the final list. We consider iTRAQ ratio above 1.25 as upper cutoff and below 0.75 as lower cutoff for fold change of protein abundance in different chromatin fractions. We found 484 proteins increased their abundance levels and 506 proteins

decreased their abundance levels in the different fractions of chromatin digests (Table 4.2). Proteins were clustered according to their relative abundance in the different chromatin digested fractions by using Pearson-correlation and the hit map in figure 4.1e showed hierarchical clustering of the proteins, which reflects the differential chromatin associations during normoxia, hypoxia and reoxygenation conditions.

Table 4.2: Data analysis of identified proteins in different chromatin digests.

	Number of proteins with significant change in iTRAQ ratio (p-value <0.05)							
Sample	**Hx48-S**	**Hx72-S**	**Rx-S**	**Nx-P**	**Hx48-P**	**Hx72-P**	**Rx-P**	**Total unique protein***
iTRAQ ratio	**114:113**	**115:113**	**116:113**	**117:113**	**118:113**	**119:113**	**121:113**	
Total	271	326	310	494	482	489	474	819
Ratio>1.2	80	100	97	195	187	194	187	484
Ratio<0.83	87	166	78	270	266	273	254	506

*The number of unique proteins with at least one ratio with $p<0.05$

4.4.2 Chromatin organization and transcription regulation during hypoxia

In rapidly growing tumor, tumor-surface was going through acute hypoxia but tumor-core exhibited chronic hypoxia due to lack of blood supply [247]. Hypoxia microenvironment in the tumor plays a central role in both local and systemic cancer proliferation and also contributes a major involvement in radio- and chemo-resistance. All pathophysiological changes occurred during hypoxia, were manifested by hypoxia induced alternation in the genetic reconciliation. Hypoxia microenvironment alters chromatin dependent events such as transcription [248], replication [249] and DNA repair [250] but also involved in genomic rearrangement [251] and genome amplification [252]. Those chromatin dependent events are directly or indirectly regulated through the structural integrity of chromatin, which is controlled by the chromatin-protein interactions. Differential chromatin association topology of the chromatin proteome provides better understanding of the global structural dynamics of chromatin during hypoxia and also explored the molecular mechanisms behind altered genomic events.

In this nuclease digestion coupled quantitative proteomic study, we identified 114 proteins which are directly involved in chromatin organization and transcription regulation Figure 4.2-4 showed their differential release by DNase I indicating their differential chromatin

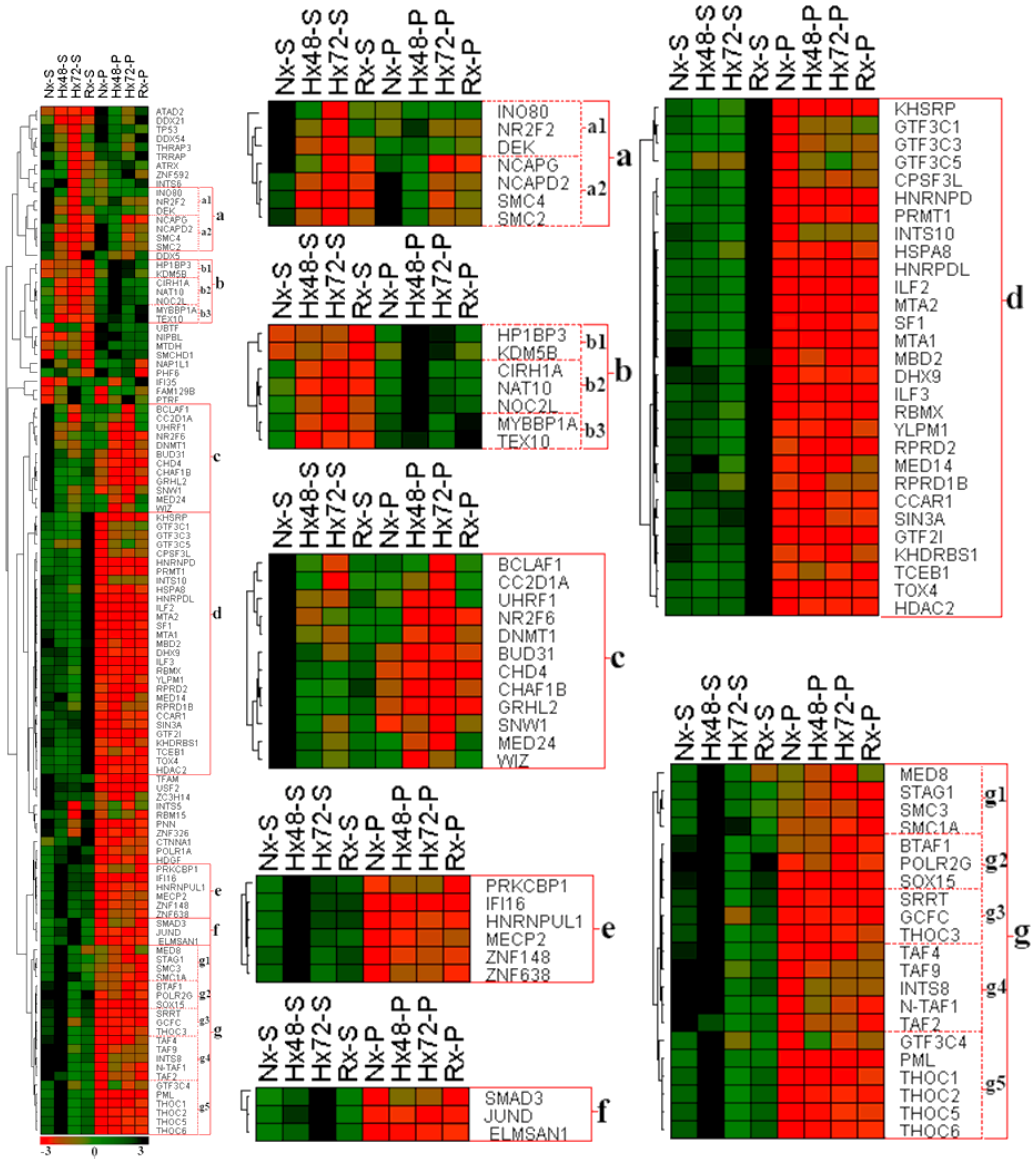

Figure 4.2: Hierarchical clustering of chromatin organizers and transcription regulators according to their release after partial DNase I digestion. 'Cluster a': Highest amount of proteins present in either Nx-S or Nx-P fractions, whereas in 'sub-cluster a1' highest concentration of proteins were present in the Nx-S and in 'sub-cluster a2' highest concentration of proteins were present in the Nx-P fraction.; 'Cluster b': Highest concentration of proteins were present in the Hx48-P fraction, while in 'sub-cluster b1' highest concentration of proteins were present in both Hx48-P and Hx72-P fractions , in 'sub-cluster b2' highest concentration of proteins were present in only in the Hx48-P fraction and in 'sub-cluster b3' highest amount of proteins were present in both Hx48-P and Rx-P fractions.; 'Cluster c': Highest concentration of proteins were present only in the Nx-S fractions.; 'Cluster d': Highest concentration of proteins present only in the Rx-S fractions. 'Cluster e': Highest amount of proteins present only in the Hx48-S fraction; 'Cluster f': Highest concentration of proteins was present only in the Hx72-S fractions; and 'Cluster g': Comparatively higher quantity of proteins was present in the Hx84-S fractions, while in 'sub-cluster g1', 'sub-cluster g3', and 'sub-cluster g5' highest amount of proteins was present in the Hx48-S fraction and in 'sub-cluster g2', and 'sub-cluster g4' highest amount of proteins was present in both Nx-S and Hx48-P fractions. Nx-S, Hx48-S, Hx72-S and Rx-S represent the corresponding supernatant fraction of partial DNase I digested normoxic, 48h hypoxic, 72h hypoxic and reoxygenated chromatins and Nx-P, Hx48-P, Hx72-P and Rx-P represent the undigested pellet fraction of the respective chromatin samples.

association topology during hypoxia and reoxygenation conditions. Further cluster analysis showed proteins in the specific protein cluster share similar chromatin association topology during different hypoxic conditions and released by DNase I in a similar manner. Seven distinct protein clusters ('cluster a-g') were identified. Among them 'cluster a', 'cluster b', and 'cluster g' were further divided into few sub-clusters which reflected the differential chromatin binding topology of the chromatome during hypoxia and reoxygenation (Fig. 4.2).

Proteins clustered in the 'cluster a' showed higher concentration of proteins present in both normoxic supernatant and pellet fractions when compared to other fractions indicating their reduced chromatin association due to hypoxia shock. Sub-cluster a1 showed proteins like DEK and INO80 were partially released by DNase I and both of them were present comparatively at a lower concentration in hypoxia and reoxygenation conditions (Fig. 4.3a and 4.3d). Condensin complex subunit SMC2, SMC4, NCAPD2, and NCAPG were grouped in 'sub-cluster a2' (Fig. 4.2). Proteomic results showed that concentration of condensin complex subunits were highly reduced in both pellet and supernatant fractions of hypoxia and reoxygenated chromatins (Fig.4.3c) indicated that their chromatin associations were decreased during hypoxia and

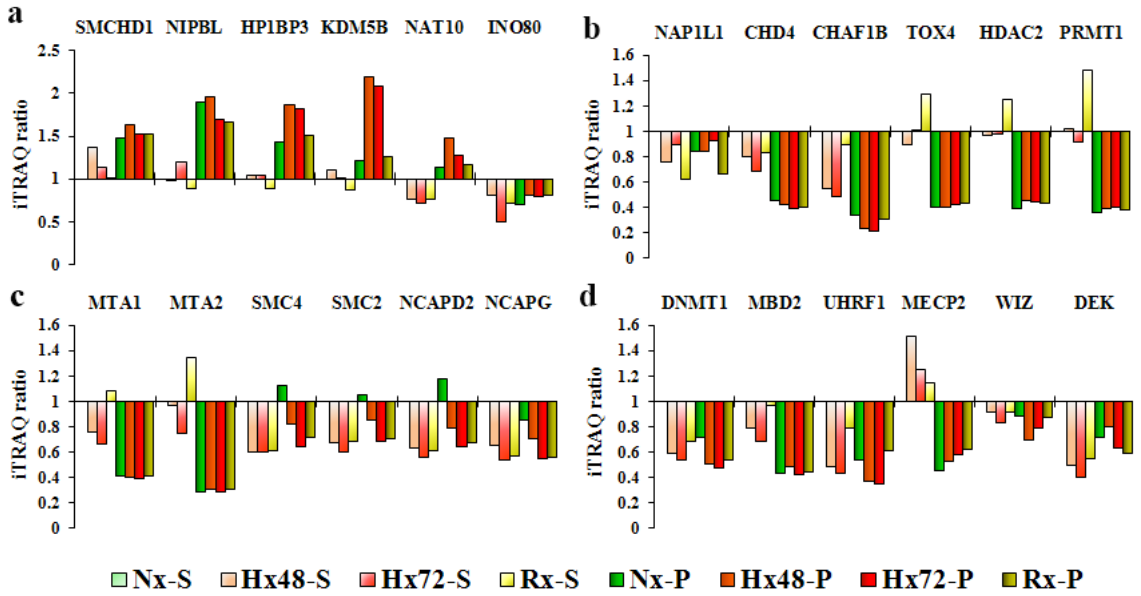

Figure 4.3: Release pattern of chromatin organizers from normoxic, hypoxic and reoxygenated chromatin during partial DNase I digestion. iTRAQ ratio represent the relative abundance of protein in the different chromatin digests. Supernatant fractions Nx-S,Hx48-S, Hx72-S and Rx-S and undigested pellet fractions Nx-P,Hx48-P, Hx72-P and Rx-P were obtain from partial digestion of normoxic, 48h hypoxic, 72h hypoxic and reoxygenated chromates.

reoxygenation. Chromatin organizer proteins like CHAF1B, DNMT1, UHRF1, and CHD4 were clustered in the 'cluster c' and their release patterns showed that these proteins were identified with highest abundance in the supernatant fraction of normoxic chromatin when compare to the other fractions. Digestion result reflected that unlike sub-cluster a2, 'cluster c' proteins were also reduced their chromatin bindings during hypoxia stress (Fig. 4.3b and 4.3d). Chromatin association of condensin was very dynamic throughout cell cycle progression and it was involved in maintenance of chromatin condensation during mitosis [253]. DNMT1 was associated with the pre-replicative chromatin in replication dependent manner but it also associated with the post-replicative heterochromatin in replication independent manner [254]. Our experimental results also showed hypoxia induced cell cycle arrest at the G_0-G_1 phase (Fig. 4.6). Proteins of the 'cluster a' and 'cluster c' might be associated with the chromatin in a cell cycle dependent manner and hypoxia induced cell cycle arrest in the G_0-G_1 phase reduced their chromatin association with hypoxic and reoxygenated cancer cell chromatin.

Proteins clustered under 'cluster d' were present relatively in a high amount in the reoxygenated supernatant fraction when compared to other supernatant and pellet fractions reflecting increment of their euchromatin association during reoxygenation. Our DNase I digestion results showed that the epigenetic regulator including NuRD complex components HDAC2, MBD2, MTA1, and MTA2 and other proteins like PRMT1 and TOX4 were released in the supernatant fractions and identified comparatively lower concentration in the pellet fractions and results also showed that protein amount was relatively high in the reoxygenated supernatant fraction (Fig. 4.3b-d). Our results suggested that euchromatin association of the NuRD complex proteins, PRMT1 and TOX4 were increased during reoxygenation condition. Recent findings suggested that HDACs regulate apoptosis and also activate VEGF and HIF-1α expression in response to the hypoxia stress [255] Clinical evidences showed overexpression of MTA family proteins in a wide range of cancer and their involvement in metastasis process [256]. Reported evidences suggested involvement of histone modifier protein arginine methyl transferees PRMTs in cell proliferation and tumor-microenvironment modulation [257]. Our experimental data suggested that during reoxygenation, NuRD complex and other chromatin organizers were associated with euchromatin to alter gene expressions, which might contribute in cancer metastasis. Proteins like CCAR1, KHSRP, GTF3C3, GTF3C5, ILF2, and ILF3 having transcription factor activity, were clustered in 'cluster d' and their release patterns indicated these

proteins in the reoxygenated supernatant fraction in a greater concentration compare to other conditions (Fig 4.3c). Proteomic result suggested that euchromatin association of these proteins and result was justified by euchromatin association of transcription factors. Their chromatin loadings during reoxygenation indicate that they might involve in the gene transcription and responsible for cancer malignancy.

Proteins clustered under 'cluster e' and 'cluster g' showed relatively grater amount in the 48h hypoxia supernatant fraction when compared with other fractions and results also reflected that short term hypoxia increased euchromatin association of these proteins but prolong hypoxia

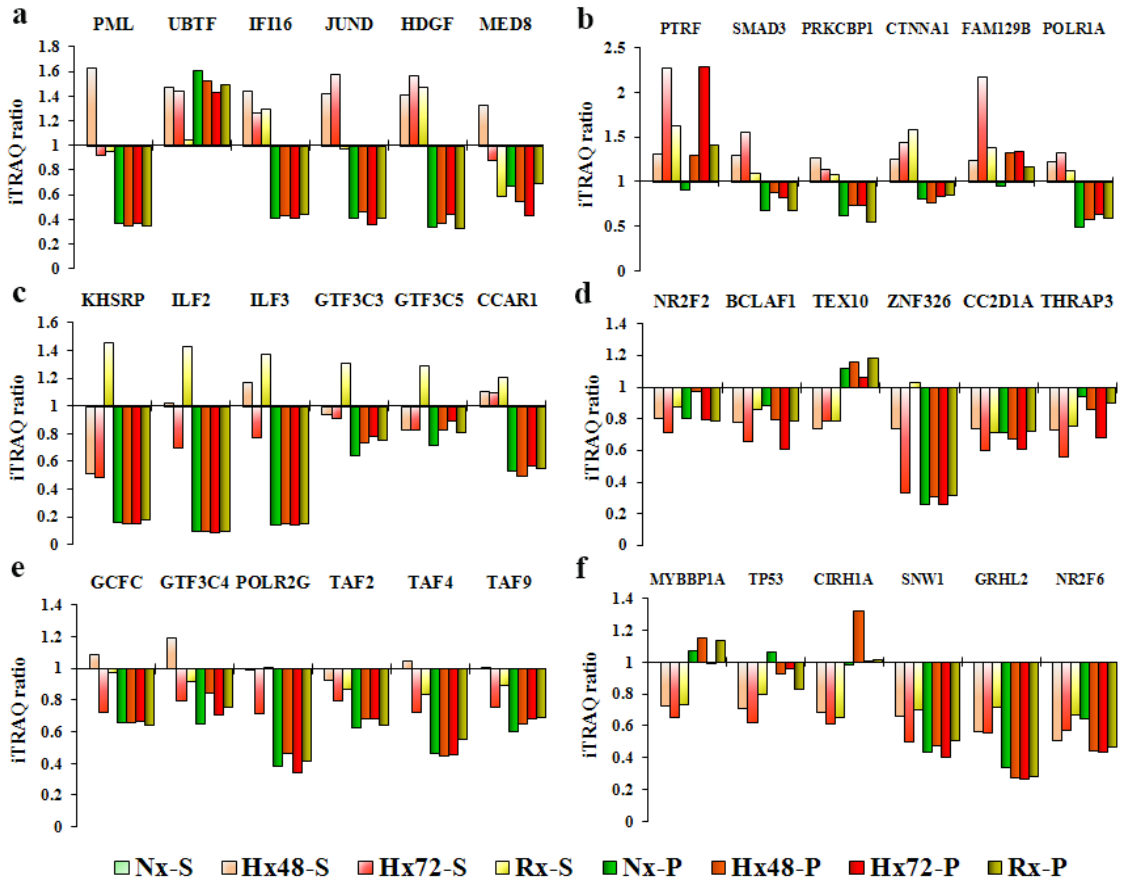

Figure 4.4: Release pattern of transcription factors and transcription regulators from normoxic, hypoxic and reoxygenated chromatin during partial DNase I digestion. iTRAQ ratio represent the relative abundance of protein in different chromatin digests. Supernatant fractions Nx-S, Hx48-S, Hx72-S and Rx-S and undigested pellet fractions Nx-P, Hx48-P, Hx72-P and Rx-P were obtain from partial digestion of normoxic, 48h hypoxic, 72h hypoxic and reoxygenated chromates.

reduced their chromatin association. Our proteomic result also showed that concentration of transcription regulator MECP2, and other transcription factors including GCFC, GTF3C4, TAF2, TAF4, TAF9 and polymerase POLR2G were highly reduced in the 72h hypoxic supernatant fraction (Fig. 4.3d and Fig. 4.4d). Hypoxia induced MECP2 binding in the hyper-methylated CpG island of euchromatin regions might repress the tumor suppressive genes [258] and increase cancer cell survival during hypoxia stress. Prolong hypoxia caused massive cell death comparing to short term hypoxia due to activation of p53 induced apoptosis pathway which reduces the chromatin binding of TAFs [259] and other transcription proteins. On the other hand concentration of 'cluster f' proteins including JUND, ELMSAN1 and SMAD3 was relatively higher in the 72h hypoxia supernatant fraction (Fig 4.4d) suggested that prolong hypoxia increased their euchromatin association. Euchromatin association of these transcription factors during prolong hypoxia might activates genes which increase cell survivability and also responsible for oncogenesis [260, 261].

Cluster analysis showed comparatively higher concentration of 'cluster b' proteins in the pellet fractions of hypoxic chromatin digests (Fig. 4.2) indicating their heterochromatin specific localization during hypoxia. Proteomic results revealed that chromatin interacting protein HP1BP3 and KDM5B remain unreleased by DNase I and identified in a greater quantity specifically in both hypoxic pellet fractions compare to other fractions (Fig.4.3a) indicated their localization inside highly condensed heterochromatin territories. Recent studies revealed the role of KDM5B in gene expression and also suggested that it was involved in regulation of E2f genes expression through heterochromatin organization during cell cycle progression [262], justifying our proteomic finding. Western blot analysis also showed that chromatin association of HP1BP3 was increased during hypoxia stress (Fig. 4.5a-b). Our previous studies in the chapter 3 showed that HP1BP3 plays an important role in maintenance of the heterochromatin integrity and depletion

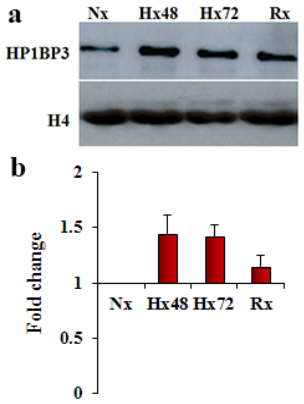

Figure 4.5: Chromatin association of HP1BP3 during different hypoxia and reoxygenation conditions. a: Western blot images represent the differential chromatin association of HP1BP3 during hypoxia and reoxygenation conditions. b: Changes of HP1BP3 chromatin association level during different hypoxia conditions. HP1BP3 level was normalized in terms of histone 4 level in respective chromatin samples and all statistical calculation was performed in basis of five experimental replicates.

of HP1BP3 caused heterochromatin unfolding and increase MNase sensitivity in the resultant phenotype. MNase digestion of normoxic and hypoxic chromatins showed hypoxic chromatins were produced relatively higher nuclease resistance (Fig. 4.6) reflected that comparatively larger amount of heterochromatins were present in the hypoxic chromatins. On the basis of proteomic and biological findings we suggest that HP1BP3 mediated heterochromatinization during hypoxia altering gene expression which might play a key role in tumorigenesis. So HP1BP3 is a potential candidate for further functional study to establish its functional roles in tumor biology. We also found that transcription regulators including NAT10, CIRH1A and NOC2L remain unreleased after nuclease digestion and their release profiles showed relatively larger amount of proteins were present in the 48h hypoxic pellet fraction, while relatively high concentration of MYBBP1A and TEX10 were observed in both 48h hypoxia and reoxygenated pellet fractions (Fig. 4.3a and Fig. 4.4e-f) indicating their heterochromatin specific chromatin binding during short term hypoxia stress. Association of these proteins might be involved in the gene repression during hypoxia which might play a crucial role in cancer metastasis [263, 264].

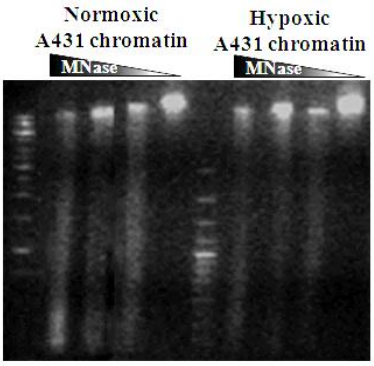

Figure 4.6: Effect of hypoxia in higher order chromatin structure. MNase figure printing of Normoxic and hypoxic A431 chromatins. Chromatins were digested with different concentration MNase (0U, 5U, 10U and 15U) for 10min and digested DNA fragments were extracted and separated in 1% agarose gel.

4.4.3 HP1BP3 is a novel regulator of tumor biology during hypoxia

In this study we found that global heterochromatinization took place during hypoxia (Fig. 4.6). Functional analysis of HP1BP3 in the chapter 3 revealed that novel chromatin associated protein HP1BP3 directly involved in the heterochromatin organization and regulates cell proliferation. Here in this study quantitative proteomic data showed that HP1BP3 increased its chromatin binding during hypoxia stress. On basis of our findings we selected HP1BP3 as a

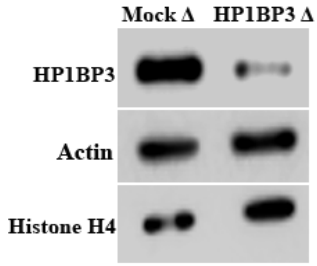

Figure 4.7: HP1BP3 knockdown in A431 cell line. Western blot images representing the expression levels of HP1BP3, actin and histone H4 in Mock and HP1BP3 depleted A431 cells.

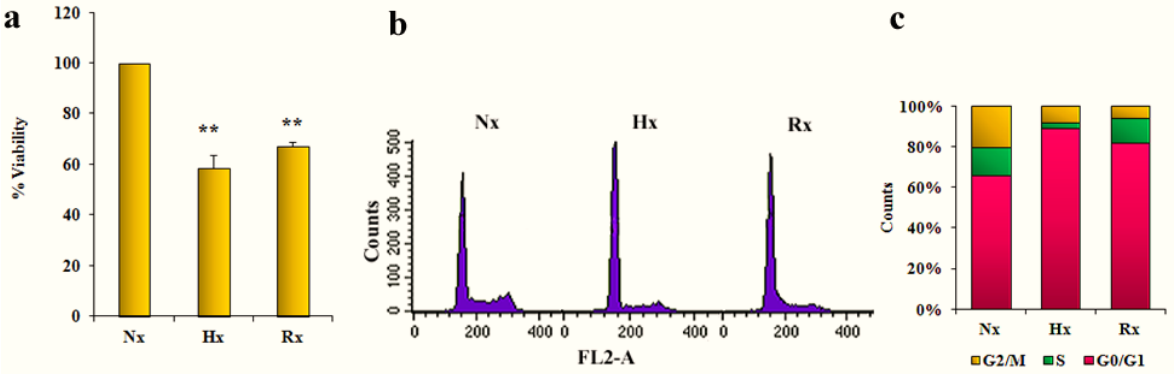

Figure 4.8: Cell viability and cell cycle progression during hypoxia. a: MTT assay result represent the percentage of viable A431 cells during normoxic, hypoxic and hypoxic-reoxygenated condition. Experiment was performed in a three biological replicates and Statistical significant was denoted as ** P-value <0.005. b: Cell cycle analysis of normoxic, hypoxic, and hypoxic-reoxygenated cells. Cells were stained with propidium iodide and DNA content was measured by flow cytometry. c: Graphical representation of G_0-G_1, S, and G_2-M phase cells distribution in the normoxic, hypoxic and hypoxic-reoxygenated condition.

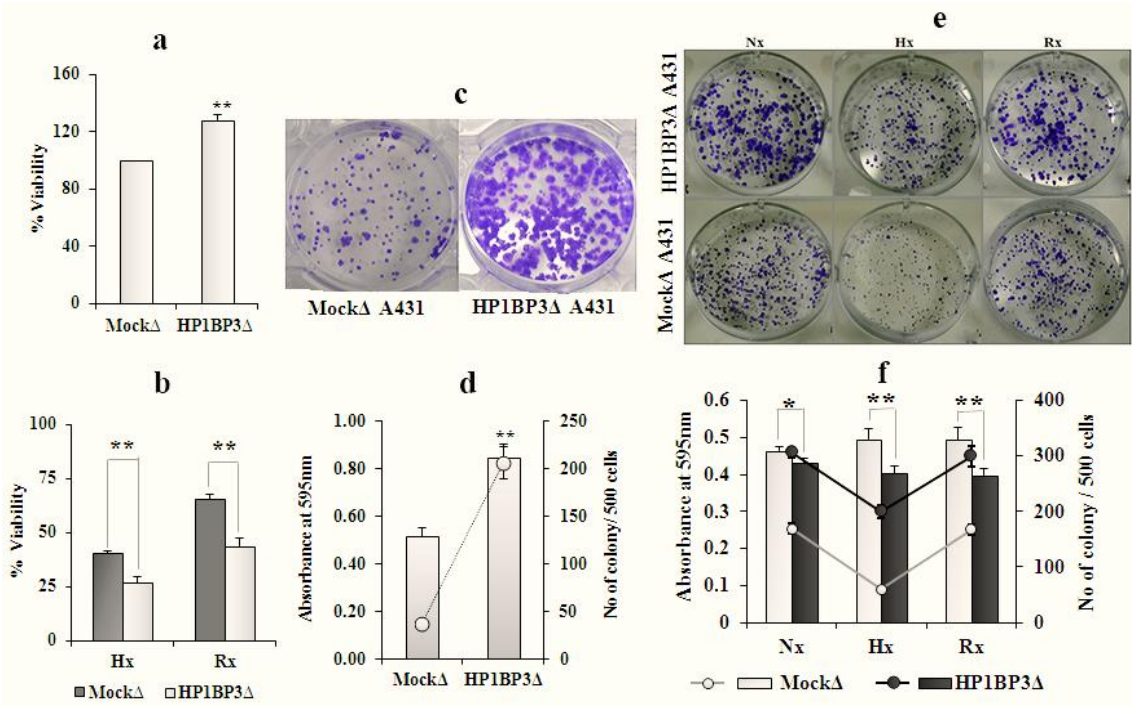

Figure 4.9: Cell viability assay and clonogenic assay for studding cell proliferation and survivability. a: Graphical represent of the relative cell viability of both Mock Δ and HP1BP3 Δ A431 phenotype after 24h and viability was measured by MTT assay. b: Relative cell viability of 48h hypoxia (Hx) and 24hypoxia and 24h reoxygenation (Rx) treated Mock Δ and HP1BP3 Δ A431 phenotypes measured by MTT assay. c-d: Clonogenicity of Mock Δ and HP1BP3 Δ A431 phenotypes. 500 viable cells/ well were seeded and incubated and after 10 day colonies were stain with crystal violet. Concentration of crystal violet used as a measurement of clonogenicity. e-f: Clonogenicity of 48h normoxia,48 hypoxia and 24h hypoxia and 24 reoxygenation treated Mock Δ and HP1BP3 Δ A431 phenotypes. Three biological replicates were used for all above experiments. Statistical significant was denoted as * P-value <0.05 and ** P-value <0.005.

potential candidate for detailed study to establish its functional roles in hypoxia induced tumorigenesis. Here we used HP1BP3 depleted A431 cells for the characterization studies. The shRNA based knock-down strategy was used to knock-down the HP1BP3 expression (Fig. 4.7).

4.4.3.1 HP1BP3 and its functional role in tumor growth

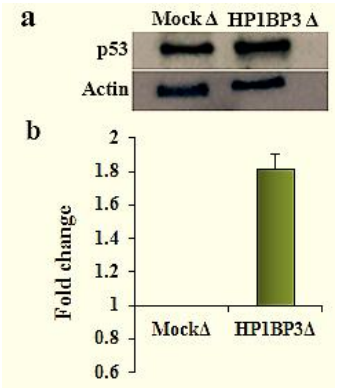

Figure 4.10: Effect of HP1BP3 depletion upon p53 expression. a: western blot images represent the p53 expression levels in mock and HP1BP3 depleted A431. b: Change of p53 expression levels in HP1BP3 depletion. P53 level was normalized by actin in the samples and five experimental replicates were used for statistical calculation.

Experimental evidences showed that cell viability was significantly decreased during hypoxia and hypoxia-reoxygenation compared to normoxia (Fig. 4.8a). Cell cycle analysis revealed that hypoxia induced cell cycle arrest at the G_0-G_1 phase (Fig. 4.8b-c). Result also showed that reoxygenation restored the cell growth by restarting the G_0-G_1 arrested cell cycle (Fig.4.8b-c). Functional studies of HP1BP3 in the chapter 3 established its regulatory role in G_1-S phase progression by promoting the G_1/S transition. Both MTT and colonigenic assay showed HP1BP3 depleted A431 phenotype was more proliferative than mock depleted phenotype (Fig. 4.9a and Fig. 4.9c-d). Both proteomic data and biological assay results suggested that HP1BP3 mediated heterochromatinization might promote G_0-G_1 arrest during hypoxia. MTT assay also showed that during both hypoxia and reoxygenation conditions viability of the HP1BP3 depleted A431 cells was significantly decreased compare to the mock depleted cells (Fig. 4.9b). Clonogenic assay results also revealed that HP1BP3 depleted cells were significantly loosed their clonogenicity during hypoxia but colonies formed by the HP1BP3 depleted cells were much larger in size compare to the colonies formed by the mock depleted cells (Fig. 4.9e-f) indicate depletion of HP1BP3 reduced cell survivability during hypoxia but increase proliferation of the survived cells. Recent evidences exhibited that during non-acidic conditions direct effect of hypoxia increases the survivability of G_0-G_1 arrested cells through bypassing p53 induced apoptosis [265]. Western blot analysis revealed that p53 level was increased by ~1.8 fold in HP1BP3 depleted A431 cells (Fig. 4.10a-b) and our proteomic data also showed that chromatin association of p53 was reduced during hypoxia stress (Fig. 4.4f). In the context of our experimental observations and evidences we hypothesize that HP1BP3 mediated

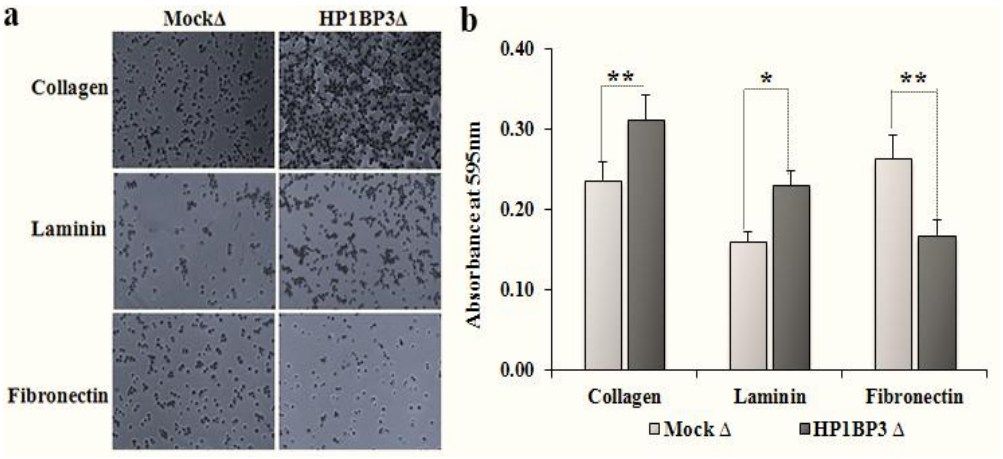

Figure 4.11: HP1BP3 mediated regulation of cell adhesion. Cell adhesion property of Mock and HP1BP3 depleted A431 phenotype with the ECM protein collagen, laminin and fibronectin. Statistical significant was denoted as * P-value <0.05 and ** P-value <0.005.

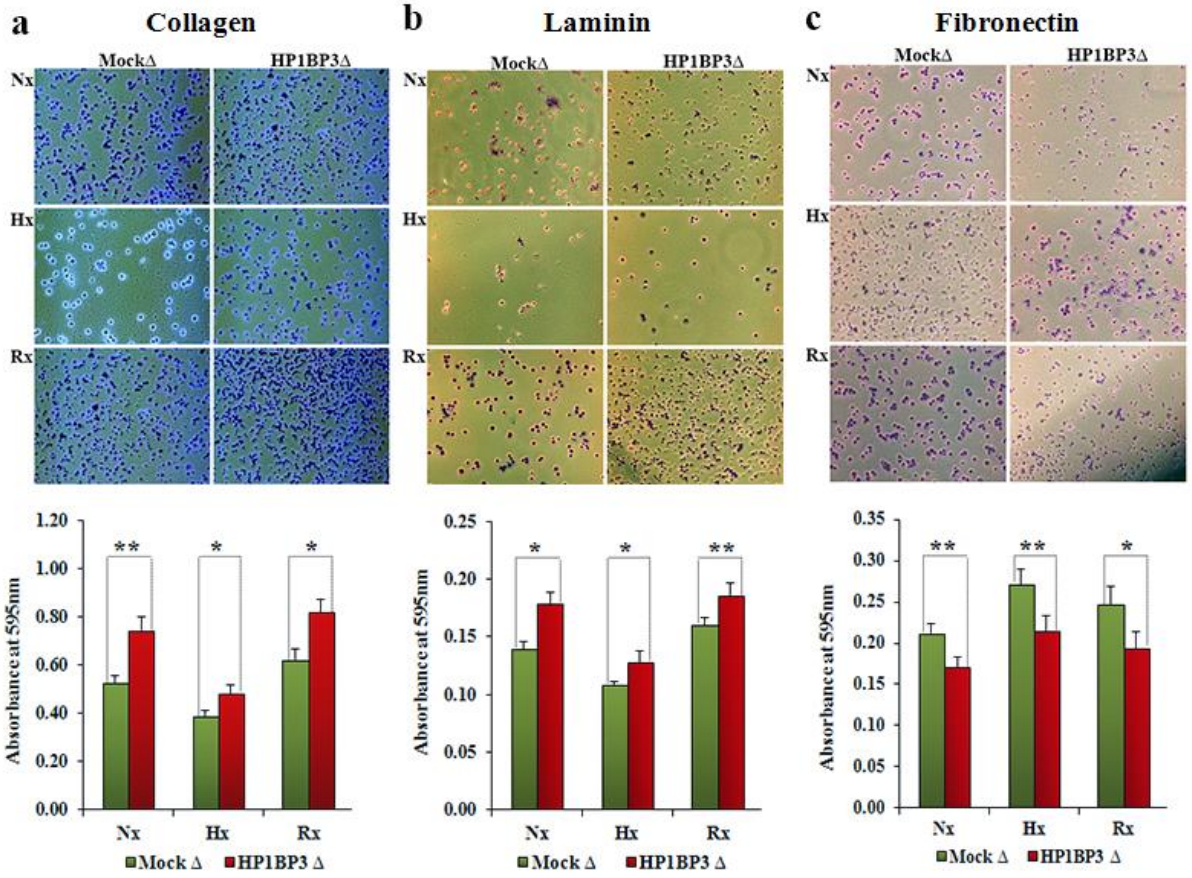

Figure 4.12: HP1BP3 mediated regulation of cell adhesion during hypoxia. 48h normoxia (Nx), 48 hypoxia (Hx), and 24h hypoxia-24h reoxygenation (Rx) pretreated cells were used for Cell adhesion assay and collagen, laminin and fibronectin were used as matrix for the assay. Statistical significant was denoted as * P-value <0.05 and ** P-value <0.005.

heterochromatinization induces transcriptional reprogramming that play a dual role during hypoxia, to prevent cellular growth by G_0-G_1 arrest and to increase cell survivability by reducing apoptotic cell death.

4.4.3.2 Regulatory role of HP1BP3 in ECM adhesion and cell migration

Inside tumor cells are surrounded by extracellular matrix (ECM). Interaction between cells and ECM plays a crucial role in tumor biology and regulates basic cellular characters including cell morphology, proliferation, survival, migration, invasion, and differentiation [266-268]. Hypoxia alters ECM mediated cell adhesion by changing their expression level [84, 269]. To study the role of HP1BP3 in cell adhesion, we performed cell adhesion assay using different ECM matrixes including collagen type I, fibronectin and laminin. During the adhesion assay, HP1BP3 depleted A431 phenotype exhibited significant increment in cell adhesion when collagen and laminin were used as adhesion matrix but cell adhesion was significantly decreased when fibronectin was used as adhesion matrix (Fig. 411a-b). Assay results also showed that the hypoxia stress caused significant reduction in collagen and laminin mediated adhesion in HP1BP3 depleted phenotype but fibronectin mediated adhesion was significantly increased and reoxygenation restore the cell adhesion property (Fig. 4.12a-c). Unlike normal cells, normoxic, hypoxic and reoxygenated HP1BP3 depleted A431 cells increased their collagen and laminin mediated cell adhesion and decreased fibronectin mediated cell adhesion comparing to mock depleted cells (Fig. 4.12a-c). Based on our experimental observation we suggested that HP1BP3 plays a crucial role in cell adhesion by regulating the expression of the cell adhesion molecules and responsible for hypoxia induced alternated cell adhesion.

Cell migration and invasion are the hallmark of metastasis. Hypoxia induced cell migration and invasion contribute to the cancer metastasis [269]. We performed scratch assay and trans-well assay to investigate the role of HP1BP3 in cell migration. Both assay results showed cell migration was significantly increased upon HP1BP3 depletion (Fig. 4.13a-b). Hypoxia and reoxygenation treated HP1BP3 depleted cells exhibited significant increment of cell migration during both wound healing scratch assay and trans-well assay and both assay results were comparable (Fig 4.13c-d). Highly migratory and invasive cancer phenotypes were characterized by disintegration of the cell-cell adhesion and increment of the cell-ECM adhesion

[270]. According to our observations we interpreted that HP1BP3 mediated heterochromatinization altered gene expressions which modify the cell-ECM interaction and reduce cell migration. Hypoxia induced HP1BP3 mediated repressed genes were reactivated during reoxygenation through withdrawal of the HP1BP3 mediated heterochromatinization which could convert normal cancer cells into a higher migratory and invasive phenotypes.

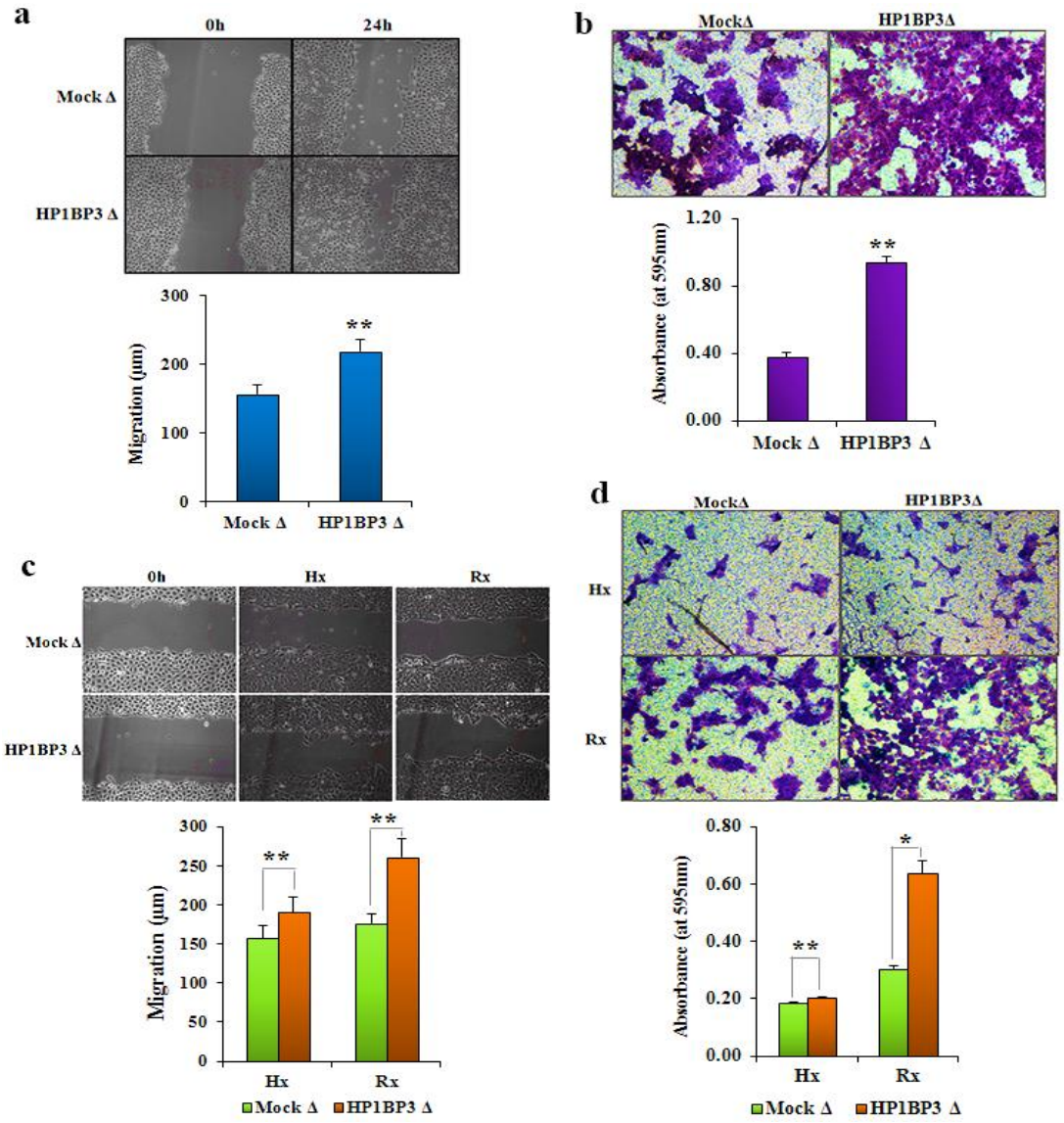

Figure 4.13: HP1BP3 mediated regulation of cell migration. a: Effect of HP1BP3 depletion in cell migration, was analyzed by wound healing scratch assay. b: Effect of HP1BP3 depletion in cell migration, cell migration towards 2.5% FBS was analyzed by trans-well assay. c: Effect of HP1BP3 depletion in cell migration during hypoxia and reoxygenation condition, was analyzed by wound healing scratch assay. d: Effect of HP1BP3 depletion in cell migration (without serum gradient) during hypoxia and reoxygenation condition, was analyzed by trans-well assay. For hypoxia and reoxygenation condition assays were performed by incubating the cells for 48h hypoxia (Hx), and 24h hypoxia and 24h reoxygenation (Rx). Statistical significant was denoted as * P-value <0.05 and ** P-value <0.005.

4.4.3.3 Hypoxia and HP1BP1 in radio- and chemo-resistance

Clinical and experimental observations established that hypoxia is solely responsible for radio- and chemo-resistance, genetic instability and systemic metastasis [271-273]. Relationship between DNA repair and genetic instability during hypoxia yet not well understood, which may have direct link with tumor progression. Ionizing radiation or chemotherapeutic agents generally causes DNA double strand breaks (DSBs) and cell death. DSBs induced genome instability was rectified through non-homologous end joining (NHEJ) and homologous recombination (HR) pathways. Our iTRAQ based proteomic data showed that NHEJ repair pathway protein XRCC5

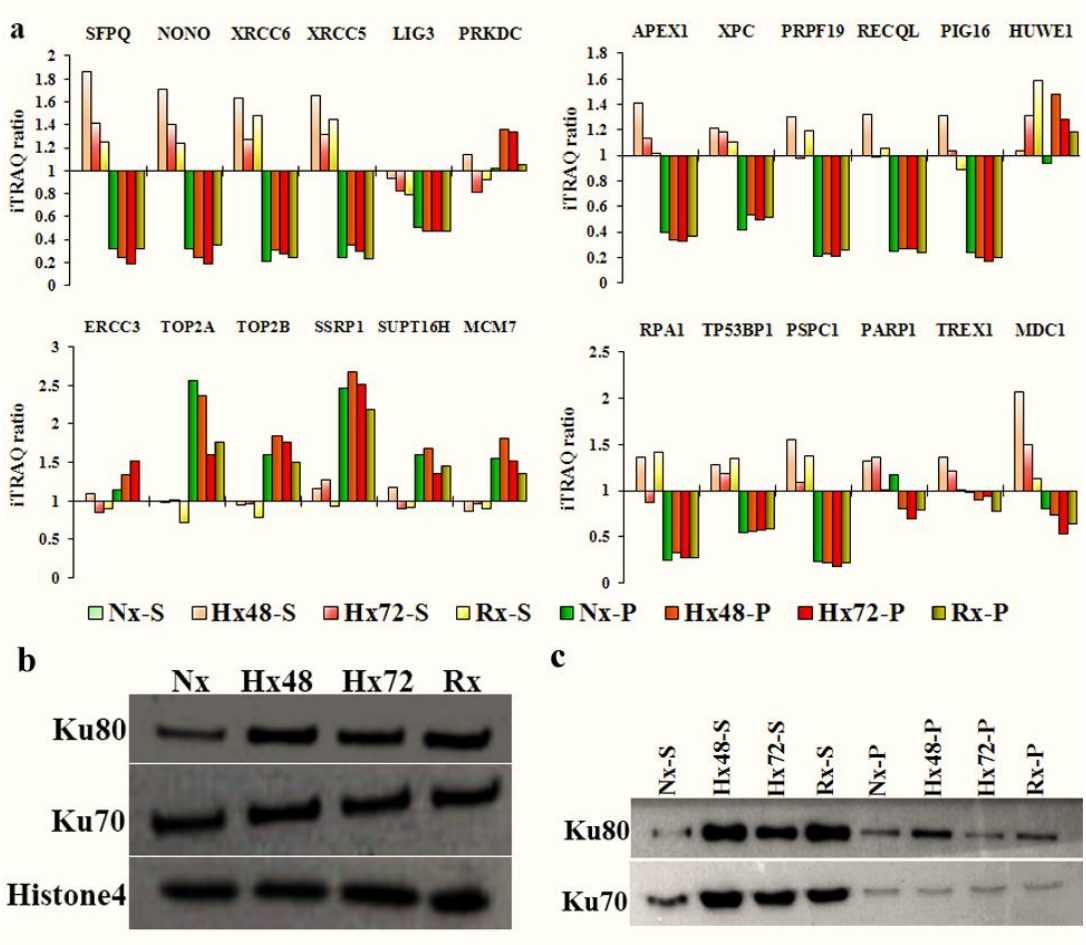

Figure 4.14: Release pattern of DNA repair proteins from normoxic, hypoxic and reoxygenated chromatin during partial DNase I digestion. a: iTRAQ ratio represent the relative abundance of protein in the samples. b: Western blot represent the chromatin-association level of Ku70, Ku80, histone H4 with 48h normoxic (Nx), 48h hypoxic (Hx48), 72h hypoxic (Hx72), and 48h hypoxic and 24h reoxygenated (Rx) chromatin. c: Western blot represent the proteins amount of Ku80 and Ku70 in different chromatin digests obtain by partial DNase I digestion of different chromatin samples.

and XRCC6 were identified with comparatively larger quantity in supernatant fractions of both hypoxic and reoxygenated chromatin samples (Hx48-S, Hx72-S and Rx-S) but another member of NHEJ pathway PRKDC was identified in a greater concentration in pellet fractions of hypoxia chromatins (Fig. 4.14a) indicate the activation of NHEJ pathway during hypoxia. Our western blot analysis showed total chromatin binding of Ku70 and Ku80 increased during both hypoxia and reoxygenation conditions (Fig. 4.14b). Western blot data also showed greater concentration of proteins were present in the DNase I digested supernatant fractions of the hypoxic and reoxygenated chromatins (Fig. 4.14d). Our recent study exhibited up-regulation of NHEJ pathway proteins during both hypoxia and reoxygenation conditions and also established their contribution in the radio- and chemo-resistance [84]. Quantitative proteomic data showed chromatin loading of NEHJ facilitator proteins including MDC1, NONO, and SFPQ were increased during hypoxia and reoxygenation conditions (Fig. 4.14a). We also identify other DSBs pathway proteins including APEX1, PIG16, PRPF19, RECQL, and XPC in our data set which showed significant increment of their chromatin binding during 48h hypoxia, while proteins like PSPC1, RPA1, and TP53BP1 were increased their chromatin binding during both 48h hypoxia and reoxygenation (Fig. 4.14a). Homologous recombination (HR) repair of DSBs was restricted between late S and G_2 phase of the cell cycle but NHEJ repair does not have such restriction [274, 275]. Our cell cycle based chromatome data suggested that the NHEJ pathway was activated throughout interphase but more activated during G_1 and G_2 phase. Based on our proteomic and biological data, we suggested that hypoxia induced G_0-G_1 arrest activated the NHEJ pathway as major DSBs repair mechanism during hypoxia stress which contributed a significant role in hypoxia induced radio- and chemo-resistance. Beside the activation of the NHEJ based DNA repair many other pathways or proteins also contributed significant roles in

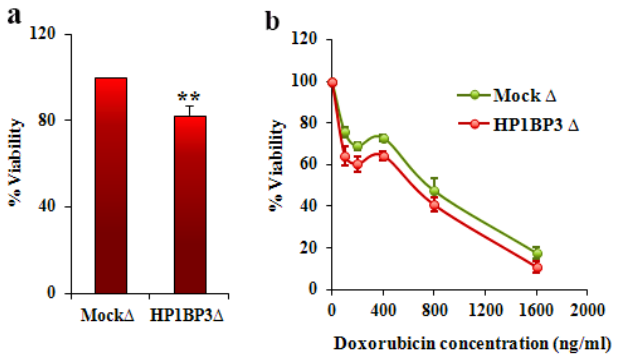

Figure 4.15: Effect of HP1BP3 depletion upon radio- and chemo-resistance. a, Cell viability of 10Gy ionization radiation treated mock and HP1BP3 depleted A431 phenotype measured by MTT assay. b, Dose-response curve represent the relative susceptibility of mock and HP1BP3 depleted A431 cells to doxorubicin over 0-1600ng/ml concentration range.

hypoxia induced radio- and chemo-resistance. Our experimental observation showed that HP1BP3 played a crucial role in the cell survivability during hypoxia which influenced us to study its role in radio- and chemo-resistance. To study its role in radio resistance we treated HP1BP3 depleted and mock depleted A431 cells with 10Gy ionization radiation and identified that HP1BP3 depletion reduced the cell viability by 18% (Fig. 4.15a). Whereas we used doxorubicin as a model chemotherapeutic agent and treat both phenotypes with different doses of doxorubicin for 24h time period. Dose-response curve showed that depletion of HP1BP3 increased the doxorubicin susceptibility in the resultant phenotype (Fig. 4.15b). HP1BP3 depletion also reduced the IC_{50} value of doxorubicin from 670.2±62ng/ml to 503.2±36ng/ml. Our biochemical assays suggested that HP1BP3 depletion produce higher radio-chemo-sensitive A431 phenotypes. Taking all experimental evidences together we first time reported that HP1BP3 induced heterochromatinization mediated gene suppression during hypoxia, contributed a significant role in the radio- and chemo-resistance.

4.4.3.4 Effect hypoxia and HP1BP3 in cancer stem cell self-renewal of A431 cells

According to the cancer stem cell (CSC) hypothesis it was thought that small populations of slowly growing stem cell like cells are responsible for initiation and development of the cancer. CSCs are characterized by their unique stem cells like self-renewal and multipotent properties. It was also thought that during hypoxia HIFs induced genetic alternation regulate the CSCs self-renewal and multipotency properties and caused further cancer progression [276, 277]. But hypoxia induced activation of CSCs is still not properly understood. Our findings indicated that HP1BP3 induced heterochromatinization and transcription reprogramming caused growth arrest and also increase

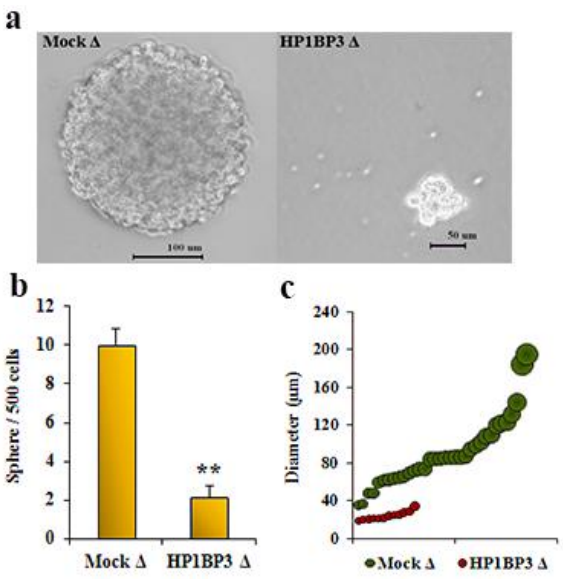

Figure 4.16: Effect of HP1BP3 depletion upon self-renewal property. a: Images of spheres formed by mock and HP1BP3 depleted A431 phenotype. b: Number of tumorspheres formed per 500 cells during sphere forming assay. c: Size distribution of mock and HP1BP3 depleted A431 tumorspheres .

cell survivability. So we suspected that HP1BP3 mediated heterochromatinization and transcription alternation during hypoxia might contribute significant roles in the CSCs activation. To study the roles of HP1BP3 on CSC self-renewal property we performed sphere formation assay for 10d (Fig. 4.16a-c). Results of the assay showed that HP1BP3 depleted A431 cells produced smaller size spheres (actually looks like a cluster of cells) of an average diameter of 25±5µm but mock depleted cells formed very prominent tumor-spheres of an average diameter of 82±15µm.The number of spheres formed by mock depleted A431 cells was ~4 times higher than HP1BP3 depleted A431 cells. Our assay results suggested that HP1BP3 mediated heterochromatinization regulates the self-renewal property of the cancer through induction of transcription reprogramming.

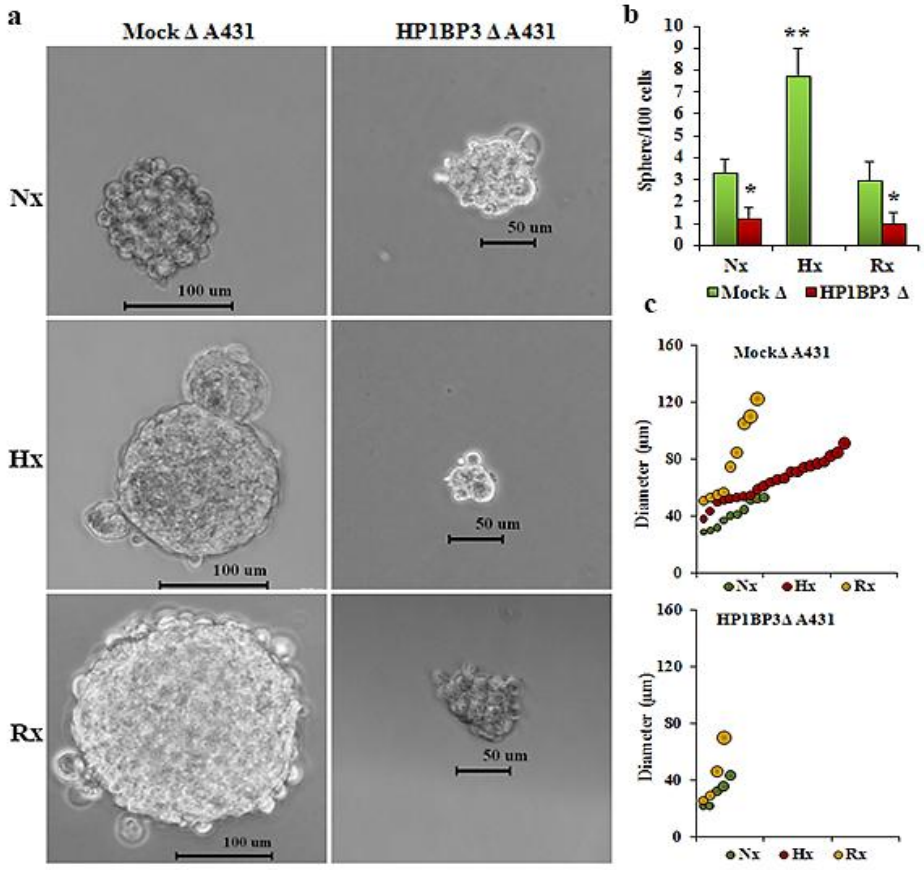

Figure 4.17: Effect of HP1BP3 depletion upon self-renewal property during hypoxia and reoxygenation. a: Tumorsphere formed by 48h normoxia (Nx), 48h Hypoxia (Hx), and 24hypoxia and 24h reoxygenation (Rx) treated mock and HP1BP3 depleted A431cells. b: Number of tumorspheres formed/100 cells seeding in different conditions as maintain c: Size distribution of spheres formed by mock and HP1BP3 depleted phenotypes during above maintained conditions.

To examine the effect of HP1BP3 depletion on CSC self-renewal efficiency during hypoxia and reoxygenation we conducted sphere formation assay using 48h normoxia, 48h hypoxia and 24h hypoxia followed by 24h reoxygenation treated A431 phenotypes (Fig. 4.17 a-c). Our assay results exhibited that during hypoxia mock depleted A431 cells increased their tumor-sphere forming efficiency by ~2.5 times comparing to normoxia and reoxygenation conditions, while HP1BP3 depleted cells reduced their sphere forming efficiency by 3 times during normoxia and reoxygenated conditions and no tumor-sphere was formed by hypoxic HP1BP3 depleted A431 cells (Fig. 3.17b). Size distribution of the tumor-spheres formed during different conditions were represented in the figure 4.17c and size distribution analysis confirmed that average sphere diameter of the mock depleted cells were increased during hypoxia (65±7µm) and reoxygenation (80±13µm) with respect to normoxia (41±5µm) condition but average sphere diameter of HP1BP3 depleted cells were not significantly changed during normoxia (30±4µm) and reoxygenated (34±6µm) conditions. Recent studies also showed that HIFs involved in the maintenance of CSCs functions during hypoxia, which contributed a significant role in radio- and chemo-resistance [278]. Based on our experimental evidences we suggested that hypoxia induced CSC self-renewal property is regulated in a HP1BP3 dependent manner.

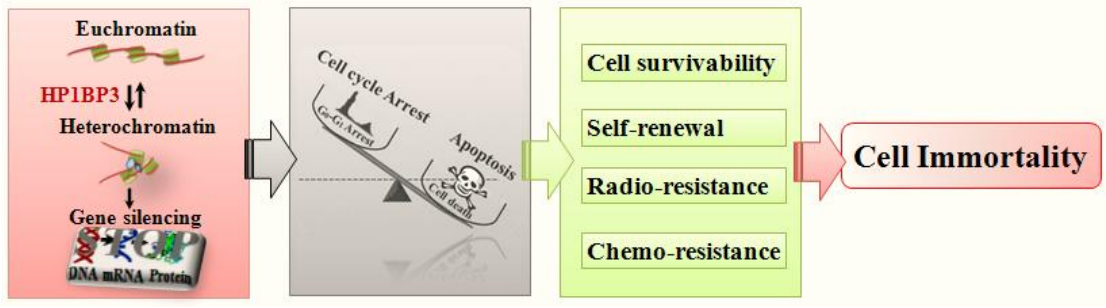

Figure 4.18: Cartoon represents the HP1BP3 induced cancer cell immortalization during hypoxia.

4.4.4 Conclusion

Hypoxia induced alternations in the chromatin biology played a significant role in cancer metastasis. In this study we applied iTRAQ based quantitative approach coupled with partial

DNase I digestion to establish the chromatin association topology of the chromatome during hypoxia to understand hypoxia induced alternation in chromatin biology. Our proteomic data revealed the picture of chromatin association dynamics of the chromatome on a global basis and provided better understanding of the hypoxia perturbed molecular pathways. We identified a novel chromatin associated protein HP1BP3 and its chromatin association was increased especially during hypoxia. Functional characterization of HP1BP3 revealed its regulatory role in cancer biology. Based on our experimental observations we hypothesized that HP1BP3 mediated heterochromatinization during hypoxia developed an imbalance between cell cycle arrest and apoptosis induced cell death. This regulatory imbalance converted normal cancer cells into immortal cancer cell phenotype by increasing some important cellular property including cell survivability, radio- and chemo-resistance and stemness. Thus HP1BP3 might be a potential therapeutic target for future cancer treatment.

Chapter 5

5 Conclusion and future direction

5.1 Concluding remarks and future perspective

Chromatin is a DNA-protein complex in which a very long DNA molecule is packed to accommodate it inside the tiny place of nucleus. Chromatin is a master regulator of all genomic events including transcription, replication, and DNA repair by regulating the DNA template accessibility through its dynamic structure. DNA-protein and protein-protein interactions play the important role in maintenance of chromatin structure and regulate its functions. Knowledge of chromatome changes in response to internal and external signals will provides invaluable information to better understand chromatin biology. Chromatin proteome and their association topology on global basis are much less extensively studied thus far. My PhD research project has established a suitable biochemical approach coupled with LC-MS/MS based high throughput proteomic technique to study the chromatome and its dynamic changes in cell cycle and hypoxia induced cancer progression. We applied enzymatic nuclease chromatin digestion to extract differentially released chromatin-associated proteins, euchromatin-associated proteins released in the supernatant fraction and heterochromatin-associated proteins remained in the pellet fraction, and in this study we used both MNase and DNase I as the digestive enzymes. Subsequently, we identified the proteins by LC-MS/MS based proteomic approach and quantify them with emPAI based label free quantification technique. We developed the technique using rat liver chromatome as model. We identified 694 high confidence proteins that were associated with either the active euchromatin or the inactive heterochromatin. Their differential release patterns upon both MNase and DNase I digestion reflected their chromatin association topology and we also validated the localization of selected proteins. The method and results are discussed in the chapter 2 of this thesis. The method can be applied to study various chromatome to understand the dynamics of the chromatin biology during different physiological and pathophysiological cellular events. We identified not only many known chromatin associated proteins but also many other proteins whose chromatin associations are not reported yet. This indicates that the chromatin associated proteome is relatively unexplored and poorly understood. There is a huge reserve of biological information waiting to be discovered. We applied our newly developed proteomic method to study cell cycle progression and hypoxia tumor to elucidate hypoxia stressed induced cancer progression and to identify key regulator potential drug target in oncogenesis for future cancer treatment.

Chapter 5

Cell cycle is a cellular event by which organism maintain their existence through multiplication of the cells. All chromatin dependent cellular events including genome and epigenome duplication, genome packaging, transcription, genome stability maintenance are conducted throughout cell cycle specifically during interphase progression and chromatin maintain its dynamic structure to performs these events. Chromatin proteomics and their chromatin association topology during interphase can provide essential information to better understand their regulatory role in cell cycle progression. We applied our nuclease digestion coupled LC-MS/MS based proteomic approach to study the chromatin dynamics during interphase progression as described in the chapter 3. We extracted chromatins from different interphase stages and partially digested them with MNase to release the chromatin associated proteins and quantitative proteomic profiling was performed by iTRAQ based shotgun proteomic approach. We identified 481 proteins with differential chromatin association topology during different stages of interphase. We also validated the iTRAQ data through western blot analysis. Our findings regarding differential chromatin association of chromatome during interphase progression help us to understand their regulatory role in cell cycle progression. As hyper-proliferation or uncontrolled cell growth due to deregulated cell cycle is the hallmark of cancer, our results might also provide critical clues to better understand the pathophysiology of cell cycle deregulation induced/related disease like cancer. Hypoxic tumor microenvironment plays the crucial role in tumorigenesis and it is well established that many epigenetic factors including HIFs regulation play a significant regulatory role in tumorigenesis through altering the chromatin biology. Chromatome and their association topology will provide the better understanding regarding the altered chromatin biology of tumorigenesis and also help us to explore the molecular mechanism of hypoxia perturbed pathways and their importance in tumorigenesis. In the chapter 4, we used *in vivo* hypoxia model to study the hypoxia induced tumorigenesis and nuclease digestion coupled to LC-MS/MS based proteomic strategy to study the hypoxia evolved chromatome and their roles in tumorigenesis. Chromatins were extracted from A431 cells cultures with different oxygen levels and partially digested with DNase I to release the chromatome to understand their association topology and iTRAQ based proteomic approach was used for quantitative proteomic profiling of the chromatome. A total of 1446 proteins were identified and quantified which were differentially associated with the different hypoxic and re-oxygenated cancer chromatins. Our findings help us to reveal the altered chromatin biology

during hypoxia induced tumorigenesis which also provides better understanding regarding few hypoxia perturbed pathways including NHEJ dependent DSBs repair pathway. The cell cycle chromatome findings provide the invaluable information which helped us to interpret the result from hypoxia induced chromatome dynamics to elucidate cancer pathogenesis.

There are driver and passenger proteins/genes in the tumorigenesis. The driver proteins are likely the key switch in tumor progression and malignancy. The studied cell cycle dynamic chromatome and hypoxia induced chromatome changes revealed the key switch in controlling cancer progression. In the PhD project, through intense studies on chromatome during both physiological cell cycle progression and hypoxia cancer pathophysiological cellular events, we identified one novel chromatin associated protein HP1BP3 which showed dynamic chromatin association during interphase progression and also during hypoxia stress, indicating this protein as potential key regulator of cancer progression and drug target for cancer treatment. Therefore, we performed extensive functional characterization on HP1BP3 to confirm its importance in cell cycle and tumorigenesis. Our experimental observations and evidences reflected that HP1BP3 is involved in the maintenance of chromatin structural integrity through heterochromatinization and in regulating protein expressions. Depletion of HP1BP3 increases the nucleus size without changing the cell size. Functional studies also showed its involvement in regulation of cell proliferation through regulating the G_1 phase length. Our data also suggested that HP1BP3 is involved in hypoxia induced growth arrest through arresting the cell cycle in G_0-G_1 phase. Cell line based functional study also revealed its involvement in cell survivability, radio- and chemo-resistance, cell adhesion, cell migration and stemness induction. Based on our proteomic, biological and biochemical evidences we hypothesized that HP1BP3 mediated heterochromatinization during hypoxia converted cancer cells into immortal aggressive malignant cancer phenotype by increasing cell-survivability, radio- and chemo-resistance and stemness properties. HP1BP3 is a relatively less characterized protein with very important potential functions in cancer progression and normal cell cycle control. To understand the molecular mechanism of HP1BP3 dependent cellular events, we need to know its interacting partners. This objective will be achieved through HP1BP3 interactome study which could reveal the molecular mechanisms of its biological function. To further establishment of its importance in tumorigenesis, we need to evaluate the tumorigenic property of the HP1BP3 depleted

phenotype in both *in vitro* and *in vivo* models based experiment which might strengthen our findings and proven its potentiality as a therapeutic target.

References

Reference

[1] Luger K, Mader AW, Richmond RK, Sargent DF, Richmond TJ. Crystal structure of the nucleosome core particle at 2.8 A resolution. *Nature*. (1997) 389: 251-260.

[2] Bednar J, Horowitz RA, Grigoryev SA, Carruthers LM, Hansen JC, Koster AJ, et al. Nucleosomes, linker DNA, and linker histone form a unique structural motif that directs the higher-order folding and compaction of chromatin. *Proceedings of the National Academy of Sciences of the United States of America*. (1998) 95: 14173-14178.

[3] Horn PJ, Peterson CL. Molecular biology. Chromatin higher order folding wrapping up transcription. *Science*. (2002) 297: 1824-1827.

[4] Ushiki T, Hoshi O, Iwai K, Kimura E, Shigeno M. The structure of human metaphase chromosomes: its histological perspective and new horizons by atomic force microscopy. *Archives of histology and cytology*. (2002) 65: 377-390.

[5] Van Bortle K, Corces VG. Nuclear organization and genome function. *Annual review of cell and developmental biology*. (2012) 28: 163-187.

[6] Dulac C. Brain function and chromatin plasticity. *Nature*. (2010) 465: 728-735.

[7] Margueron R, Trojer P, Reinberg D. The key to development: interpreting the histone code? *Current opinion in genetics & development*. (2005) 15: 163-176.

[8] Black J, Van Rechem C, Whetstine J. Histone lysine methylation dynamics: establishment, regulation, and biological impact. *Molecular Cell*. (2012) 48: 491-507.

[9] Sims RJ, 3rd, Nishioka K, Reinberg D. Histone lysine methylation: a signature for chromatin function. *Trends in genetics : TIG*. (2003) 19: 629-639.

[10] Bannister AJ, Schneider R, Kouzarides T. Histone methylation: dynamic or static? *Cell*. (2002) 109: 801-806.

[11] Dormann HL, Tseng BS, Allis CD, Funabiki H, Fischle W. Dynamic regulation of effector protein binding to histone modifications: the biology of HP1 switching. *Cell cycle (Georgetown, Tex.)*. (2006) 5: 2842-2851.

Reference

[12] Caiafa P, Zampieri M. DNA methylation and chromatin structure: the puzzling CpG islands. *Journal of cellular biochemistry*. (2005) 94: 257-265.

[13] Kalashnikova AA, Porter-Goff ME, Muthurajan UM, Luger K, Hansen JC. The role of the nucleosome acidic patch in modulating higher order chromatin structure. *Journal of the Royal Society, Interface / the Royal Society*. (2013) 10: 20121022.

[14] Schuettengruber B, Cavalli G. Polycomb domain formation depends on short and long distance regulatory cues. *PloS one*. (2013) 8: e56531.

[15] Thomas JO, Stott K. H1 and HMGB1: modulators of chromatin structure. *Biochemical Society transactions*. (2012) 40: 341-346.

[16] Calo E, Wysocka J. Modification of enhancer chromatin: what, how, and why? *Molecular cell*. (2013) 49: 825-837.

[17] Kouzarides T. SnapShot: Histone-modifying enzymes. *Cell*. (2007) 128: 802.

[18] Ruthenburg AJ, Allis CD, Wysocka J. Methylation of lysine 4 on histone H3: intricacy of writing and reading a single epigenetic mark. *Molecular cell*. (2007) 25: 15-30.

[19] Thompson LL, Guppy BJ, Sawchuk L, Davie JR, McManus KJ. Regulation of chromatin structure via histone post-translational modification and the link to carcinogenesis. *Cancer metastasis reviews*. (2013).

[20] Santos-Rosa H, Caldas C. Chromatin modifier enzymes, the histone code and cancer. *European journal of cancer (Oxford, England : 1990)*. (2005) 41: 2381-2402.

[21] Delcuve GP, Rastegar M, Davie JR. Epigenetic control. *Journal of cellular physiology*. (2009) 219: 243-250.

[22] Jeong S, Stein A. Micrococcal nuclease digestion of nuclei reveals extended nucleosome ladders having anomalous DNA lengths for chromatin assembled on non-replicating plasmids in transfected cells. *Nucleic acids research*. (1994) 22: 370-375.

Reference

[23] Sun YL, Xu YZ, Bellard M, Chambon P. Digestion of the chicken beta-globin gene chromatin with micrococcal nuclease reveals the presence of an altered nucleosomal array characterized by an atypical ladder of DNA fragments. *The EMBO journal*. (1986) 5: 293-300.

[24] Roth SL, Malani N, Bushman FD. Gammaretroviral integration into nucleosomal target DNA in vivo. *Journal of virology*.(2011) 85: 7393-7401.

[25] Weisbrod S. Active chromatin. *Nature*. (1982) 297: 289-295.

[26] Parnaik VK. DNAase-I-hypersensitive sites in the mouse albumin gene. *Biochim Biophys Acta*. (1987) 910: 27-33.

[27] Wood WI, Felsenfeld G. Chromatin structure of the chicken beta-globin gene region. Sensitivity to DNase I, micrococcal nuclease, and DNase II. *The Journal of biological chemistry*. (1982) 257: 7730-7736.

[28] Dynan WS, Tjian R. The promoter-specific transcription factor Sp1 binds to upstream sequences in the SV40 early promoter. *Cell*. (1983) 35: 79-87.

[29] Aebersold R, Mann M. Mass spectrometry-based proteomics. *Nature*. (2003) 422: 198-207.

[30] Ong SE, Mann M. Mass spectrometry-based proteomics turns quantitative. *Nature chemical biology*. (2005) 1: 252-262.

[31] Schulze WX, Usadel B. Quantitation in mass-spectrometry-based proteomics. *Annual review of plant biology*. (2010) 61: 491-516.

[32] Bantscheff M, Schirle M, Sweetman G, Rick J, Kuster B. Quantitative mass spectrometry in proteomics: a critical review. *Analytical and bioanalytical chemistry*. (2007) 389: 1017-1031.

[33] Ong SE, Blagoev B, Kratchmarova I, Kristensen DB, Steen H, Pandey A, et al. Stable isotope labeling by amino acids in cell culture, SILAC, as a simple and accurate approach to expression proteomics. *Molecular & cellular proteomics : MCP*. (2002) 1: 376-386.

Reference

[34] Ross PL, Huang YN, Marchese JN, Williamson B, Parker K, Hattan S, et al. Multiplexed protein quantitation in Saccharomyces cerevisiae using amine-reactive isobaric tagging reagents. *Molecular & cellular proteomics : MCP*. (2004) 3: 1154-1169.

[35] Hao P, Qian J, Ren Y, Sze SK. Electrostatic repulsion-hydrophilic interaction chromatography (ERLIC) versus strong cation exchange (SCX) for fractionation of iTRAQ-labeled peptides. *Journal of proteome research*. (2011) 10: 5568-5574.

[36] Ishihama Y, Oda Y, Tabata T, Sato T, Nagasu T, Rappsilber J, et al. Exponentially modified protein abundance index (emPAI) for estimation of absolute protein amount in proteomics by the number of sequenced peptides per protein. *Molecular & Cellular Proteomics*. (2005) 4: 1265-1272.

[37] Cooper GM. The eukaryotic cell cycle. The cell: a molecular approach. 2nd edition ed. Sunderland (MA): Sinauer Associates; 2000.

[38] Alberts B, Johnson A, Lewis J, et al. An overview of the cell cycle. molecular biology of the cell. 4th edition ed. New York: Garland Science; 2002.

[39] Sherr CJ. Mammalian G1 cyclins. *Cell*. (1993) 73: 1059-1065.

[40] Sherr CJ, Roberts JM. Inhibitors of mammalian G1 cyclin-dependent kinases. *Genes & development*. (1995) 9: 1149-1163.

[41] Farmer H, McCabe N, Lord CJ, Tutt AN, Johnson DA, Richardson TB, et al. Targeting the DNA repair defect in BRCA mutant cells as a therapeutic strategy. *Nature*. (2005) 434: 917-921.

[42] Novák B, Sible JC, Tyson JJ. Checkpoints in the Cell Cycle. *eLS*: John Wiley & Sons, Ltd; (2001).

[43] Vleugel M, Hoogendoorn E, Snel B, Kops GJ. Evolution and function of the mitotic checkpoint. *Developmental cell*. (2012) 23: 239-250.

Reference

[44] Hartwell L. Defects in a cell cycle checkpoint may be responsible for the genomic instability of cancer cells. *Cell*. (1992) 71: 543-546.

[45] Morgan SE, Kastan MB. p53 and ATM: Cell cycle, cell death, and cancer. *Advances in cancer research.* (1997). 71: 1-25.

[46] Andreeff M GD, Pardee AB. Cell proliferation, differentiation, and apoptosis. in: bast RC JR KD, Pollock RE, et al., editor. Holland-Frei Cancer Medicine. 5th edition ed. Hamilton (ON): BC Decker; 2000.

[47] Johnson DG, Walker CL. Cyclins and cell cycle checkpoints. *Annual review of pharmacology and toxicology*. (1999) 39: 295-312.

[48] Weinberg RA. The retinoblastoma protein and cell cycle control. *Cell*. (1995) 81: 323-330.

[49] Sherr CJ. Tumor surveillance via the ARF-p53 pathway. *Genes and Development*. (1998) 12: 2984-2991.

[50] Nevins JR. The Rb/E2F pathway and cancer. *Human Molecular Genetics*. (2001) 10: 699-703.

[51] Bartek J, Bartkova J, Lukas J. The retinoblastoma protein pathway in cell cycle control and cancer. *Experimental cell research.* (1997) 237: 1-6.

[52] Giancotti FG, Ruoslahti E. Integrin signaling. *Science*. (1999) 285: 1028-1032.

[53] Mizuguchi T, Hui T, Palm K, Sugiyama N, Mitaka T, Demetriou AA, et al. Fibronectin, integrins, and growth control. *Journal of cellular physiology*. (2001) 189: 1-13.

[54] Pelengaris S, Khan M, Evan G. c-MYC: More than just a matter of life and death. *Nature Reviews Cancer*. (2002) 2: 764-776.

[55] Shaulian E, Karin M. AP-1 as a regulator of cell life and death. *Nature Cell Biology*. (2002) 4: E131-E136.

[56] Ryan A, Al-Jehani RM, Mulligan KT, Jacobs IJ. No evidence exists for methylation inactivation of the p16 tumor suppressor gene in ovarian carcinogenesis. *Gynecologic oncology*. (1998) 68: 14-17.

[57] Barra V, Schillaci T, Lentini L, Costa G, Di Leonardo A. Bypass of cell cycle arrest induced by transient DNMT1 post-transcriptional silencing triggers aneuploidy in human cells. *Cell division*. (2012) 7: 2.

[58] Fan H, Chen L, Zhang F, Quan Y, Su X, Qiu X, et al. MTSS1, a novel target of DNA methyltransferase 3B, functions as a tumor suppressor in hepatocellular carcinoma. *Oncogene*. (2012) 31: 2298-2308.

[59] Zhou JX, Niehans GA, Shar A, Rubins JB, Frizelle SP, Kratzke RA. Mechanisms of G1 checkpoint loss in resected early stage non-small cell lung cancer. *Lung cancer (Amsterdam, Netherlands)*. (2001) 32: 27-38.

[60] Ferreira R, Naguibneva I, Pritchard LL, Ait-Si-Ali S, Harel-Bellan A. The Rb/chromatin connection and epigenetic control: opinion. *Oncogene*. (2001) 20: 3128-3133.

[61] Clurman BE, Roberts JM. Cell cycle and cancer. *Journal of the National Cancer Institute*. (1995) 87: 1499-1501.

[62] Kamb A. Cell-cycle regulators and cancer. *Trends in genetics : TIG*. (1995) 11: 136-140.

[63] Porter PL, Malone KE, Heagerty PJ, Alexander GM, Gatti LA, Firpo EJ, et al. Expression of cell-cycle regulators p27(Kip1) and cyclin E, alone and in combination, correlate with survival in young breast cancer patients. *Nature Medicine*. (1997) 3: 222-225.

[64] Musgrove EA, Lee CSL, Buckley MF, Sutherland RL. Cyclin D1 induction in breast cancer cells shortens G1 and is sufficient for cells arrested in G1 to complete the cell cycle. *Proceedings of the National Academy of Sciences of the United States of America*. (1994) 91: 8022-8026.

[65] Mehlen P, Puisieux A. Metastasis: a question of life or death. *Nature reviews. Cancer*. (2006) 6: 449-458.

[66] Gonzalez-Angulo AM, Morales-Vasquez F, Hortobagyi GN. Overview of resistance to systemic therapy in patients with breast cancer. *Advances in experimental medicine and biology*. (2007) 608: 1-22.

[67] Wolfer A, Wittner BS, Irimia D, Flavin RJ, Lupien M, Gunawardane RN, et al. MYC regulation of a "poor-prognosis" metastatic cancer cell state. *Proceedings of the National Academy of Sciences of the United States of America*. (2010) 107: 3698-3703.

[68] Jakobisiak M, Lasek W, Golab J. Natural mechanisms protecting against cancer. *Immunology letters*. (2003) 90: 103-122.

[69] Bhat TA, Singh RP. Tumor angiogenesis--a potential target in cancer chemoprevention. *Food and chemical toxicology : an international journal published for the British Industrial Biological Research Association*. (2008) 46: 1334-1345.

[70] Pouyssegur J, Dayan F, Mazure NM. Hypoxia signalling in cancer and approaches to enforce tumour regression. *Nature*. (2006) 441: 437-443.

[71] Denko NC. Hypoxia, HIF1 and glucose metabolism in the solid tumour. *Nature reviews. Cancer*. (2008) 8: 705-713.

[72] Bertout JA, Patel SA, Simon MC. The impact of O2 availability on human cancer. *Nature reviews. Cancer*. (2008) 8: 967-975.

[73] Ruan K, Song G, Ouyang G. Role of hypoxia in the hallmarks of human cancer. *Journal of cellular biochemistry*. (2009) 107: 1053-1062.

[74] Brizel DM, Dodge RK, Clough RW, Dewhirst MW. Oxygenation of head and neck cancer: changes during radiotherapy and impact on treatment outcome. *Radiotherapy and Oncology*. (1999) 53: 113-117.

[75] Nordsmark M, Overgaard M, Overgaard J. Pretreatment oxygenation predicts radiation response in advanced squamous cell carcinoma of the head and neck. *Radiotherapy and oncology : journal of the European Society for Therapeutic Radiology and Oncology*. (1996) 41: 31-39.

[76] Ghattass K, Assah R, El-Sabban M, Gali-Muhtasib H. Targeting hypoxia for sensitization of tumors to radio-and chemo-therapy. *Current cancer drug targets*. (2013) 13: 670-685.

[77] Brown JM. Tumor microenvironment and the response to anticancer therapy. *Cancer biology & therapy*. (2002) 1: 453-458.

[78] Cuisnier O, Serduc R, Lavieille JP, Longuet M, Reyt E, Riva C. Chronic hypoxia protects against gamma-irradiation-induced apoptosis by inducing bcl-2 up-regulation and inhibiting mitochondrial translocation and conformational change of bax protein. *International journal of oncology*. (2003) 23: 1033-1041.

[79] Powell SN, Abraham EH. The biology of radioresistance: similarities, differences and interactions with drug resistance. *Cytotechnology*. (1993) 12: 325-345.

[80] Yasuda H. Solid tumor physiology and hypoxia-induced chemo/radio-resistance: novel strategy for cancer therapy: nitric oxide donor as a therapeutic enhancer. *Nitric oxide : biology and chemistry / official journal of the Nitric Oxide Society*. (2008) 19: 205-216.

[81] Nurwidya F, Takahashi F, Minakata K, Murakami A, Takahashi K. From tumor hypoxia to cancer progression: the implications of hypoxia-inducible factor-1 expression in cancers. *Anatomy & cell biology*. (2012) 45: 73-78.

[82] Pathak R, Sarma A, Sengupta B, Dey SK, Khuda-Bukhsh AR. Response to high LET radiation 12C (LET, 295 keV/microm) in M5 cells, a radio resistant cell strain derived from Chinese hamster V79 cells. *International journal of radiation biology*. (2007) 83: 53-63.

[83] Tsioli PG, Patsouris ES, Giaginis C, Theocharis SE. DNA repair systems in rhabdomyosarcoma. *Histology and histopathology*. (2013) 28: 971-984.

[84] Ren Y, Hao P, Dutta B, Cheow ES, Sim KH, Gan CS, et al. Hypoxia modulates A431 cellular pathways association to tumor radioresistance and enhanced migration revealed by comprehensive proteomic and functional studies. *Molecular & cellular proteomics : MCP*. (2013) 12: 485-498.

[85] Fu Y, Zheng S, Zheng Y, Huang R, An N, Liang A, et al. Glioma derived isocitrate dehydrogenase-2 mutations induced up-regulation of HIF-1alpha and beta-catenin signaling: possible impact on glioma cell metastasis and chemo-resistance. *The international journal of biochemistry & cell biology*. (2012) 44: 770-775.

[86] Doublier S, Belisario DC, Polimeni M, Annaratone L, Riganti C, Allia E, et al. HIF-1 activation induces doxorubicin resistance in MCF7 3-D spheroids via P-glycoprotein expression: a potential model of the chemo-resistance of invasive micropapillary carcinoma of the breast. *BMC cancer*. (2012) 12: 4.

[87] Dangi-Garimella S, Sahai V, Ebine K, Kumar K, Munshi HG. Three-dimensional collagen i promotes gemcitabine resistance in vitro in pancreatic cancer cells through HMGA2-dependent histone acetyltransferase expression. *PloS one*. (2013) 8: e64566.

[88] Fukumura D, Jain RK. Tumor microvasculature and microenvironment: targets for anti-angiogenesis and normalization. *Microvascular research*. (2007) 74: 72-84.

[89] Mareel MM, Bracke ME, Boghaert ER. Tumour invasion and metastasis: therapeutic implications? *Radiotherapy and oncology : journal of the European Society for Therapeutic Radiology and Oncology*. (1986) 6: 135-142.

[90] Gatenby RA, Smallbone K, Maini PK, Rose F, Averill J, Nagle RB, et al. Cellular adaptations to hypoxia and acidosis during somatic evolution of breast cancer. *British journal of cancer*. (2007) 97: 646-653.

[91] Paszek MJ, Zahir N, Johnson KR, Lakins JN, Rozenberg GI, Gefen A, et al. Tensional homeostasis and the malignant phenotype. *Cancer cell*. (2005) 8: 241-254.

[92] Moore SW, Roca-Cusachs P, Sheetz MP. Stretchy proteins on stretchy substrates: the important elements of integrin-mediated rigidity sensing. *Developmental cell*. (2010) 19: 194-206.

[93] Roussos ET, Condeelis JS, Patsialou A. Chemotaxis in cancer. *Nature reviews. Cancer*. (2011) 11: 573-587.

[94] Polacheck WJ, Zervantonakis IK, Kamm RD. Tumor cell migration in complex microenvironments. *Cellular and Molecular Life Sciences*. (2013) 70: 1335-1356.

[95] Tsai YP, Wu KJ. Hypoxia-regulated target genes implicated in tumor metastasis. *Journal of biomedical science*. (2012) 19: 102.

[96] Fu L, Chen L, Yang J, Ye T, Chen Y, Fang J. HIF-1alpha-induced histone demethylase JMJD2B contributes to the malignant phenotype of colorectal cancer cells via an epigenetic mechanism. *Carcinogenesis*. (2012) 33: 1664-1673.

[97] Kim JG, Yi JM, Park SJ, Kim JS, Son TG, Yang K, et al. Histone demethylase JMJD2B-mediated cell proliferation regulated by hypoxia and radiation in gastric cancer cell. *Biochim Biophys Acta*. (2012) 1819: 1200-1207.

[98] Heddleston JM, Wu Q, Rivera M, Minhas S, Lathia JD, Sloan AE, et al. Hypoxia-induced mixed-lineage leukemia 1 regulates glioma stem cell tumorigenic potential. *Cell death and differentiation*. (2012) 19: 428-439.

[99] Wicha MS, Liu S, Dontu G. Cancer stem cells: An old idea - A paradigm shift. *Cancer Research*. (2006) 66: 1883-1890.

[100] Lobo NA, Shimono Y, Qian D, Clarke MF. The biology of cancer stem cells. *Annual review of cell and developmental biology*. (2007). 23: 675-699.

[101] Reya T, Clevers H. Wnt signalling in stem cells and cancer. *Nature*. (2005) 434: 843-850.

[102] Voronkov A, Krauss S. Wnt/beta-catenin signaling and small molecule inhibitors. *Current Pharmaceutical Design*. (2013) 19: 634-664.

[103] Liu S, Dontu G, Mantle ID, Patel S, Ahn NS, Jackson KW, et al. Hedgehog signaling and Bmi-1 regulate self-renewal of normal and malignant human mammary stem cells. *Cancer research*. (2006) 66: 6063-6071.

[104] Nanta R, Kumar D, Meeker D, Rodova M, Van Veldhuizen PJ, Shankar S, et al. NVP-LDE-225 (Erismodegib) inhibits epithelial-mesenchymal transition and human prostate cancer

stem cell growth in NOD/SCID IL2Rgamma null mice by regulating Bmi-1 and microRNA-128. *Oncogenesis*. (2013) 2: e42.

[105] Arima Y, Hayashi N, Hayashi H, Sasaki M, Kai K, Sugihara E, et al. Loss of p16 expression is associated with the stem cell characteristics of surface markers and therapeutic resistance in estrogen receptor-negative breast cancer. *International journal of cancer. Journal international du cancer*. (2012) 130: 2568-2579.

[106] Garvalov BK, Acker T. Cancer stem cells: a new framework for the design of tumor therapies. *International journal of molecular medicine (Berl)*. (2011) 89: 95-107.

[107] Li P, Zhou C, Xu L, Xiao H. Hypoxia enhances stemness of cancer stem cells in Glioblastoma: An in vitro study. *International Journal of Medical Sciences*. (2013) 10: 399-407.

[108] Gustafsson MV, Zheng X, Pereira T, Gradin K, Jin S, Lundkvist J, et al. Hypoxia requires notch signaling to maintain the undifferentiated cell state. *Developmental cell*. (2005) 9: 617-628.

[109] Jogi A, Ora I, Nilsson H, Lindeheim A, Makino Y, Poellinger L, et al. Hypoxia alters gene expression in human neuroblastoma cells toward an immature and neural crest-like phenotype. *Proceedings of the National Academy of Sciences of the United States of America*. (2002) 99: 7021-7026.

[110] Covello KL, Kehler J, Yu H, Gordan JD, Arsham AM, Hu CJ, et al. HIF-2alpha regulates Oct-4: effects of hypoxia on stem cell function, embryonic development, and tumor growth. *Genes & development*. (2006) 20: 557-570.

[111] Gordan JD, Bertout JA, Hu CJ, Diehl JA, Simon MC. HIF-2alpha promotes hypoxic cell proliferation by enhancing c-myc transcriptional activity. *Cancer cell*. (2007) 11: 335-347.

[112] Cannito S, Novo E, Compagnone A, Valfre di Bonzo L, Busletta C, Zamara E, et al. Redox mechanisms switch on hypoxia-dependent epithelial-mesenchymal transition in cancer cells. *Carcinogenesis*. (2008) 29: 2267-2278.

[113] Ji F, Wang Y, Qiu L, Li S, Zhu J, Liang Z, et al. Hypoxia inducible factor 1alpha-mediated LOX expression correlates with migration and invasion in epithelial ovarian cancer. *International journal of oncology*. (2013) 42: 1578-1588.

[114] Staller P, Sulitkova J, Lisztwan J, Moch H, Oakeley EJ, Krek W. Chemokine receptor CXCR4 downregulated by von Hippel-Lindau tumour suppressor pVHL. *Nature*. (2003) 425: 307-311.

[115] Zhu S, Zhou Y, Wang L, Zhang J, Wu H, Xiong J, et al. Transcriptional upregulation of MT2-MMP in response to hypoxia is promoted by HIF-1alpha in cancer cells. *Molecular carcinogenesis*. (2011) 50: 770-780.

[116] Ward C, Langdon SP, Mullen P, Harris AL, Harrison DJ, Supuran CT, et al. New strategies for targeting the hypoxic tumour microenvironment in breast cancer. *Cancer Treatment Reviews*. (2013) 39: 171-179.

[117] Hendrich B, Bickmore W. Human diseases with underlying defects in chromatin structure and modification. *Human molecular genetics*. (2001) 10: 2233-2242.

[118] Cho KS, Elizondo LI, Boerkoel CF. Advances in chromatin remodeling and human disease. *Current opinion in genetics & development*. (2004) 14: 308-315.

[119] Li G, Reinberg D. Chromatin higher-order structures and gene regulation. *Current opinion in genetics & development*. (2011) 21: 175-186.

[120] Sidoli S, Cheng L, Jensen ON. Proteomics in chromatin biology and epigenetics: Elucidation of post-translational modifications of histone proteins by mass spectrometry. *Journal of proteomics*. (2012) 75: 3419-3433.

[121] Kitagawa H, Fujiki R, Yoshimura K, Mezaki Y, Uematsu Y, Matsui D, et al. The chromatin-remodeling complex WINAC targets a nuclear receptor to promoters and is impaired in Williams syndrome. *Cell*. (2003) 113: 905-917.

[122] Xue YT, Gibbons R, Yan ZJ, Yang DF, McDowell TL, Sechi S, et al. The ATRX syndrome protein forms a chromatin-remodeling complex with Daxx and localizes in

promyelocytic leukemia nuclear bodies. *Proceedings of the National Academy of Sciences of the United States of America*. (2003) 100: 10635-10640.

[123] Gibbons RJ, Higgs DR. Molecular-clinical spectrum of the ATR-X syndrome. *American Journal of Medical Genetics*. (2000) 97: 204-212.

[124] Boerkoel CF, Takashima H, John J, Yan J, Stankiewicz P, Rosenbarker L, et al. Mutant chromatin remodeling protein SMARCAL1 causes Schimke immuno-osseous dysplasia. *Nature genetics*. (2002) 30: 215-220.

[125] Shiio Y, Eisenman RN, Yi EC, Donohoe S, Goodlett DR, Aebersold R. Quantitative proteomic analysis of chromatin-associated factors. *Journal of the American Society for Mass Spectrometry*. (2003) 14: 696-703.

[126] Gassmann R, Henzing AJ, Earnshaw WC. Novel components of human mitotic chromosomes identified by proteomic analysis of the chromosome scaffold fraction. *Chromosoma*. (2005) 113: 385-397.

[127] Uchiyama S, Kobayashi S, Takata H, Ishihara T, Hori N, Higashi T, et al. Proteome analysis of human metaphase chromosomes. *The Journal of biological chemistry*. (2005) 280: 16994-17004.

[128] Chu DS, Liu H, Nix P, Wu TF, Ralston EJ, Yates JR, 3rd, et al. Sperm chromatin proteomics identifies evolutionarily conserved fertility factors. *Nature*. (2006) 443: 101-105.

[129] Franklin S, Chen H, Mitchell-Jordan S, Ren S, Wang Y, Vondriska TM. Quantitative analysis of the chromatin proteome in disease reveals remodeling principles and identifies high mobility group protein B2 as a regulator of hypertrophic growth. *Molecular & cellular proteomics : MCP*. (2012) 11: M111 014258.

[130] Fischle W, Wang Y, Allis CD. Binary switches and modification cassettes in histone biology and beyond. *Nature*. (2003) 425: 475-479.

[131] Felsenfeld G, Groudine M. Controlling the double helix. *Nature*. (2003) 421: 448-453.

[132] Jaenisch R, Bird A. Epigenetic regulation of gene expression: how the genome integrates intrinsic and environmental signals. *Nature genetics*. (2003) 33 Suppl: 245-254.

[133] Cheung P, Allis CD, Sassone-Corsi P. Signaling to chromatin through histone modifications. *Cell*. (2000) 103: 263-271.

[134] Du YC, Gu S, Zhou J, Wang T, Cai H, Macinnes MA, et al. The dynamic alterations of H2AX complex during DNA repair detected by a proteomic approach reveal the critical roles of Ca(2+)/calmodulin in the ionizing radiation-induced cell cycle arrest. *Molecular & cellular proteomics : MCP*. (2006) 5: 1033-1044.

[135] Brajenovic M, Joberty G, Kuster B, Bouwmeester T, Drewes G. Comprehensive proteomic analysis of human Par protein complexes reveals an interconnected protein network. *The Journal of biological chemistry*. (2004) 279: 12804-12811.

[136] Ewing RM, Chu P, Elisma F, Li H, Taylor P, Climie S, et al. Large-scale mapping of human protein-protein interactions by mass spectrometry. *Molecular systems biiology*. (2007) 3: 89.

[137] Gavin AC, Aloy P, Grandi P, Krause R, Boesche M, Marzioch M, et al. Proteome survey reveals modularity of the yeast cell machinery. *Nature*. (2006) 440: 631-636.

[138] Lambert JP, Mitchell L, Rudner A, Baetz K, Figeys D. A novel proteomics approach for the discovery of chromatin-associated protein networks. *Molecular & cellular proteomics : MCP*. (2009) 8: 870-882.

[139] Shechter D, Dormann HL, Allis CD, Hake SB. Extraction, purification and analysis of histones. *Nature protocal*. (2007) 2: 1445-1457.

[140] Yaniv M, Cereghini S. Structure of transcriptionally active chromatin. *CRC Critical reviews in biochemistry*. (1986) 21: 1-26.

[141] Reeves R. Transcriptionally active chromatin. *Biochim Biophys Acta*. (1984) 782: 343-393.

Reference

[142] Cartwright IL, Abmayr SM, Fleischmann G, Lowenhaupt K, Elgin SC, Keene MA, et al. Chromatin structure and gene activity: the role of nonhistone chromosomal proteins. *CRC Critical reviews in biochemistry*. (1982) 13: 1-86.

[143] Guo T, Gan CS, Zhang H, Zhu Y, Kon OL, Sze SK. Hybridization of pulsed-Q dissociation and collision-activated dissociation in linear ion trap mass spectrometer for iTRAQ quantitation. *Journal of proteome research*. (2008) 7: 4831-4840.

[144] Dutta B, Adav SS, Koh CG, Lim SK, Meshorer E, Sze SK. Elucidating the temporal dynamics of chromatin-associated protein release upon DNA digestion by quantitative proteomic approach. *Journal of Proteomics*. (2012) 75: 5493-5506.

[145] Wilkins RJ, Hart RW. Preferential DNA repair in human cells. *Nature*. (1974) 247: 35-36.

[146] Misteli T, Gunjan A, Hock R, Bustin M, Brown DT. Dynamic binding of histone H1 to chromatin in living cells. *Nature*. (2000) 408: 877-881.

[147] Gilbert N, Gilchrist S, Bickmore WA. Chromatin organization in the mammalian nucleus. *International review of cytology*. (2005) 242: 283-336.

[148] Ichimura S, Mita K, Zama M. Essential role of arginine residues in the folding of deoxyribonucleic acid into nucleosome cores. *Biochemistry*. (1982) 21: 5329-5334.

[149] Vandamme J, Volkel P, Rosnoblet C, Le Faou P, Angrand PO. Interaction proteomics analysis of polycomb proteins defines distinct PRC1 complexes in mammalian cells. *Molecular & cellular proteomics : MCP*. (2011) 10: M110 002642.

[150] Hake SB, Allis CD. Histone H3 variants and their potential role in indexing mammalian genomes: the "H3 barcode hypothesis". *Proceedings of the National Academy of Sciences of the United States of America*. (2006) 103: 6428-6435.

[151] Bianchi ME, Agresti A. HMG proteins: dynamic players in gene regulation and differentiation. *Current opinion in genetics & development.* (2005) 15: 496-506.

Reference

[152] Phair RD, Scaffidi P, Elbi C, Vecerova J, Dey A, Ozato K, et al. Global nature of dynamic protein-chromatin interactions in vivo: Three-dimensional genome scanning and dynamic interaction networks of chromatin proteins. *Molecular and cellular biology*. (2004) 24: 6393-6402.

[153] Scaffidi P, Misteli T, Bianchi ME. Release of chromatin protein HMGB1 by necrotic cells triggers inflammation. *Nature*. (2002) 418: 191-195.

[154] Bustin M. Regulation of DNA-dependent activities by the functional motifs of the high-mobility-group chromosomal proteins. *Molecular and cellular biology*. (1999) 19: 5237-5246.

[155] Reeves R. Molecular biology of HMGA proteins: hubs of nuclear function. *Gene*. (2001) 277: 63-81.

[156] Cherukuri S, Hock R, Ueda T, Catez F, Rochman M, Bustin M. Cell cycle-dependent binding of HMGN proteins to chromatin. *Molecular biology of the cell*. (2008) 19: 1816-1824.

[157] Tsukiyama T, Wu C. Chromatin remodeling and transcription. *Current opinion in genetics & development*. (1997) 7: 182-191.

[158] Peterson CL, Tamkun JW. The SWI-SNF complex: a chromatin remodeling machine? *Trends in biochemical sciences*. (1995) 20: 143-146.

[159] Khetani RS, Bickel SE. Regulation of meiotic cohesion and chromosome core morphogenesis during pachytene in Drosophila oocytes. *Journal of cell science*. (2007) 120: 3123-3137.

[160] Kim HS, Brill SJ. Rfc4 interacts with Rpa1 and is required for both DNA replication and DNA damage checkpoints in Saccharomyces cerevisiae. *Molecular and Cellular Biology*. (2001) 21: 3725-3737.

[161] Durand-Dubief M, Svensson JP, Persson J, Ekwall K. Topoisomerases, chromatin and transcription termination. *Transcription*. (2011) 2: 66-70.

[162] Quinn J, Fyrberg AM, Ganster RW, Schmidt MC, Peterson CL. DNA-binding properties of the yeast SWI/SNF complex. *Nature*. (1996) 379: 844-847.

[163] Zhu XD, Kuster B, Mann M, Petrini JH, de Lange T. Cell-cycle-regulated association of RAD50/MRE11/NBS1 with TRF2 and human telomeres. *Nature genetics.* (2000) 25: 347-352.

[164] Ciapponi L, Cenci G, Ducau J, Flores C, Johnson-Schlitz D, Gorski MM, et al. The Drosophila Mre11/Rad50 complex is required to prevent both telomeric fusion and chromosome breakage. *Current biology : CB*. (2004) 14: 1360-1366.

[165] Dorner D, Gotzmann J, Foisner R. Nucleoplasmic lamins and their interaction partners, LAP2alpha, Rb, and BAF, in transcriptional regulation. *FEBS journal*. (2007) 274: 1362-1373.

[166] Prokocimer M, Davidovich M, Nissim-Rafinia M, Wiesel-Motiuk N, Bar DZ, Barkan R, et al. Nuclear lamins: key regulators of nuclear structure and activities. *Journal of cellular and molecular medicine*. (2009) 13: 1059-1085.

[167] Albiez H, Cremer M, Tiberi C, Vecchio L, Schermelleh L, Dittrich S, et al. Chromatin domains and the interchromatin compartment form structurally defined and functionally interacting nuclear networks. *Chromosome research*. (2006) 14: 707-733.

[168] Bonenfant D, Towbin H, Coulot M, Schindler P, Mueller DR, van Oostrum J. Analysis of Dynamic Changes in Post-translational Modifications of Human Histones during Cell Cycle by Mass Spectrometry. *Molecular & cellular proteomics : MCP*. (2007) 6: 1917-1932.

[169] Jin T, Guo F, Serebriiskii IG, Howard A, Zhang YZ. A 1.55 A resolution X-ray crystal structure of HEF2/ERH and insights into its transcriptional and cell-cycle interaction networks. *Proteins*. (2007) 68: 427-437.

[170] Onyango P, Feinberg AP. A nucleolar protein, H19 opposite tumor suppressor (HOTS), is a tumor growth inhibitor encoded by a human imprinted H19 antisense transcript. *Proceedings of the National Academy of Sciences of the United States of America* (2011) 108: 16759-16764.

Reference

[171] Morillo-Huesca M, Maya D, Munoz-Centeno MC, Singh RK, Oreal V, Reddy GU, et al. FACT prevents the accumulation of free histones evicted from transcribed chromatin and a subsequent cell cycle delay in G1. *PLoS genetic.* (2010) 6: e1000964.

[172] Obuse C, Yang H, Nozaki N, Goto S, Okazaki T, Yoda K. Proteomics analysis of the centromere complex from HeLa interphase cells: UV-damaged DNA binding protein 1 (DDB-1) is a component of the CEN-complex, while BMI-1 is transiently co-localized with the centromeric region in interphase. *Genes Cells*. (2004) 9: 105-120.

[173] Dai Y, Ngo D, Jacob J, Forman LW, Faller DV. Prohibitin and the SWI/SNF ATPase subunit BRG1 are required for effective androgen antagonist-mediated transcriptional repression of androgen receptor-regulated genes. *Carcinogenesis*. (2008) 29: 1725-1733.

[174] Erard MS, Belenguer P, Caizergues-Ferrer M, Pantaloni A, Amalric F. A major nucleolar protein, nucleolin, induces chromatin decondensation by binding to histone H1. *European journal of biochemistry / FEBS*. (1988) 175: 525-530.

[1784] Meng L, Hsu JK, Zhu Q, Lin T, Tsai RY. Nucleostemin inhibits TRF1 dimerization and shortens its dynamic association with the telomere. *Journal of cell science*. (2011) 124: 3706-3714.

[176] Pombo A. Advances in imaging the interphase nucleus using thin cryosections. *Histochemistry and cell biology*. (2007) 128: 97-104.

[177] Bailis JM, Forsburg SL. It's all in the timing: linking S phase to chromatin structure and chromosome dynamics. *Cell cycle (Georgetown, Tex.)*. (2003) 2: 303-306.

[178] Probst AV, Dunleavy E, Almouzni G. Epigenetic inheritance during the cell cycle. *Nature reviews. Molecular cell biology*. (2009) 10: 192-206.

[179] Liu Q, Gong Z. The coupling of epigenome replication with DNA replication. *Current opinion in plant biology*. (2011) 14: 187-194.

Reference

[180] Gehring M, Huh JH, Hsieh TF, Penterman J, Choi Y, Harada JJ, et al. DEMETER DNA glycosylase establishes MEDEA polycomb gene self-imprinting by allele-specific demethylation. *Cell*. (2006) 124: 495-506.

[181] Zhang C, Su ZY, Khor TO, Shu L, Kong AN. Sulforaphane enhances Nrf2 expression in prostate cancer TRAMP C1 cells through epigenetic regulation. *Biochemical pharmacology*. (2013) 85: 1398-1404.

[182] Ng MH, Wong IH, Lo KW. DNA methylation changes and multiple myeloma. *Leukemia & lymphoma*. (1999) 34: 463-472.

[183] Halley-Stott RP, Gurdon JB. Epigenetic memory in the context of nuclear reprogramming and cancer. *Briefings in functional genomics*. (2013) 12: 164-173.

[184] Martin C, Zhang Y. Mechanisms of epigenetic inheritance. *Current opinion in cell biology*. (2007) 19: 266-272.

[185] Huang C, Zhang Z, Xu M, Li Y, Li Z, Ma Y, et al. H3.3-h4 tetramer splitting events feature cell-type specific enhancers. *PLoS genetics*. (2013) 9: e1003558.

[186] Wysocka J, Swigut T, Milne TA, Dou Y, Zhang X, Burlingame AL, et al. WDR5 associates with histone H3 methylated at K4 and is essential for H3 K4 methylation and vertebrate development. *Cell*. (2005) 121: 859-872.

[187] Ahmad K, Henikoff S. The histone variant H3.3 marks active chromatin by replication-independent nucleosome assembly. *Molecular cell*. (2002) 9: 1191-1200.

[188] Mora-Bermudez F, Ellenberg J. Measuring structural dynamics of chromosomes in living cells by fluorescence microscopy. *Methods (San Diego, Calif.)*. (2007) 41: 158-167.

[189] Hartl P, Gottesfeld J, Forbes DJ. Mitotic repression of transcription in vitro. *The Journal of cell biology*. (1993) 120: 613-624.

[190] Yong KJ, Milenic DE, Baidoo KE, Brechbiel MW. (212)Pb-radioimmunotherapy induces G(2) cell-cycle arrest and delays DNA damage repair in tumor xenografts in a model for disseminated intraperitoneal disease. *Molecular cancer therapeutics*. (2012) 11: 639-648.

[191] Sinha M, Peterson CL. Chromatin dynamics during repair of chromosomal DNA double-strand breaks. *Epigenomics*. (2009) 1: 371-385.

[192] Mosesso P, Palitti F, Pepe G, Pinero J, Bellacima R, Ahnstrom G, et al. Relationship between chromatin structure, DNA damage and repair following X-irradiation of human lymphocytes. *Mutation research*. (2010) 701: 86-91.

[193] Audit B, Zaghloul L, Vaillant C, Chevereau G, d'Aubenton-Carafa Y, Thermes C, et al. Open chromatin encoded in DNA sequence is the signature of 'master' replication origins in human cells. *Nucleic acids research*. (2009) 37: 6064-6075.

[194] Zhang X, Yu Q, Olsen L, Bi X. Functions of protosilencers in the formation and maintenance of heterochromatin in Saccharomyces cerevisiae. *PloS one*. (2012) 7: e37092.

[195] Aird KM, Zhang R. Detection of senescence-associated heterochromatin foci (SAHF). *Methods in molecular biology (Clifton, N.J.)*. (2013) 965: 185-196.

[196] Tu Z, Aird K, Zhang R. Chromatin remodeling, BRCA1, SAHF and cellular senescence. *Cell cycle (Georgetown, Tex.)*. (2013) 12: 1653-1654.

[197] Jespersen C, Soragni E, James Chou C, Arora PS, Dervan PB, Gottesfeld JM. Chromatin structure determines accessibility of a hairpin polyamide-chlorambucil conjugate at histone H4 genes in pancreatic cancer cells. *Bioorganic & medicinal chemistry letters*. (2012) 22: 4068-4071.

[198] Di Paola D, Rampakakis E, Chan MK, Zannis-Hadjopoulos M. Differential chromatin structure encompassing replication origins in transformed and normal cells. *Genes & cancer*. (2012) 3: 152-176.

[199] Chadwick BP, Willard HF. Cell cycle-dependent localization of macroH2A in chromatin of the inactive X chromosome. *The Journal of cell biology*. (2002) 157: 1113-1123.

[200] Izuta H, Ikeno M, Suzuki N, Tomonaga T, Nozaki N, Obuse C, et al. Comprehensive analysis of the ICEN (Interphase Centromere Complex) components enriched in the CENP-A chromatin of human cells. *Genes Cells*. (2006) 11: 673-684.

[201] Agostinho M, Rino J, Braga J, Ferreira F, Steffensen S, Ferreira J. Human topoisomerase IIalpha: targeting to subchromosomal sites of activity during interphase and mitosis. *Molecular biology of the cell*. (2004) 15: 2388-2400.

[202] Iwasaki O, Noma K. Global genome organization mediated by RNA polymerase III-transcribed genes in fission yeast. *Gene*. (2012) 493: 195-200.

[203] Minc E, Courvalin JC, Buendia B. HP1gamma associates with euchromatin and heterochromatin in mammalian nuclei and chromosomes. *Cytogenetics and cell genetics*. (2000) 90: 279-284.

[204] Hayakawa T, Haraguchi T, Masumoto H, Hiraoka Y. Cell cycle behavior of human HP1 subtypes: distinct molecular domains of HP1 are required for their centromeric localization during interphase and metaphase. *Journal of cell science*. (2003) 116: 3327-3338.

[205] Kubota T, Stead DA, Hiraga S, ten Have S, Donaldson AD. Quantitative proteomic analysis of yeast DNA replication proteins. *Methods (San Diego, Calif.)*. (2012) 57: 196-202.

[206] Choi S, Srivas R, Fu KY, Hood BL, Dost B, Gibson GA, et al. Quantitative proteomics reveal ATM kinase-dependent exchange in DNA damage response complexes. *Journal of proteome research*. (2012) 11: 4983-4991.

[207] Rousseaux S, Khochbin S. Combined proteomic and in silico approaches to decipher post-meiotic male genome reprogramming in mice. *Systems biology in reproductive medicine*. (2012) 58: 191-196.

[208] Kunkel TA, Erie DA. DNA mismatch repair. *Annual review of biochemistry*. (2005) 74: 681-710.

[209] Zhang Y, Yuan F, Presnell SR, Tian K, Gao Y, Tomkinson AE, et al. Reconstitution of 5'-directed human mismatch repair in a purified system. *Cell*. (2005) 122: 693-705.

[210] Pena-Diaz J, Jiricny J. Mammalian mismatch repair: error-free or error-prone? *Trends in biochemical sciences*. (2012) 37: 206-214.

[211] Larson ED, Iams K, Drummond JT. Strand-specific processing of 8-oxoguanine by the human mismatch repair pathway: inefficient removal of 8-oxoguanine paired with adenine or cytosine. *DNA Repair*. (2003) 2: 1199-1210.

[212] Davis AJ, Lee KJ, Chen DJ. The N-terminal region of the DNA-dependent protein kinase catalytic subunit is required for its DNA double-stranded break-mediated activation. *The Journal of biological chemistry*. (2013) 288: 7037-7046.

[213] Shibata A, Conrad S, Birraux J, Geuting V, Barton O, Ismail A, et al. Factors determining DNA double-strand break repair pathway choice in G2 phase. *EMBO journal*. (2011) 30: 1079-1092.

[214] Kongruttanachok N, Phuangphairoj C, Thongnak A, Ponyeam W, Rattanatanyong P, Pornthanakasem W, et al. Replication independent DNA double-strand break retention may prevent genomic instability. *Molecular cancer*. (2010) 9: 70.

[215] Kocher S, Rieckmann T, Rohaly G, Mansour WY, Dikomey E, Dornreiter I, et al. Radiation-induced double-strand breaks require ATM but not Artemis for homologous recombination during S-phase. *Nucleic acids research*. (2012) 40: 8336-8347.

[216] Storici F, Henneke G, Ferrari E, Gordenin DA, Hübscher U, Resnick MA. The flexible loop of human FEN1 endonuclease is required for flap cleavage during DNA replication and repair. *EMBO Journal*. (2002) 21: 5930-5942.

[217] Verdun RE, Karlseder J. The DNA damage machinery and homologous recombination pathway act consecutively to protect human telomeres. *Cell*. (2006) 127: 709-720.

[218] Stein GS, van Wijnen AJ, Stein JL, Lian JB, Montecino M, Zaidi SK, et al. An architectural perspective of cell-cycle control at the G1/S phase cell-cycle transition. *Journal of cellular physiology*. (2006) 209: 706-710.

Reference

[219] Guan D, Altan-Bonnet N, Parrott AM, Arrigo CJ, Li Q, Khaleduzzaman M, et al. Nuclear factor 45 (NF45) is a regulatory subunit of complexes with NF90/110 involved in mitotic control. *Molecular and cellular biology*. (2008) 28: 4629-4641.

[220] Winnicki K, Polit JT, Maszewski J. Increased transcription in hydroxyurea-treated root meristem cells of Vicia faba. *Protoplasma*. (2013) 250: 251-259.

[221] Steinberg XP, Hepp MI, Fernandez Garcia Y, Suganuma T, Swanson SK, Washburn M, et al. Human CCAAT/enhancer-binding protein beta interacts with chromatin remodeling complexes of the imitation switch subfamily. *Biochemistry*. (2012) 51: 952-962.

[222] Tan BC, Yang CC, Hsieh CL, Chou YH, Zhong CZ, Yung BY, et al. Epigeneitc silencing of ribosomal RNA genes by Mybbp1a. *Journal of biomedical science*. (2012) 19: 57.

[223] Jerabek H, Heermann DW. Expression-dependent folding of interphase chromatin. *PloS one*. (2012) 7: e37525.

[224] Piluso D, Bilan P, Capone JP. Host cell factor-1 interacts with and antagonizes transactivation by the cell cycle regulatory factor Miz-1. *The Journal of biological chemistry*. (2002) 277: 46799-46808.

[225] Ma Y, Jacobs SB, Jackson-Grusby L, Mastrangelo MA, Torres-Betancourt JA, Jaenisch R, et al. DNA CpG hypomethylation induces heterochromatin reorganization involving the histone variant macroH2A. *Journal of cell science*. (2005) 118: 1607-1616.

[226] Nair SS, Nair BC, Cortez V, Chakravarty D, Metzger E, Schule R, et al. PELP1 is a reader of histone H3 methylation that facilitates oestrogen receptor-alpha target gene activation by regulating lysine demethylase 1 specificity. *EMBO reports*. (2010) 11: 438-444.

[227] Sakane N, Kwon HS, Pagans S, Kaehlcke K, Mizusawa Y, Kamada M, et al. Activation of HIV transcription by the viral Tat protein requires a demethylation step mediated by lysine-specific demethylase 1 (LSD1/KDM1). *PLoS pathogens*. (2011) 7: e1002184.

[228] Hayashihara K, Uchiyama S, Shimamoto S, Kobayashi S, Tomschik M, Wakamatsu H, et al. The middle region of an HP1-binding protein, HP1-BP74, associates with linker DNA at the entry/exit site of nucleosomal DNA. *Journal of biological chemistry*. (2010) 285: 6498-6507.

[229] Butchko RA, Brown DW, Busman M, Tudzynski B, Wiemann P. Lae1 regulates expression of multiple secondary metabolite gene clusters in Fusarium verticillioides. *Fungal genetics and biology : FG & B*. (2012) 49: 602-612.

[230] Yuan HX, Xiong Y, Guan KL. Nutrient sensing, metabolism, and cell growth control. *Molecular cell*. (2013) 49: 379-387.

[231] Owa T, Yoshino H, Yoshimatsu K, Nagasu T. Cell cycle regulation in the G1 phase: a promising target for the development of new chemotherapeutic anticancer agents. *Current medicinal chemistry*. (2001) 8: 1487-1503.

[232] Huang Y, Wu G, Fan H, Ye J, Liu X. Electroacupuncture promotes chondrocyte proliferation via accelerated G1/S transition in the cell cycle. *International journal of molecular medicine*. (2013) 31: 1443-1448.

[233] Uttam S, Bista RK, Staton K, Alexandrov S, Choi S, Bakkenist CJ, et al. Investigation of depth-resolved nanoscale structural changes in regulated cell proliferation and chromatin decondensation. *Biomedical optics express*. (2013) 4: 596-613.

[234] Cohen-Fix O. Cell biology: Import and nuclear size. *Nature*. (2010) 468: 513-516.

[235] van Zanten M, Koini MA, Geyer R, Liu Y, Brambilla V, Bartels D, et al. Seed maturation in Arabidopsis thaliana is characterized by nuclear size reduction and increased chromatin condensation. *Proceedings of the National Academy of Sciences of the United States of America*. (2011) 108: 20219-20224.

[236] Levy DL, Heald R. Nuclear size is regulated by importin alpha and Ntf2 in Xenopus. *Cell*. (2010) 143: 288-298.

[237] Moyer MW. Targeting hypoxia brings breath of fresh air to cancer therapy. *Nature medicine*. (2012) 18: 636-637.

[238] Nguyen MP, Lee S, Lee YM. Epigenetic regulation of hypoxia inducible factor in diseases and therapeutics. *Archives of pharmacal research*. (2013) 36: 252-263.

[239] Wu CY, Tsai YP, Wu MZ, Teng SC, Wu KJ. Epigenetic reprogramming and post-transcriptional regulation during the epithelial-mesenchymal transition. *Trends in genetics : TIG*. (2012) 28: 454-463.

[240] Johnson AB, Barton MC. Hypoxia-induced and stress-specific changes in chromatin structure and function. *Mutation research*. (2007) 618: 149-162.

[241] Wang F, Zhang R, Beischlag TV, Muchardt C, Yaniv M, Hankinson O. Roles of Brahma and Brahma/SWI2-related gene 1 in hypoxic induction of the erythropoietin gene. *Journal of biological chemistry*. (2004) 279: 46733-46741.

[242] Isaacs JT, Antony L, Dalrymple SL, Brennen WN, Gerber S, Hammers H, et al. Tasquinimod Is an Allosteric Modulator of HDAC4 survival signaling within the compromised cancer microenvironment. *Cancer research.* (2013) 73: 1386-1399.

[243] Steinmann K, Richter AM, Dammann RH. Epigenetic silencing of erythropoietin in human cancers. *Genes & cancer*. (2011) 2: 65-73.

[244] Ponnaluri VK, Vadlapatla RK, Vavilala DT, Pal D, Mitra AK, Mukherji M. Hypoxia induced expression of histone lysine demethylases: implications in oxygen-dependent retinal neovascular diseases. *Biochemical and biophysical research communications*. (2011) 415: 373-377.

[245] Tsai YP, Wu KJ. Epigenetic regulation of hypoxia-responsive gene expression: Focusing on chromatin and DNA modifications. *International journal of cancer.* (2013) 134: 249-256.

[246] Robinson CM, Neary R, Levendale A, Watson CJ, Baugh JA. Hypoxia-induced DNA hypermethylation in human pulmonary fibroblasts is associated with Thy-1 promoter methylation and the development of a pro-fibrotic phenotype. *Respiratory research*. (2012) 13: 74.

[247] Chaplin DJ, Olive PL, Durand RE. Intermittent blood flow in a murine tumor: radiobiological effects. *Cancer research.* (1987) 47: 597-601.

[248] Johnson AB, Denko N, Barton MC. Hypoxia induces a novel signature of chromatin modifications and global repression of transcription. *Mutation research*. (2008) 640: 174-179.

[249] Young SD, Marshall RS, Hill RP. Hypoxia induces DNA overreplication and enhances metastatic potential of murine tumor cells. *Proceedings of the National Academy of Sciences of the United States of America*. (1988) 85: 9533-9537.

[250] Bristow RG, Hill RP. Hypoxia and metabolism. Hypoxia, DNA repair and genetic instability. *Nature reviews. Cancer*. (2008) 8: 180-192.

[251] Coquelle A, Toledo F, Stern S, Bieth A, Debatisse M. A new role for hypoxia in tumor progression: induction of fragile site triggering genomic rearrangements and formation of complex DMs and HSRs. *Molecular cell.* (1998) 2: 259-265.

[252] Rice GC, Hoy C, Schimke RT. Transient hypoxia enhances the frequency of dihydrofolate reductase gene amplification in Chinese hamster ovary cells. *Proceedings of the National Academy of Sciences of the United States of America*. (1986) 83: 5978-5982.

[253] Thadani R, Uhlmann F, Heeger S. Condensin, chromatin crossbarring and chromosome condensation. *Current biology : CB.* (2012) 22: R1012-1021.

[254] Schneider K, Fuchs C, Dobay A, Rottach A, Qin W, Wolf P, et al. Dissection of cell cycle-dependent dynamics of Dnmt1 by FRAP and diffusion-coupled modeling. *Nucleic acids research*. (2013) 41: 4860-4876.

[255] Mizuno S, Yasuo M, Bogaard HJ, Kraskauskas D, Natarajan R, Voelkel NF. Inhibition of histone deacetylase causes emphysema. *American Journal of Physiology - Lung Cellular and Molecular Physiology*. (2011) 300: L402-L413.

[256] Toh Y, Nicolson GL. The role of the MTA family and their encoded proteins in human cancers: Molecular functions and clinical implications. *Clinical and Experimental Metastasis*. (2009) 26: 215-227.

[257] Lim JH, Choi YJ, Cho CH, Park JW. Protein arginine methyltransferase 5 is an essential component of the hypoxia-inducible factor 1 signaling pathway. *Biochemical and biophysical research communications*. (2012) 418: 254-259.

[258] Agrawal S, Hofmann WK, Tidow N, Ehrich M, van den Boom D, Koschmieder S, et al. The C/EBPdelta tumor suppressor is silenced by hypermethylation in acute myeloid leukemia. *Blood*. (2007) 109: 3895-3905.

[259] Riley T, Sontag E, Chen P, Levine A. Transcriptional control of human p53-regulated genes. *Nature reviews. Molecular cell biology*. (2008) 9: 402-412.

[260] Chen D, Reierstad S, Fang F, Bulun SE. JunD and JunB integrate prostaglandin E2 activation of breast cancer-associated proximal aromatase promoters. *Molecular endocrinology (Baltimore, Md.)*. (2011) 25: 767-775.

[261] Abdul-Hafez A, Shu R, Uhal BD. JunD and HIF-1alpha mediate transcriptional activation of angiotensinogen by TGF-beta1 in human lung fibroblasts. *FASEB journal : official publication of the Federation of American Societies for Experimental Biology*. (2009) 23: 1655-1662.

[262] Nijwening JH, Geutjes EJ, Bernards R, Beijersbergen RL. The histone demethylase Jarid1b (Kdm5b) is a novel component of the Rb pathway and associates with E2f-target genes in MEFs during senescence. *PloS one*. (2011) 6: e25235.

[263] Lv J, Liu H, Wang Q, Tang Z, Hou L, Zhang B. Molecular cloning of a novel human gene encoding histone acetyltransferase-like protein involved in transcriptional activation of hTERT. *Biochemical and biophysical research communications*. (2003) 311: 506-513.

[264] Liu H, Ling Y, Gong Y, Sun Y, Hou L, Zhang B. DNA damage induces N-acetyltransferase NAT10 gene expression through transcriptional activation. *Molecular and cellular biochemistry*. (2007) 300: 249-258.

[265] Schmaltz C, Hardenbergh PH, Wells A, Fisher DE. Regulation of proliferation-survival decisions during tumor cell hypoxia. *Molecular and cellular biology*. (1998) 18: 2845-2854.

[266] Gumbiner BM. Cell adhesion: the molecular basis of tissue architecture and morphogenesis. *Cell*. (1996) 84: 345-357.

[267] Schlie-Wolter S, Ngezahayo A, Chichkov BN. The selective role of ECM components on cell adhesion, morphology, proliferation and communication in vitro. *Experimental cell research.* (2013) 319: 1553-1561.

[268] Hynes RO, Lander AD. Contact and adhesive specificities in the associations, migrations, and targeting of cells and axons. *Cell*. (1992) 68: 303-322.

[269] Park JE, Tan HS, Datta A, Lai RC, Zhang H, Meng W, et al. Hypoxic tumor cell modulates its microenvironment to enhance angiogenic and metastatic potential by secretion of proteins and exosomes. *Molecular & cellular proteomics : MCP*. (2010) 9: 1085-1099.

[270] Phillips-Mason PJ, Craig SE, Brady-Kalnay SM. Should I stay or should I go? Shedding of RPTPs in cancer cells switches signals from stabilizing cell-cell adhesion to driving cell migration. *Cell adhesion & migration*. (2011) 5: 298-305.

[271] Kumareswaran R, Ludkovski O, Meng A, Sykes J, Pintilie M, Bristow RG. Chronic hypoxia compromises repair of DNA double-strand breaks to drive genetic instability. *Journal of cell science*. (2012) 125: 189-199.

[272] Huang LE, Bindra RS, Glazer PM, Harris AL. Hypoxia-induced genetic instability--a calculated mechanism underlying tumor progression. *Journal of cellular and molecular medicine(Berl)*. (2007) 85: 139-148.

[273] Banath JP, Sinnott L, Larrivee B, MacPhail SH, Olive PL. Growth of V79 cells as xenograft tumors promotes multicellular resistance but does not increase spontaneous or radiation-induced mutant frequency. *Radiation research*. (2005) 164: 733-744.

[274] Lieber MR. The mechanism of double-strand DNA break repair by the nonhomologous DNA end-joining pathway. *Annual review of biochemistry*. (2010) 79: 181-211.

[275] Takashima Y, Sakuraba M, Koizumi T, Sakamoto H, Hayashi M, Honma M. Dependence of DNA double strand break repair pathways on cell cycle phase in human lymphoblastoid cells. *Environmental and molecular mutagenesis*. (2009) 50: 815-822.

[276] Keith B, Simon MC. Hypoxia-inducible factors, stem cells, and cancer. *Cell*. (2007) 129: 465-472.

[277] Mazumdar J, Dondeti V, Simon MC. Hypoxia-inducible factors in stem cells and cancer. *Journal of cellular and molecular medicine*. (2009) 13: 4319-4328.

[278] Bao B, Ahmad A, Kong DJ, Ali S, Azmi AS, Li YW, et al. Hypoxia induced aggressiveness of prostate cancer cells is linked with deregulated expression of VEGF, IL-6 and miRNAs that are attenuated by CDF. *PloS one*. (2012) 7.

Appendix A

Publications

1. **Dutta, B.**, Ren, Y., Lim S. K., Tam J. P., and Sze, S. K. (2014) Quantitative profiling of chromatome dynamics reveals a novel role for HP1BP3 in hypoxia-induced oncogenesis *Mol Cell Proteomics* **(In preparation).**

2. **Dutta, B.**, Ren, Y., Hao, P., Sim, K. H., Cheow, E. S., Adav, S. S., Tam J. P., and Sze, S. K. (2013) Profiling of the Chromatin-Associated Proteome Identifies HP1BP3 as a Novel Regulator of Cell Cycle Progression. *Mol Cell Proteomics* **(Submitted).**

3. Ren, Y., Hao, P., **Dutta, B.**, Cheow, E. S., Sim, K. H., Gan, C. S., Lim, S. K., and Sze, S. K. (2013) Hypoxia modulates A431 cellular pathways association to tumor radioresistance and enhanced migration revealed by comprehensive proteomic and functional studies. *Mol Cell Proteomics* 12, 485-498.

4. Hao, P., Ren, Y., **Dutta, B.**, and Sze, S. K. (2013) Comparative evaluation of electrostatic repulsion-hydrophilic interaction chromatography (ERLIC) and high-pH reversed phase (Hp-RP) chromatography in profiling of rat kidney proteome. *J Proteomics* 82, 254-262.

5. **Dutta, B.**, Adav, S. S., Koh, C. G., Lim, S. K., Meshorer, E., and Sze, S. K. (2012) Elucidating the temporal dynamics of chromatin-associated protein release upon DNA digestion by quantitative proteomic approach. *J Proteomics* 75, 5493-5506.

6. Adav, S. S., Cheow, E. S., Ravindran, A., **Dutta, B.**, and Sze, S. K. (2012) Label free quantitative proteomic analysis of secretome by Thermobifida fusca on different lignocellulosic biomass. *J Proteomics* 75, 3694-3706.

7. Hao, P., Qian, J., **Dutta, B.**, Cheow, E. S., Sim, K. H., Meng, W., Adav, S. S., Alpert, A., and Sze, S. K. (2012) Enhanced separation and characterization of deamidated peptides with RP-ERLIC-based multidimensional chromatography coupled with tandem mass spectrometry. *J Proteome Res* 11, 1804-1811.

Appendix B

Conference Presentations

Invited talks

1. SBS Graduate Student Retreat, Nanyang Technological University, Singapore. 05th October 2012.

   Title: Elucidating Dynamic Regulation on Chromatin Structure by Chromatin-associated Proteome Using Quantitative Proteomic Approach.

Posters

1. SSMS Conference, Singapore from 22nd to 23rd September 2011.

   Title: Elucidating Dynamic Interaction of Chromatin-associated Proteome with Chromatin by Quantitative Proteomics Approach.

2. 2nd Asian and Oceanic Mass Spectrometry Conference, Busan, Korea from 17th to 19th August 2011.

   Title: Elucidating Dynamic Interaction of Chromatin-associated Proteome with Chromatin by Quantitative Proteomics Approach.

3. Natural Products and Health 2013, Singapore from 5th to 7th September 2013.

   Title: Proteomic and Functional Studies of Chromatome Dynamics during Tumor Hypoxia to Elucidate Their Role in Tumorigenesis.